

REPORT 1115

DESIGN OF TWO-DIMENSIONAL CHANNELS WITH PRESCRIBED VELOCITY DISTRIBUTIONS ALONG THE CHANNEL WALLS¹

By JOHN D. STANITZ

SUMMARY

A general method of design is developed for two-dimensional unbranched channels with prescribed velocities as a function of arc length along the channel walls. The method is developed for both compressible and incompressible, irrotational, nonviscous flow and applies to the design of elbows, diffusers, nozzles, and so forth. Two types of compressible flow are considered: the general type, with the ratio of specific heats γ equal to 1.4, for example, and the linearized type, in which γ is -1.0 . Two methods of solution are used: In part I solutions are obtained by relaxation methods; in part II solutions are obtained by a Green's function.

Five numerical examples are given in part I including three elbow designs with the same prescribed velocity as a function of arc length along the channel walls but with incompressible, linearized compressible, and compressible flow. It is concluded that if a nonviscous gas with arbitrary γ (1.4, for example) were to flow through a channel designed for linearized compressible flow ($\gamma = -1.0$), the resulting velocity distribution along the channel walls would be nearly the velocity distribution prescribed for the linearized compressible flow.

One numerical example is presented in part II for an accelerating elbow with linearized compressible flow, and the time required for the solution by a Green's function in part II was considerably less than the time required for the same solution by relaxation methods in part I.

INTRODUCTION

There are two general types of theoretical problem in two-dimensional fluid motion: (1) the direct problem, in which the distribution of velocity is determined for a prescribed shape of boundary, and (2) the inverse problem, in which the shape of boundary is determined for a prescribed distribution of velocity along the boundary. The direct problem is an analysis problem; the inverse problem is a design problem. This report is concerned with the inverse, or design, problem for two-dimensional, irrotational flow in unbranched channels with prescribed velocities as a function of arc length along the channel walls.

The design of channels with prescribed velocities is important because: (1) Boundary-layer separation losses can be avoided by prescribed velocities that do not decelerate rapidly enough to cause separation, (2) shock losses in com-

pressible flow and cavitation in incompressible flow can be avoided by prescribed velocities that do not exceed certain maximum values dictated by these phenomena, and (3) for compressible flow the desired flow rate can be assured by prescribed velocities that do not result in "choke flow" conditions.

Several methods of channel design have been developed for particular application (refs. 1 and 2, for example). In reference 1 a design method is developed for accelerating elbows in which the velocity increases monotonically along the channel walls. The method is developed for incompressible and linearized ($\gamma = -1.0$) compressible flow. The velocity distribution along the channel walls is not arbitrary and the design method applies to elbows only. In reference 2 a design method is developed for straight, symmetrical channels with contracting or expanding walls. The method is developed for incompressible flow and the velocities are prescribed not as a function of arc length along the channel walls but as a function of circle angle in the transformed circle plane. A more general design is suggested in reference 3, but no attempt is made to develop and apply the method.

In the present report a general method of design is developed for two-dimensional, unbranched channels with prescribed velocities as a function of arc length along the channel walls. The method is developed for both compressible and incompressible, irrotational, nonviscous flow and applies to the design of elbows, diffusers, nozzles, and so forth. Two types of compressible flow are considered: the general type with arbitrary value of γ (1.4, for example) and the linearized type with γ equal to -1.0 . In general, if the prescribed velocity along one channel-wall differs from that along the other, the channel turns so that the downstream flow direction is different from the upstream direction. This change in flow direction cannot be arbitrarily chosen but depends on the prescribed velocity distribution along the walls. Equations are developed for computing this change in flow direction for an arbitrary prescribed velocity distribution with incompressible or linearized compressible flow. Two methods of solution have been developed for the design method and are presented in separate parts of this report. In part I solutions are obtained by relaxation methods (ref. 4). This method of solution results in complete information concerning the distribution of flow conditions throughout the

¹Supersedes NACA TN 2593, "Design of Two-Dimensional Channels with Prescribed Velocity Distributions Along the Channel Walls. I—Relaxation Solutions" by John D. Stanitz, 1952, and NACA TN 2595, "Design of Two-Dimensional Channels with Prescribed Velocity Distributions Along the Channel Walls. II—Solution by Green's Function" by John D. Stanitz, 1952.

channel and, in addition, can be used to obtain nonlinear solutions for compressible flow with arbitrary values of γ . In part II solutions are obtained by means of a Green's function. This method of solution is limited to incompressible and linearized ($\gamma = -1.0$) compressible flow, but the method is more rapid than relaxation methods, provided information within the channel is not required.

The design method reported herein was developed at the NACA Lewis laboratory during 1950 and is part of a doctoral thesis conducted with the advice of Professor Ascher H. Shapiro of the Massachusetts Institute of Technology.

PART I

GENERAL THEORY AND SOLUTION BY RELAXATION METHODS

A general method of design is developed for two-dimensional, unbranched channels with prescribed velocities as functions of arc length along the channel walls. The method is developed for both incompressible and compressible, irrotational, nonviscous flow. Two types of compressible flow are considered: the general type with arbitrary value for the ratio of specific heats γ (1.4, for example), and the linearized type in which γ is equal to -1.0 . The solutions in part I of this report are obtained by relaxation methods and give complete information concerning the flow throughout the channel. Five numerical examples are given, including three elbow designs with the same prescribed velocity as a function of arc length along the channel walls but with incompressible, linearized compressible, and compressible flow.

THEORY OF DESIGN METHOD

The design method is developed for two-dimensional channels with prescribed velocities along the channel walls. The prescribed velocity is arbitrary except that stagnation points cannot be prescribed. This exception limits the design method to unbranched channels.

PRELIMINARY CONSIDERATIONS

Assumptions.—The fluid is assumed to be nonviscous and either compressible or incompressible. The flow is assumed to be two dimensional and irrotational.

The assumption of two-dimensional, nonviscous, irrotational motion limits the design method in practice to channels with thin (negligible) boundary layers, such as exist near the entrance to the channel or after a rapid acceleration of the flow through a contraction in the channel. Even if the boundary layer is thin, the design method is limited to (and finds its most useful application for) prescribed velocity distributions that, from boundary-layer theory, do not decelerate fast enough to result in separation of the boundary layer, which separation alters the "effective" shape of the channel and completely changes the character of the flow.

In some channels with fully developed turbulent boundary layers, the design method might be expected to yield results that are satisfactory, although approximate, because for this

type of flow the rotational motion occurs primarily in regions close to the channel walls. In channel walls with thick or fully developed laminar boundary layers the design method cannot be used, because not only is the rotation of the flow important in most of the channel but, if the channel bends, important secondary flows develop that are not considered by the two-dimensional design method.

Flow field.—The flow field of the two-dimensional channel is considered to lie in the physical xy -plane where x and y are Cartesian coordinates expressed as ratios of a characteristic length equal to the constant channel width downstream at infinity. (All symbols are defined in appendix A.)

At each point in the channel (fig. 1) the velocity vector has a magnitude Q and a direction θ where Q is the fluid velocity expressed as the ratio of a characteristic velocity equal to the constant channel velocity downstream at infinity. For convenience, the velocity Q is related to a velocity q by

$$q = Qq_d \quad (1)$$

where q is the velocity expressed as a ratio of the stagnation speed of sound and the subscript d refers to conditions downstream at infinity.

The flow direction θ at each point in the channel is measured counterclockwise from the positive x -axis. From figure 1

$$dx = ds \cos \theta \quad (2a)$$

$$dy = ds \sin \theta \quad (2b)$$

where ds is a differential distance in the direction of Q , that is, along a streamline.

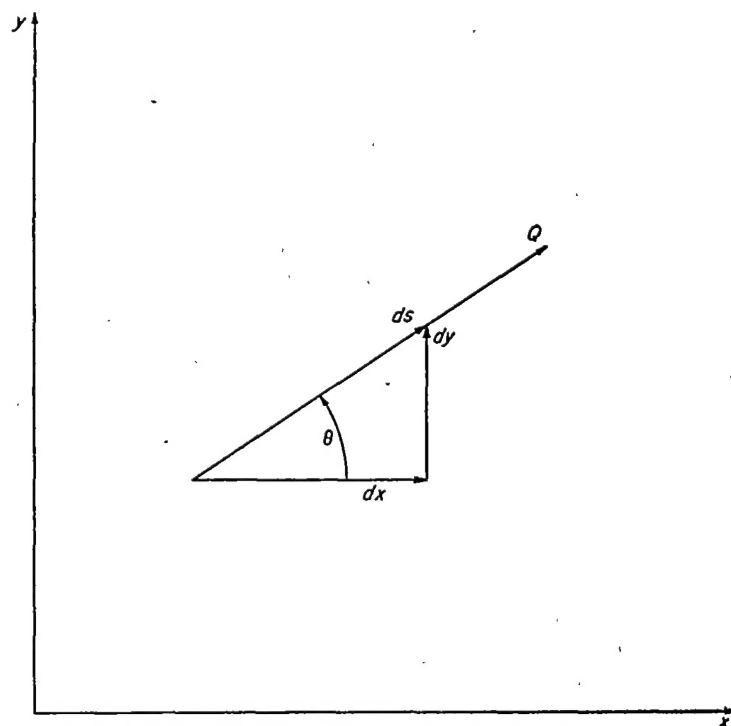


FIGURE 1.—Magnitude and direction of velocity at point in xy -plane.

Stream function and velocity potential.—If the condition of continuity is satisfied, a stream function ψ can be defined such that

$$d\psi = \rho Q \, dn \quad (3)$$

where ρ is the fluid density expressed as the ratio of a characteristic density equal to the stagnation density and where dn is a differential distance measured normal to the direction of Q , that is, normal to a streamline. Along a streamline, dn is zero so that from equation (3) the stream function ψ is constant.

If the condition of irrotational fluid motion is satisfied, a velocity potential φ can be defined such that

$$d\varphi = Q \, ds \quad (4)$$

Normal to a streamline, ds is zero so that from equation (4) the velocity potential φ is constant. Thus lines of constant φ and ψ are orthogonal in the physical xy -plane.

Outline of method.—Solutions of two-dimensional flow depend on known conditions imposed along the boundaries of the problem. In the inverse problem of channel design, the geometry of the channel walls in the physical xy -plane is unknown. This unknown geometry apparently precludes the possibility of solving the problem in the physical plane and necessitates the use of some new set of coordinates, that is, a transformed plane, in which to solve the problem. These new coordinates must be such that the geometric boundaries along which the velocities are prescribed are known in the transformed plane. It is also desirable, for mathematical simplicity, that the coordinate system in the transformed plane be orthogonal in the physical plane. A set of coordinates that satisfies these requirements is provided by φ and ψ , which are orthogonal in the physical xy -plane and for which the geometric boundaries are known constant values of ψ in the transformed $\varphi\psi$ -plane. The distribution of velocity as a function of φ along these boundaries of constant ψ is known because, if

$$Q = Q(s)$$

is prescribed, equation (4) integrates to give

$$\varphi = \varphi(s)$$

from which equations,

$$Q = Q(\varphi)$$

The technique of the proposed method of channel design is therefore to obtain a differential equation for the distribution of velocity in the $\varphi\psi$ -plane. The velocity distribution obtained from the solution of this equation is then used to obtain the distribution of flow direction, from which distribution the channel walls in the physical xy -plane are obtained directly. The differential equation for the distribution of velocity in the $\varphi\psi$ -plane is nonlinear (for compressible flow with γ other than -1.0) and is solved by numerical methods (relaxation methods).

DIFFERENTIAL EQUATION FOR DISTRIBUTION OF VELOCITY IN TRANSFORMED $\varphi\psi$ -PLANE

The differential equation for the distribution of velocity in the transformed $\varphi\psi$ -plane is obtained from the equations for

continuity and irrotational fluid motion expressed in terms of the transformed coordinates φ and ψ .

Continuity.—The continuity equation expressed in terms of φ and ψ becomes (appendix B):

$$\frac{1}{\rho} \left(\frac{\partial \log_e \rho}{\partial \varphi} + \frac{\partial \log_e Q}{\partial \psi} \right) + \frac{\partial \theta}{\partial \psi} = 0 \quad (5)$$

Irrotational fluid motion.—The equation for irrotational fluid motion, expressed in terms of φ and ψ , becomes (appendix B):

$$\rho \frac{\partial \log_e Q}{\partial \psi} - \frac{\partial \theta}{\partial \varphi} = 0 \quad (6)$$

Differential equation for distribution of velocity.—The second-order partial differential equation for the distribution of $\log_e Q$ in the transformed $\varphi\psi$ -plane is obtained by differentiating equations (5) and (6) with respect to φ and ψ , respectively, and combining to eliminate $\frac{\partial^2 \theta}{\partial \varphi \partial \psi}$. Thus,

$$\begin{aligned} \frac{\partial^2 \log_e \rho}{\partial \varphi^2} + \frac{\partial^2 \log_e Q}{\partial \varphi^2} - \frac{\partial \log_e \rho}{\partial \varphi} \left(\frac{\partial \log_e \rho}{\partial \varphi} + \frac{\partial \log_e Q}{\partial \psi} \right) + \\ \rho^2 \frac{\partial \log_e Q}{\partial \psi} \frac{\partial \log_e \rho}{\partial \psi} + \rho^2 \frac{\partial^2 \log_e Q}{\partial \psi^2} = 0 \end{aligned} \quad (7)$$

Equation (7), together with a relation between ρ , Q , and q_a , determines the distribution of $\log_e Q$ in the $\varphi\psi$ -plane for compressible flow with a given value of q_a and for arbitrarily prescribed variations in $\log_e Q$ along the boundaries of constant ψ .

Density.—The density ρ is related to the velocity q by (ref. 5, p. 26, for example)

$$\rho = \left(1 - \frac{\gamma-1}{2} q^2 \right)^{\frac{1}{\gamma-1}} \quad (8a)$$

which, from equation (1), becomes

$$\rho = \left(1 - \frac{\gamma-1}{2} Q^2 q_a^2 \right)^{\frac{1}{\gamma-1}} \quad (8b)$$

Equation (8b) relates the density ρ to the velocity Q for a given value of q_a .

Incompressible flow.—For incompressible flow ρ is constant and equal to 1.0 so that equation (7) becomes

$$\frac{\partial^2 \log_e Q}{\partial \varphi^2} + \frac{\partial^2 \log_e Q}{\partial \psi^2} = 0 \quad (9)$$

Equation (9) determines the distribution of $\log_e Q$ in the $\varphi\psi$ -plane for incompressible flow.

CHANNEL-WALL GEOMETRY

After equation (7) or (9) has been solved to obtain the distribution of $\log_e Q$ in the transformed $\varphi\psi$ -plane (for the arbitrary specified variations in $\log_e Q$ with φ along the boundaries of constant ψ), the geometry of the channel walls in the physical xy -plane can be determined from the resulting distribution of flow direction θ .

Flow direction θ .—The distribution of flow direction θ along a streamline (constant ψ) is obtained from equation (6), which integrates to give

$$\theta = \int_{\psi} \rho \frac{\partial \log_e Q}{\partial \psi} d\psi \quad (10a)$$

where the subscript ψ indicates that the integration is taken along a line of constant ψ and where the constant of integration is selected to give a known value of θ at one value of φ along each streamline. The integrand in equation (10a) is obtained from the distribution of $\log_e Q$, which is known from the solution of equation (7) or (9).

The distribution of flow direction θ along a velocity-potential line (constant φ) is obtained from equation (5), which integrates to give

$$\theta = - \int_{\varphi} \frac{1}{\rho} \left(\frac{\partial \log_e \rho}{\partial \varphi} + \frac{\partial \log_e Q}{\partial \varphi} \right) d\varphi \quad (10b)$$

where the subscript φ indicates that the integration is taken along a line of constant φ and where the constant of integration is selected to give a known value of θ at one value of ψ along each velocity-potential line. As for equation (10a), the integrand in equation (10b) is known from the distribution of $\log_e Q$ obtained from the solution of equation (7) or (9).

Channel-wall coordinates.—The variation in x along a line of constant ψ in the $\varphi\psi$ -plane is given by

$$\frac{\partial x}{\partial \varphi} = \left(\frac{dx}{ds} \frac{ds}{d\varphi} \right)_{\psi}$$

which, combined with equations (2a) and (4), integrates to give

$$x = \int_{\psi} \frac{\cos \theta}{Q} d\varphi \quad (11a)$$

Likewise,

$$x = - \int_{\psi} \frac{\sin \theta}{\rho Q} d\psi \quad (11b)$$

$$y = \int_{\psi} \frac{\sin \theta}{Q} d\varphi \quad (11c)$$

$$y = \int_{\varphi} \frac{\cos \theta}{\rho Q} d\psi \quad (11d)$$

where the constants of integration are selected to give known values of x or y at one value of φ along each streamline or at one value of ψ along each velocity-potential line. Equations (11a) to (11d) determine the distribution of x and y in the transformed $\varphi\psi$ -plane or, which is the same thing, the shape of the streamlines and velocity-potential lines in the physical xy -plane. In particular, equations (11a) and (11c) when integrated along the boundaries of constant ψ in the $\varphi\psi$ -plane determine the shape of the channel walls.

Turning angle.—In general, if the prescribed velocity distribution along one channel wall differs from the distribution along the other wall, the channel deflects an amount $\Delta\theta$, which is the difference in flow direction far downstream and far upstream of the region in which the prescribed velocity

distribution varies. In part II it is shown that for incompressible flow the turning angle $\Delta\theta$ is given by

$$\Delta\theta = \theta_a - \theta_u \\ = - \int_{-\infty}^{\infty} \varphi \left[\left(\frac{\partial \log_e Q}{\partial \varphi} \right)_{1.0} - \left(\frac{\partial \log_e Q}{\partial \varphi} \right)_0 \right] d\varphi \quad (12)$$

where the subscript u refers to conditions upstream at infinity and where the subscripts 0 and 1.0 refer to the channel boundaries along which ψ equals 0 and 1.0, respectively. A similar equation will be given later for the case of linearized compressible flow.

LINEARIZED COMPRESSIBLE FLOW

The nonlinear differential equation (7) for the distribution of velocity in the $\varphi\psi$ -plane with compressible flow becomes linear and is considerably simplified if a linear variation in pressure with specific volume ($1/\rho$) is assumed. This linear relation between pressure and specific volume was first suggested by Chaplygin (ref. 6) in order to linearize the differential equations for two-dimensional compressible flow in the hodograph plane.

Density.—If a linear variation in pressure with specific volume is assumed, the density ρ^* is related to the velocity q^* by (appendix C)

$$\rho^* = (1 + q^{*2})^{-1/2} \quad (13)$$

where

$$\rho^* = k_1 \rho \quad (13a)$$

and

$$q^* = k_2 q \quad (13b)$$

where the constants k_1 and k_2 have been determined so that values of ρ given by equation (13) equal the values of ρ given by equation (8a) for any two selected values of q (designated by q_a and q_b). Thus,

$$k_1 = \frac{1}{\rho_a} \sqrt{\frac{1 - \left(\frac{\rho_a q_a}{\rho_b q_b} \right)^2}{1 - \left(\frac{q_a}{q_b} \right)^2}} \quad (14a)$$

and

$$k_2 = \frac{1}{q_b} \sqrt{\frac{\left(\frac{\rho_a}{\rho_b} \right)^2 - 1}{1 - \left(\frac{\rho_a q_a}{\rho_b q_b} \right)^2}} \quad (14b)$$

where ρ_a and ρ_b are determined by equation (8a) for the selected values of q_a and q_b , respectively. A discussion of the selection of q_a and q_b is given in appendix C. It will be noted that, if γ is equal to -1.0 , equation (8a) has the same form as equation (13).

Stream function and velocity potential.—For the case of linearized compressible flow it is convenient to define the stream function ψ^* and the velocity potential φ^* by

$$d\psi^* = \rho^* q^* dn \quad (15)$$

and

$$d\varphi^* = q^* ds \quad (16)$$

Continuity.—The continuity equation expressed in terms of φ^* and ψ^* becomes (appendix D)

$$\frac{\partial \log_e u}{\partial \varphi^*} + \frac{\partial \theta}{\partial \psi^*} = 0 \quad (17)$$

where

$$u = \frac{q^*}{1 + \sqrt{1 + q^{*2}}} \quad (18)$$

or, conversely,

$$q^* = \frac{2u}{1 - u^2} \quad (19)$$

Irrotational fluid motion.—The equation for irrotational fluid motion, expressed in terms of φ^* and ψ^* , becomes (appendix D)

$$\frac{\partial \log_e u}{\partial \psi^*} - \frac{\partial \theta}{\partial \varphi^*} = 0 \quad (20)$$

Differential equation for distribution of $\log_e u$.—The partial differential equation for the distribution of $\log_e u$ in the $\varphi^*\psi^*$ -plane is obtained by differentiating equations (17) and (20) with respect to φ^* and ψ^* , respectively, and combining to eliminate $\frac{\partial^2 \theta}{\partial \varphi^* \partial \psi^*}$. Thus

$$\frac{\partial^2 \log_e u}{\partial \varphi^{*2}} + \frac{\partial^2 \log_e u}{\partial \psi^{*2}} = 0 \quad (21)$$

Equation (21) determines the distribution of $\log_e u$ in the $\varphi^*\psi^*$ -plane for linearized compressible flow with a given value of q_a and for arbitrarily prescribed variations in $\log_e Q$, related to $\log_e u$ by equations (1), (13b), and (18), along the boundaries of constant ψ^* . Equation (21) is linear and is, like equation (9) for the case of incompressible flow, the equation of Laplace. Thus an incompressible flow solution for the distribution of $\log_e Q$ in the $\varphi\psi$ -plane is also a linearized compressible flow solution for the distribution of $\log_e u$ in the $\varphi^*\psi^*$ -plane. The transformation from the $\varphi\psi$ -plane is different, however, from the transformation from the $\varphi^*\psi^*$ -plane so that different channel shapes result in the xy -plane.

Flow direction θ .—The distribution of flow direction θ along a streamline (constant ψ^*) is obtained from equation (20), which integrates to give

$$\theta = \int_{\varphi^*} \frac{\partial \log_e u}{\partial \psi^*} d\varphi^* \quad (22a)$$

Likewise, the distribution of flow direction θ along a velocity-potential line (constant φ^*) is obtained from equation (17), which integrates to give

$$\theta = - \int_{\psi^*} \frac{\partial \log_e u}{\partial \varphi^*} d\psi^* \quad (22b)$$

Equations (22a) and (22b) for linearized compressible flow correspond to, and are used in the same manner as, equations (10a) and (10b) for the usual type of compressible or incompressible flow.

Channel-wall coordinates.—The variation in x along a line of constant ψ^* in the $\varphi^*\psi^*$ -plane is given by

$$\frac{\partial x}{\partial \varphi^*} = \left(\frac{dx}{ds} \frac{ds}{d\varphi^*} \right)_{\psi^*}$$

which combined with equations (2a) and (16) integrates to give

$$x = \int_{\varphi^*} \frac{\cos \theta}{q^*} d\varphi^* \quad (23a)$$

Likewise,

$$x = - \int_{\psi^*} \frac{\sin \theta}{\rho^* q^*} d\psi^* \quad (23b)$$

$$y = \int_{\varphi^*} \frac{\sin \theta}{q^*} d\varphi^* \quad (23c)$$

$$y = \int_{\psi^*} \frac{\cos \theta}{\rho^* q^*} d\psi^* \quad (23d)$$

Equations (23a) to (23d) determine the distribution of x and y in the transformed $\varphi^*\psi^*$ -plane or, which is the same thing, the shape of the streamline and velocity-potential lines in the physical xy -plane. In particular, equations (23a) and (23c), when integrated along the boundaries of constant ψ^* in the $\varphi^*\psi^*$ -plane, determine the shape of the channel walls. Equations (23a) to (23d) for linearized compressible flow correspond to, and are used in the same manner as, equations (11a) to (11d) for the usual type of compressible or incompressible flow.

Turning angle.—In part II it is shown that for linearized compressible flow the turning angle, or difference in flow direction far downstream and far upstream of the region in which the prescribed velocity distribution varies along the channel walls, is given by

$$\Delta \theta = \frac{-1}{\Delta \psi^*} \int_{-\infty}^{\infty} \varphi^* \left[\left(\frac{\partial \log_e u}{\partial \varphi^*} \right)_{\Delta \psi^*} - \left(\frac{\partial \log_e u}{\partial \varphi^*} \right)_0 \right] d\varphi^* \quad (24)$$

where $\Delta \psi^*$ is the value of ψ^* along the left boundary (channel wall) when faced in the direction of flow if the value of ψ^* along the right boundary is zero, and where the subscript $\Delta \psi^*$ refers to the boundary along which ψ^* is equal to $\Delta \psi^*$.

NUMERICAL PROCEDURE

The channel design method in part I of this report was developed for three types of fluid flow: (1) compressible, (2) incompressible, and (3) linearized compressible. Although the numerical procedures of the design method are similar for each type of fluid, the procedures differ in detail and are therefore considered separately in this section.

COMPRESSIBLE FLOW

The numerical procedure for channel design with compressible flow ($\gamma=1.4$, for example) is as follows:

(1) The velocity is specified as a function of arc length along that portion of the channel walls over which the velocity varies

$$q = q(s)$$

or q_a is specified and

$$Q=Q(s) \quad (25)$$

where s is arbitrarily equal to zero at that point along one channel wall where the velocity first begins to vary.

(2) The channel-wall boundaries of the flow field in the transformed $\varphi\psi$ -plane are straight, parallel lines of constant ψ extending indefinitely far upstream and downstream between φ equals $\pm\infty$, where φ is arbitrarily equal to zero at that point on the channel wall at which s is equal to zero. The value of ψ along the right channel wall when faced in the direction of flow (direction of positive φ) is arbitrarily set equal to zero in which case the value of ψ along the left channel wall ($\Delta\psi$) is obtained by integrating equation (3) across the channel at a position far downstream where flow conditions are uniform

$$\Delta\psi=\rho_a \quad (26)$$

(3) The distribution of $\log_e Q$ as a function of φ along the boundaries in the $\varphi\psi$ -plane is obtained by integrating equation (4) between limits so that

$$\varphi=\int_0^s Q ds=\varphi(s) \quad (27)$$

which together with equation (25) gives the distribution of $\log_e Q$ along the boundaries in the $\varphi\psi$ -plane

$$\log_e Q=f(\varphi) \quad (28)$$

The integration indicated by equation (27) is carried out numerically for arbitrary distributions of Q as a function of s .

(4) If the velocities prescribed along one channel wall differ from those along the other wall, the channel will, in general, turn the flow. This turning angle cannot be determined exactly for compressible flow until the channel design is completed. However, it will be shown that this turning angle is only slightly greater than that resulting for linearized compressible flow with the same prescribed velocity and with a suitable selection for q_a and q_b in equations (14a) and (14b). This latter turning angle for linearized compressible flow is given by equation (24), which can be integrated numerically for the arbitrary distribution of $\log_e u=f(\varphi)$ corresponding to equation (28).

(5) In order to solve equation (7) for the distribution of $\log_e Q$ in the $\varphi\psi$ -plane, it is convenient to eliminate the density terms from equation (7) by means of equation (8b). Thus, equation (7) becomes

$$A \frac{\partial^2 \log_e q}{\partial \varphi^2} + B \frac{\partial^2 \log_e q}{\partial \psi^2} + 4C \left(\frac{\partial \log_e q}{\partial \varphi} \right)^2 + 4D \left(\frac{\partial \log_e q}{\partial \psi} \right)^2 = 0 \quad (29)$$

where

$$A = \frac{1 - \frac{\gamma+1}{2} q^2}{\left(1 - \frac{\gamma-1}{2} q^2 \right)^{\frac{\gamma+1}{\gamma-1}}}$$

$$B=1.0$$

$$4C = \frac{-q^2 \left(1 + \frac{\gamma+1}{2} q^2 \right)}{\left(1 - \frac{\gamma-1}{2} q^2 \right)^{\frac{2\gamma}{\gamma-1}}}$$

and

$$4D = \frac{-q^2}{1 - \frac{\gamma-1}{2} q^2}$$

Equation (29) is nonlinear, and it can be solved by relaxation methods (refs. 4 and 7, for example). A grid of equally spaced points, at each of which the value of $\log_e Q$ is to be determined, is placed in the flow field between the channel-wall boundaries. The grid is extended upstream and downstream sufficiently far so that constant values of $\log_e Q$ are obtained across the channel by the relaxation methods. In the numerical examples to be presented six or eight grid spaces were used across the channel. In example III the number of grid spaces was reduced from eight to four with negligible effect on the resulting channel design. The values of $\log_e Q$ at each grid point were relaxed to five significant figures. If the same velocity distribution is prescribed along both walls, the channel is symmetrical so that the velocity distribution in only one half of the channel need be determined by relaxation methods.

(6) After $\log_e Q$ has been determined at each grid point in the $\varphi\psi$ -plane, the distribution of θ is determined by equations (10a) and (10b), which are integrated numerically. The constants of integration in equations (10a) and (10b) are determined to give a specified value of θ at one point in the channel (far upstream, for example). The integrands in equations (10a) and (10b) are determined by numerical methods (tables I to VII, ref. 4, for example) from the known values of ρ and $\log_e Q$ at each of the grid points. If it is desired to know the flow direction along the channel-walls only, equation (10a) can be solved along the channel-wall boundaries $\psi=0$ and $\psi=\Delta\psi$ only. If it is desired to know θ everywhere in the channel, the recommended procedure is to determine the variation in θ along the mean streamline ($\psi=(\Delta\psi)/2$) by equation (10a) and to determine the variation in θ along each velocity-potential line from the previously determined values on the mean streamline by equation (10b).

(7) After the distributions of $\log_e Q$ and θ are known in the $\varphi\psi$ -plane, the shapes of the streamlines and the velocity-potential lines in the physical xy -plane or, which is the same thing, the distributions of x and y in the transformed $\varphi\psi$ -plane are determined by the numerical integration of equations (11a) to (11d). The constants of integration in these equations are determined so that specified values of x and y occur at one point in the flow field. The recommended procedure is to determine the variation in x and y along the mean streamline by equations (11a) and (11c) and to determine the variation in x and y along each velocity-potential line for the previously determined values on the mean streamline by equations (11b) and (11d). If it is desired to know the x and y coordinates for the channel walls only, equations (11a) and (11c) can be solved along the channel-wall boundaries $\psi=0$ and $\psi=\Delta\psi$ only.

INCOMPRESSIBLE FLOW

The numerical procedure for channel design with incompressible flow ($\rho=1$) is similar to that just outlined for compressible flow, but with the following differences:

- (1) The velocity is specified as a function of arc length by equation (25) alone.
- (2) The value of ψ along the left channel wall ($\Delta\psi$) is equal to 1.0 instead of the value given by equation (26).
- (3) The distribution of $\log_e Q$ as a function of φ along the channel-wall boundaries in the $\varphi\psi$ -plane is the same as that obtained from equations (25) and (27) and given by equation (28).
- (4) The turning angle $\Delta\theta$ of the channel is given by equation (12).
- (5) The distribution of $\log_e Q$ in the $\varphi\psi$ -plane is obtained from the solution of equation (9) by relaxation methods.
- (6) After $\log_e Q$ has been determined at each grid point between the channel-wall boundaries in the $\varphi\psi$ -plane, the distribution of θ is determined by equations (10a) and (10b) as indicated previously for compressible flow, but with ρ equal to unity.
- (7) After the distributions of $\log_e Q$ and θ are known in the $\varphi\psi$ -plane, the shapes of the streamlines and velocity-potential lines in the physical xy -plane are determined by equations (11a) to (11d) as indicated previously for compressible flow, but with ρ equal to unity.

LINEARIZED COMPRESSIBLE FLOW

The numerical procedure for channel design with linearized compressible flow ($\gamma=-1.0$) is similar to that previously outlined for compressible flow, but with the following differences:

- (1) The velocity q is specified as a function of arc length along the channel walls by $q(s)$ or by q_a and equation (25). For each prescribed velocity, there are an infinite number of linearized compressible flow solutions depending on the selected values of q_a and q_b in equations (14a) and (14b). However, for values of q_a and q_b within the range of q prescribed along the channel walls (and therefore everywhere in the channel), the solutions, that is, channel shapes, probably differ only in small detail. The best solution is that most nearly like the nonlinear compressible solution with arbitrary value of γ (1.4, for example). In the numerical examples of this report it is shown that, if q_a and q_b are equal to the maximum and minimum values of q , a good solution results, at least if the ratio of these prescribed velocities is not too large (2:1 in the numerical examples). On the other hand, if continuity is to be satisfied for a gas with the correct value of γ (1.4, for example) upstream and downstream of the region of the channel in which the prescribed velocities vary, then q_a and q_b must equal q_u and q_d .

After q_a and q_b have been selected, the velocity distribution $q(s)$ is expressed as $q^*(s)$ by equation (13b) where k_2 is given by equation (14b) so that

$$q^*=q^*(s) \quad (30)$$

The velocity q^* is then expressed as u by equation (18) so that

$$u=u(s) \quad (31)$$

In the particular case where the selected value of q_a is equal to q_b , the value of k_2 is given by equation (C4b) in appendix C, where the significance of this particular case is also discussed.

- (2) The solution is obtained in the transformed $\varphi^*\psi^*$ -plane where φ^* and ψ^* are defined by equations (16) and (15), respectively. If the value of ψ^* along the right channel wall when faced in the direction of q^* is zero, the value of ψ^* along the left wall ($\Delta\psi^*$) is obtained by integrating equation (15) across the channel at a position far downstream where flow conditions are uniform

$$\Delta\psi^*=p_a^*q_a^* \quad (32)$$

- (3) The distribution of $\log_e u$ as a function of φ^* along the channel-wall boundaries in the $\varphi^*\psi^*$ -plane is obtained by integrating equation (16) between limits similar to those discussed previously for compressible flow so that

$$\varphi^*=\int_0^s q^* ds=\varphi^*(s) \quad (33)$$

which together with equation (31) determines the distribution of $\log_e u$ along the channel-wall boundaries in the $\varphi^*\psi^*$ -plane

$$\log_e u=f(\varphi^*) \quad (34)$$

- (4) The turning angle $\Delta\theta$ of the channel is given by equation (24).
- (5) The distribution of $\log_e u$ in the $\varphi^*\psi^*$ -plane is obtained from the solution of equation (21) by relaxation methods.
- (6) After $\log_e u$ has been determined at each grid point between the channel-wall boundaries in the $\varphi^*\psi^*$ -plane, the distribution of θ is determined by equations (22a) and (22b) in a manner similar to that outlined previously for compressible flow.
- (7) After the distributions of $\log_e u$ and θ are known in the $\varphi^*\psi^*$ -plane, the shapes of the streamlines and the velocity-potential lines in the physical xy -plane are determined by equations (23a) to (23d) in a manner similar to that outlined previously for compressible flow. The velocities q^* in equations (23) are obtained from the known values of u , and the densities ρ^* are given by equation (13).

NUMERICAL EXAMPLES

The channel design method has been applied in part I to the five examples listed below:

Examples	Type of channel	Type of flow
I	Reducing section	Incompressible
II	Converging section	Incompressible
III	Elbow	Incompressible
IV	Elbow	Linearized compressible
V	Elbow	Compressible ($\gamma=1.4$)

EXAMPLE I

The first numerical example is the design of a reducing section in a straight channel such that the upstream velocity is half the downstream velocity. The solution is for incompressible flow.

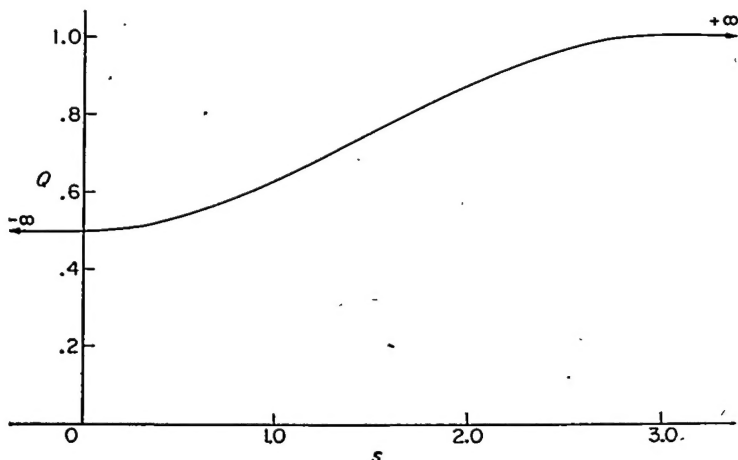


FIGURE 2.—Prescribed velocity distribution as function of arc length along channel wall for examples I, III, IV, and V. Equation (35).

Prescribed velocity distribution.—The prescribed velocity as a function of arc length s along both channel walls is given by

$$\left. \begin{aligned} Q &= 0.5 & (s \leq 0) \\ Q &= \frac{1}{2} + \frac{s^2}{6} - \frac{s^3}{27} & (0 \leq s \leq 3.0) \\ Q &= 1.0 & (s \geq 3.0) \end{aligned} \right\} \quad (35)$$

The prescribed velocity given by equation (35) is plotted in figure 2.

Equation (35) together with equation (27) results in

$$\left. \begin{aligned} \varphi &= 0.5s & (s \leq 0) \\ \varphi &= \frac{s}{2} + \frac{s^3}{18} - \frac{s^4}{108} & (0 \leq s \leq 3.0) \\ \varphi &= -0.75 + s & (s \geq 3.0) \end{aligned} \right\} \quad (36)$$

From equations (35) and (36), $\log_e Q$ is a known function of φ , which function is plotted in figure 3.

Results.—The results of example I are presented in figures 4 to 7.

In figure 4, lines of constant velocity Q and flow direction θ are plotted in the transformed $\varphi\psi$ -plane. The flow direction θ is constant and equal to zero along the mean streamline ($\psi=0.5$), indicating that the center line of the channel is straight. The maximum absolute values of θ occur along the channel walls. The solution is symmetrical about the mean streamline. The lines of constant Q and θ are orthogonal.

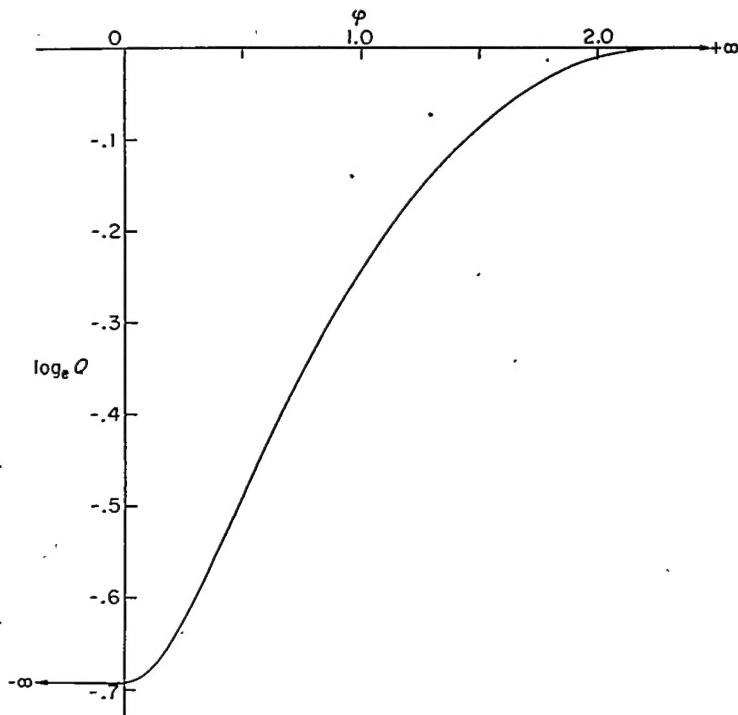


FIGURE 3.—Prescribed distribution of $\log_e Q$ as function of φ along channel walls for example I.

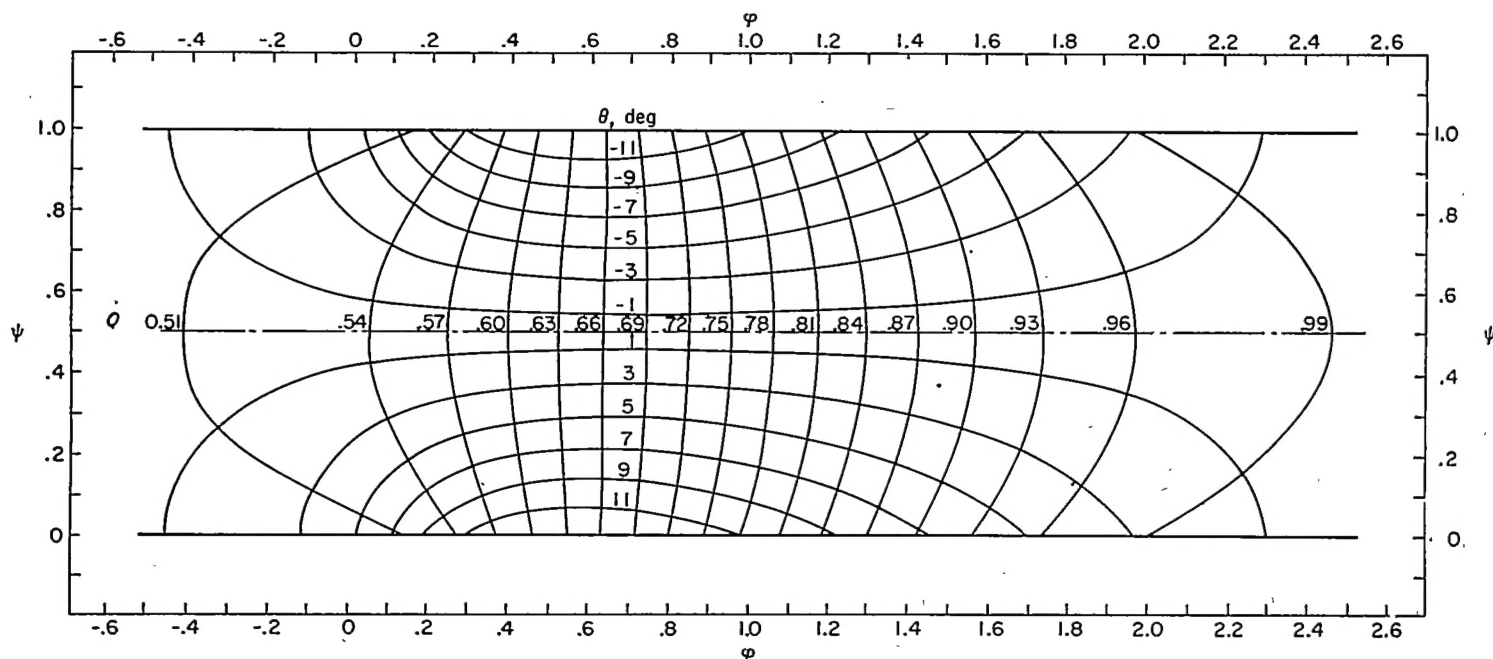
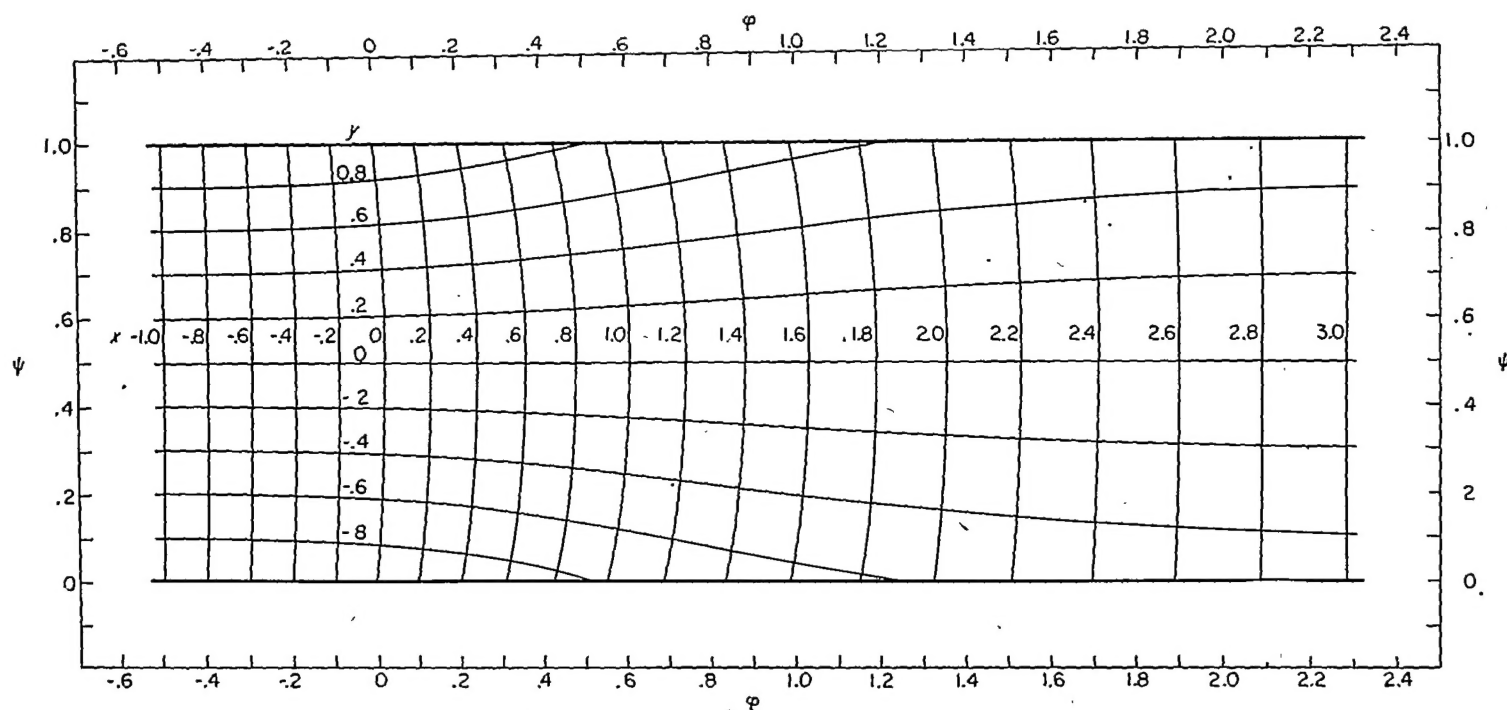
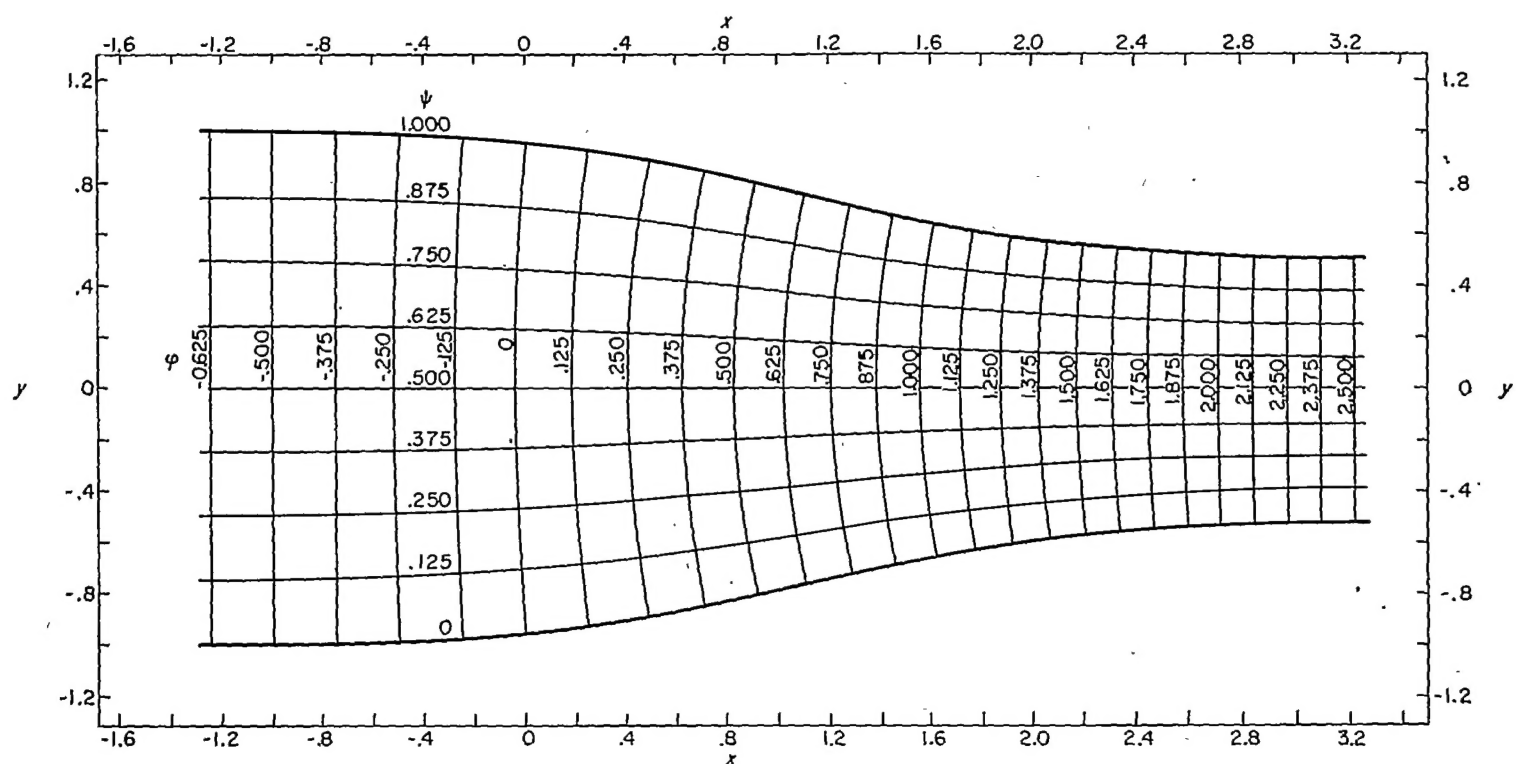


FIGURE 4.—Lines of constant velocity Q and flow direction θ in transformed $\varphi\psi$ -plane for example I. Incompressible flow; prescribed velocity given in figure 2.


 FIGURE 5.—Lines of constant x and y coordinates in transformed $\phi\psi$ -plane for example I. Incompressible flow; prescribed velocity given in figure 2.

 FIGURE 6.—Streamlines and velocity-potential lines on physical xy -plane for example I. Incompressible flow; prescribed velocity given in figure 2.

In figure 5, lines of constant x and y are plotted on the transformed $\phi\psi$ -plane. Along the mean streamline ($\psi=0.5$) the value of y is constant and equal to zero indicating, as before, that the center line of the channel is straight. The lines of constant x and y are orthogonal, and the system of curves forms a square network. The solution is symmetrical.

In figure 6, lines of constant ϕ and ψ (velocity potential and streamlines, respectively) are plotted in the physical xy -plane. The shape of the channel walls is that required to result in the prescribed velocity distribution given by equation (35) and plotted in figure 2. The downstream channel width is 1.0 by definition. The upstream channel width is 2.0 in order that the upstream velocity be half the down-

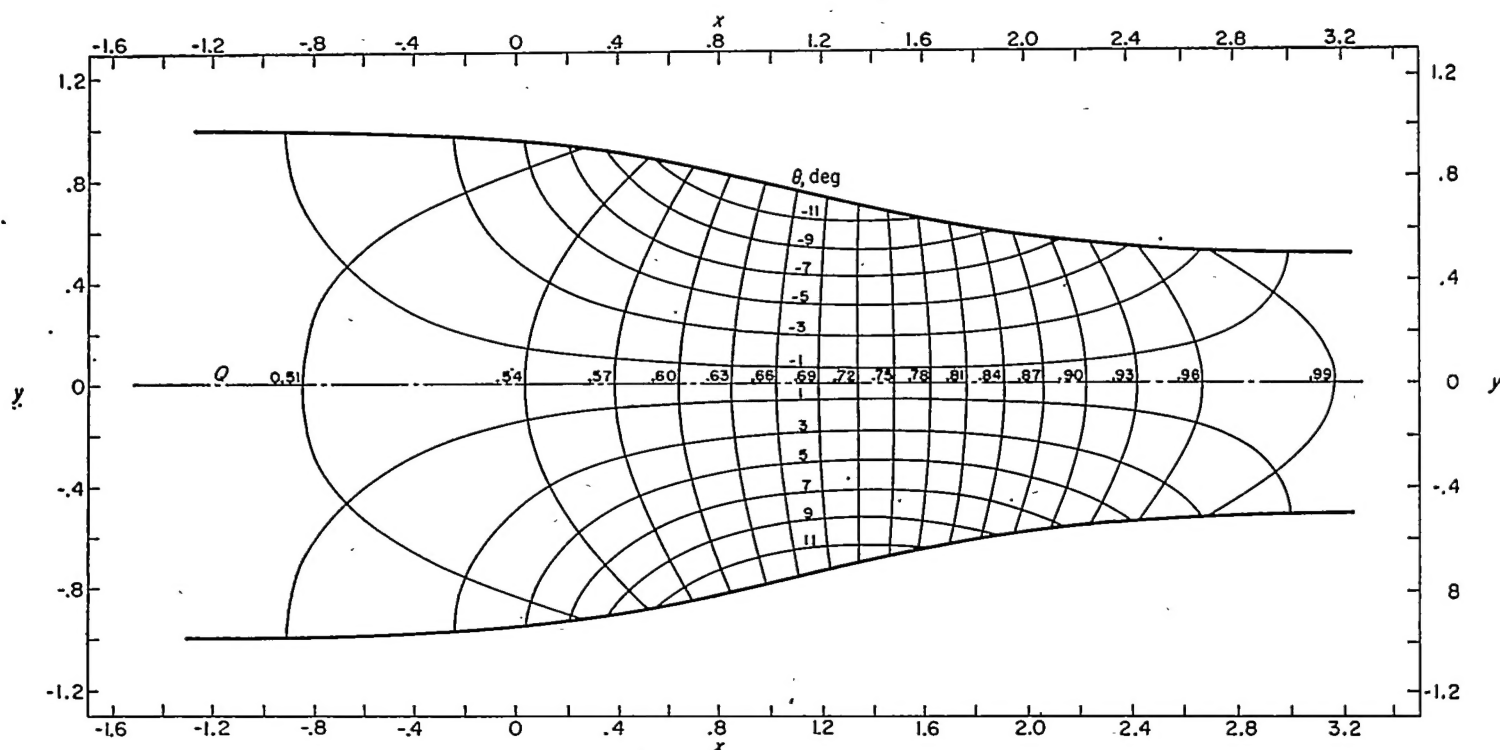


FIGURE 7.—Lines of constant velocity Q and flow direction θ in physical xy -plane for example I. Incompressible flow; prescribed velocity given in figure 2.

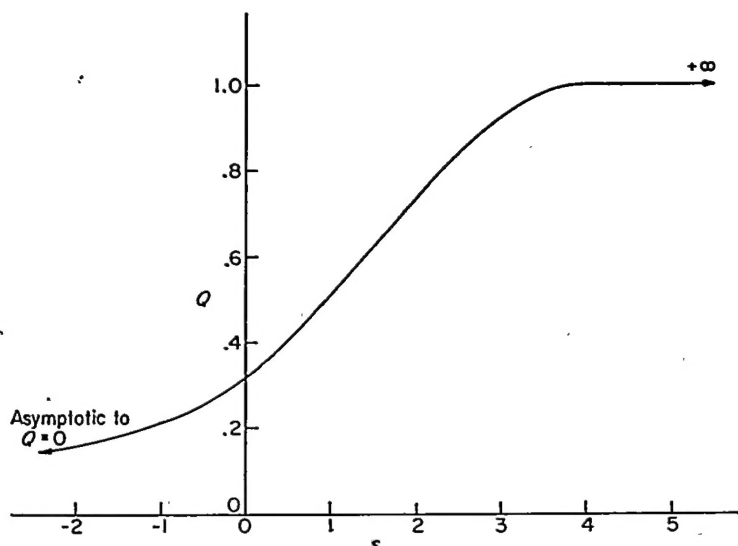


FIGURE 8.—Prescribed velocity distribution as function of arc length along channel wall for example II. Equation (38).

stream velocity. As usual, the streamlines and velocity potential lines are orthogonal and, with equal increments of φ and ψ , form a square network for incompressible flow.

In figure 7, lines of constant Q and θ are plotted in the physical xy -plane. The lines of constant Q and θ are orthogonal.

EXAMPLE II

The second numerical example is the design of a converging section that funnels the fluid from an infinite expanse into a

straight channel of unit width. Far upstream the channel walls are straight and converge at a 90° angle. The solution is for incompressible flow.

Prescribed velocity distribution.—The prescribed velocity as a function of arc length s along both channel walls is given by

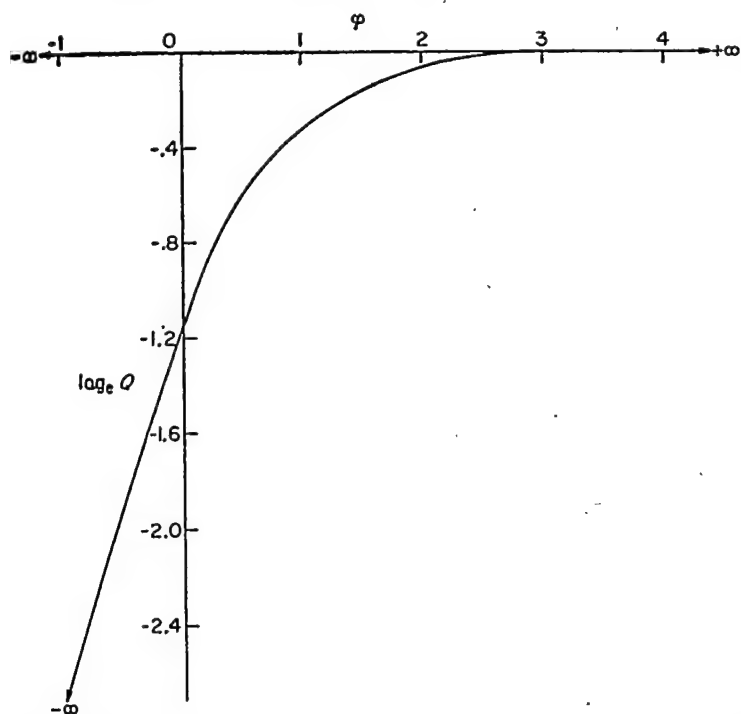
$$\left. \begin{aligned} Q &= \frac{-2}{\pi(s-2)} & (s \leq 0) \\ Q &= \frac{1}{\pi} + \frac{1}{2\pi}s - \frac{1}{8}\left(\frac{7}{2\pi} - \frac{3}{2}\right)s^2 + \frac{1}{32}\left(\frac{2}{\pi} - 1\right)s^3 & (0 \leq s \leq 4) \\ Q &= 1.0 & (s \geq 4) \end{aligned} \right\} \quad (37)$$

The prescribed velocity given by equation (37) is plotted in figure 8.

Equation (37) together with equation (27) results in

$$\left. \begin{aligned} \varphi &= \frac{-2}{\pi} \log_e \left(1 - \frac{s}{2}\right) & (s \leq 0) \\ \varphi &= \frac{1}{\pi}s + \frac{1}{2\pi}\frac{s^2}{2} - \frac{1}{8}\left(\frac{7}{2\pi} - \frac{3}{2}\right)\frac{s^3}{3} + \frac{1}{32}\left(\frac{2}{\pi} - 1\right)\frac{s^4}{4} & (0 \leq s \leq 4) \\ \varphi &= \frac{8}{3\pi} - 2 + s & (s \geq 4) \end{aligned} \right\} \quad (38)$$

From equations (37) and (38), $\log_e Q$ is a known function of φ , which function is plotted in figure 9.


 FIGURE 9.—Prescribed distribution of $\log_e Q$ as function of φ along channel walls for example II.

Results.—The results of example II are presented in figures 10 to 12.

In figure 10, lines of constant velocity Q and flow direction θ are plotted in the transformed $\varphi\psi$ -plane. The flow direction θ is constant and equal to zero along the mean streamline ($\psi=0.5$), indicating that the center line of the channel is straight. The solution is symmetrical about the mean streamline. As for example I, the lines of constant Q and θ are orthogonal.

In figure 11, lines of constant φ and ψ are plotted in the physical xy -plane. The shape of the channel walls is that

required to result in the prescribed velocity distribution given by equation (37) and plotted in figure 8. As usual, the streamlines and velocity-potential lines are orthogonal and, for incompressible flow with equal increments of φ and ψ , form a square network.

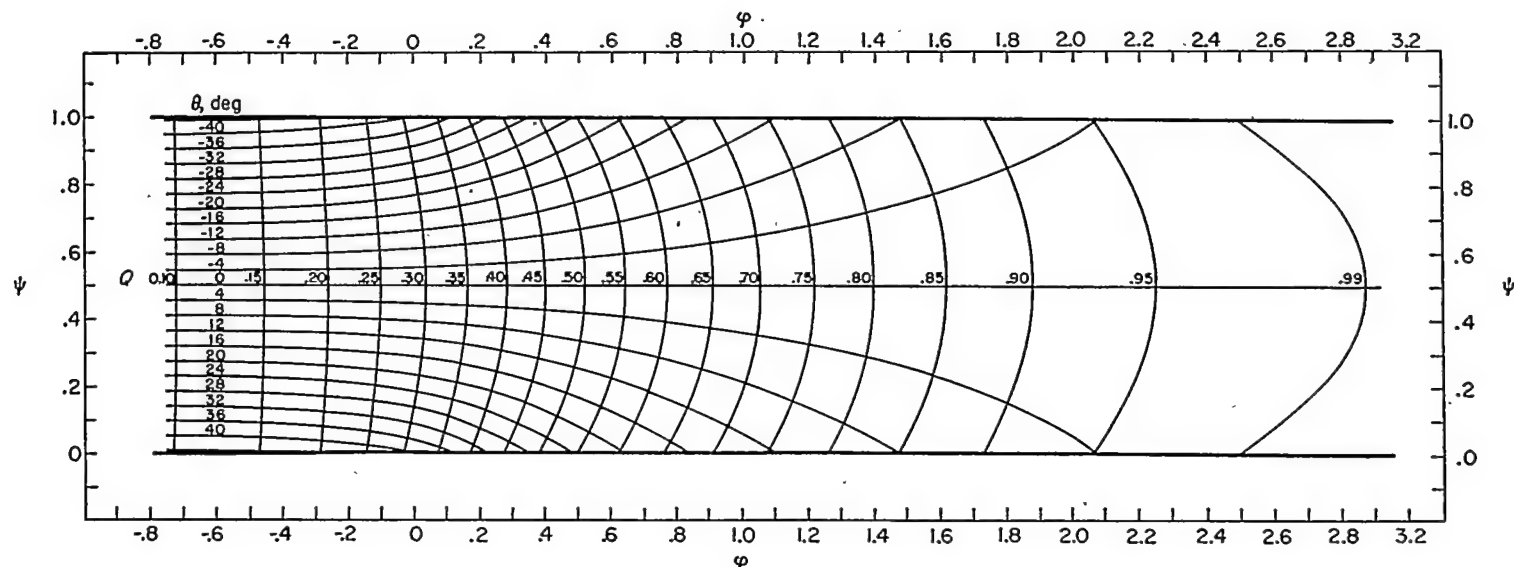
In figure 12, lines of constant Q and θ are plotted in the physical xy -plane. The lines of constant Q and θ are orthogonal.

EXAMPLE III

The third numerical example is the design of an elbow for which the upstream velocity is half the downstream velocity. The prescribed velocities are such that no deceleration occurs anywhere along the channel walls. The solution is for incompressible flow.

Prescribed velocity distribution.—Along both walls upstream of the elbow the velocity Q is equal to 0.5, and along both walls downstream of the elbow Q is equal to 1.0. The transition from Q equals 0.5 to 1.0 along both walls of the elbow will be the prescribed velocity distribution as a function of arc length given by equation (35) for example I and plotted in figure 2. In terms of $\log_e Q$ as a function of φ , this prescribed velocity distribution is given by equation (36) and is plotted in figure 3. Although this velocity distribution is the same for both walls, the distribution on the outer wall (wall with larger radii of curvature) is shifted in the positive φ direction an amount equal to 2.25 relative to the distribution on the inner wall. Thus, a velocity difference exists on the two walls at equal values of φ , as shown in figure 13. The greater this difference in velocity and the greater the range in φ over which velocity differences exist, the greater is the elbow turning angle. For the prescribed velocity distribution given in figure 13, the elbow turning angle given by equation (12) was 89.37° compared with a value of 89.36° obtained from the relaxation solution.

Results.—The results of example III are presented in figures 14 to 16 and in tables I and II. (The numerical


 FIGURE 10.—Lines of constant velocity Q and flow direction θ in transformed $\varphi\psi$ -plane for example II. Incompressible flow; prescribed velocity given in figure 8.

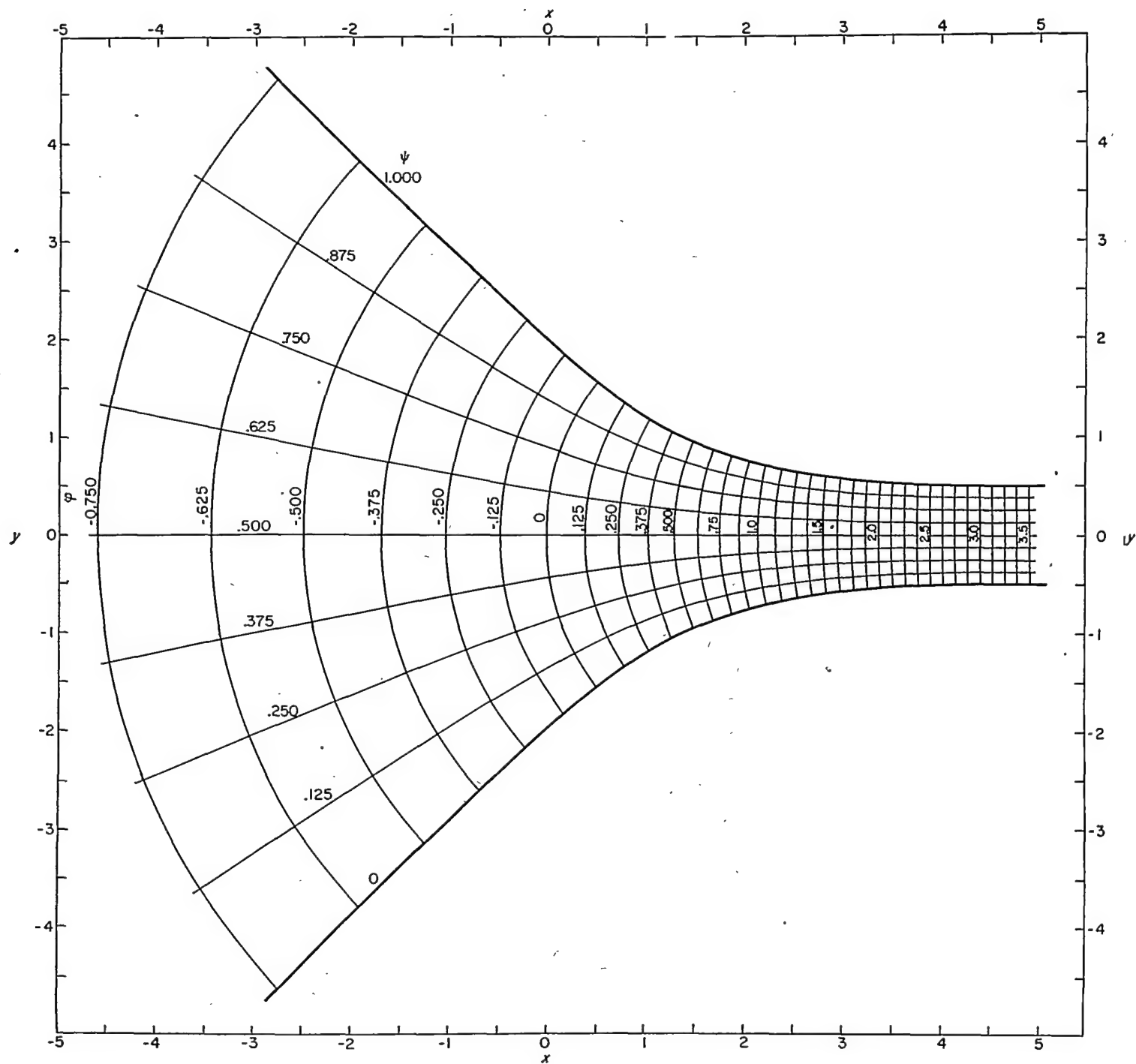


FIGURE 11.—Streamlines and velocity-potential lines in physical xy -plane for example II. Incompressible flow; prescribed velocity given in figure 8.

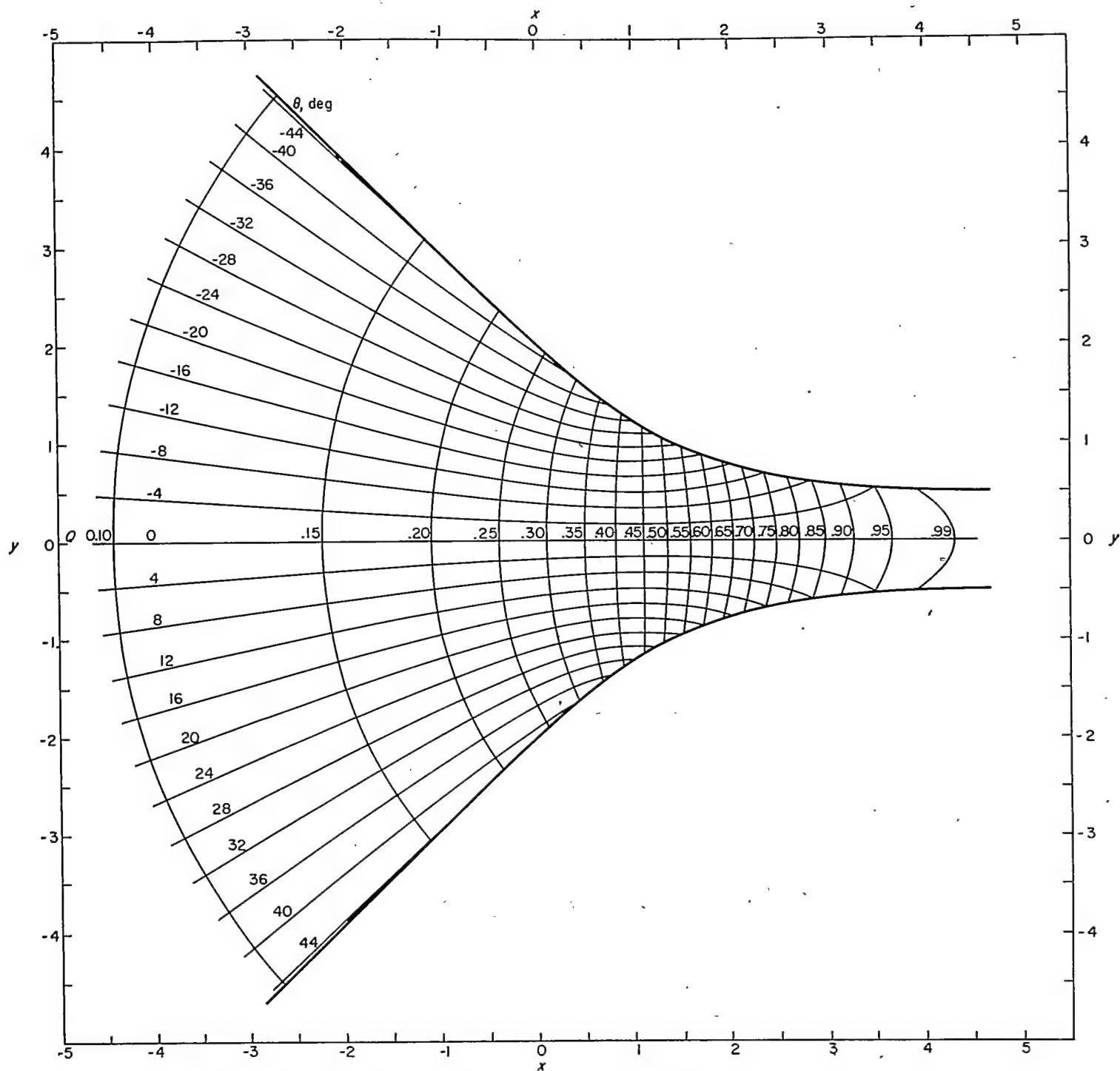


FIGURE 12.—Lines of constant velocity Q and flow direction θ in physical xy -plane for example II. Incompressible flow; prescribed velocity given in figure 8.

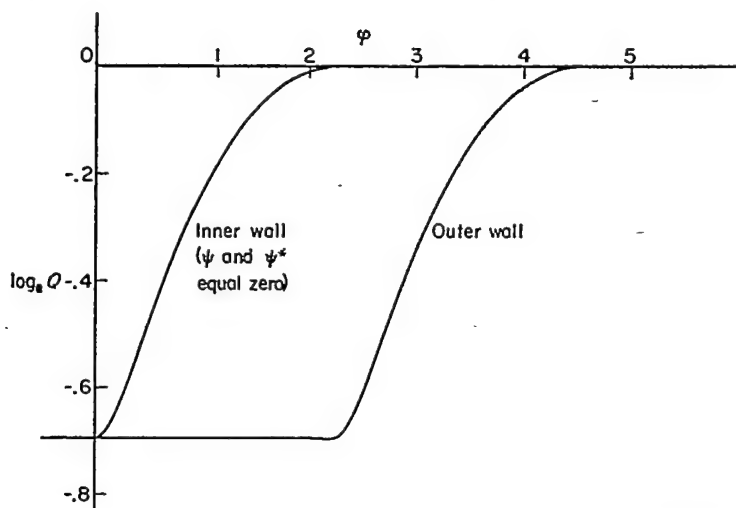


FIGURE 13.—Prescribed distribution of $\log_e Q$ as function of ϕ along channel walls for examples III, IV, and V.

results for examples III, IV, and V are tabulated in tables I to VI to enable a detailed comparison of the three elbow designs with the same prescribed velocity Q distribution as a function of arc length but with incompressible (example III), linearized compressible (example IV), and compressible (example V) flow.)

In figure 14, lines of constant Q and θ are plotted in the $\phi\psi$ -plane. The flow direction θ varies along the mean streamline ($\psi=0.5$), indicating that the channel is curved. The solution is unsymmetrical. As for examples I and II, the lines of constant Q and θ are orthogonal.

In figure 15, lines of constant ϕ and ψ are plotted in the physical xy -plane. The shape of the channel walls is that required to result in the prescribed velocity distribution given by equations (35) and (36) and plotted in figures 2 and 13. The upstream channel width is twice the downstream width in order that the upstream velocity be half the downstream velocity. It is interesting to note that, before curving in the direction of the elbow turning angle, the inner wall first curves in the opposite direction. This behavior of the inner-wall geometry is necessary in order to

maintain the prescribed constant velocity along the outer wall where the velocity would otherwise decelerate because of the necessary curvature in the direction of elbow turning. This feature of the elbow geometry will also be noted in examples IV and V. As usual, the streamlines and velocity-potential lines are orthogonal and, for equal increments of ϕ and ψ , form a square network.

In figure 16, lines of constant Q and θ are plotted in the physical xy -plane. The lines of constant Q and θ are orthogonal.

EXAMPLE IV

The fourth numerical example is the design of an elbow with the same prescribed velocity Q , as a function of arc length, used in example III but for linearized compressible flow ($\gamma=-1.0$).

Prescribed velocity distribution.—The prescribed velocity distribution Q is the same as that for example III and with q_a equal to 0.80176. The variation in Q with s along one channel wall is plotted in figure 2. The values of q_a and q_b in equations (14a) and (14b) are equal to q_a and q_b , or 0.40088 and 0.80176, respectively. For these values of q_a and q_b and for the prescribed velocity distribution with linearized compressible flow, the elbow turning angle given by equation (24) was 104.08° compared with a value of 104.07° obtained from the relaxation solution and a value of 89.36° obtained for incompressible flow (example III).

Results.—The results of example IV are presented in figures 17 to 19 and in tables III and IV.

In figure 17, lines of constant q and θ are plotted in the transformed $\phi^*\psi^*$ -plane. The solution is unsymmetrical and the lines of constant q and θ are orthogonal.

In figure 18, lines of constant $\phi^*/\Delta\psi^*$ and $\psi^*/\Delta\psi^*$ are plotted in the physical xy -plane (where the constant $\Delta\psi^*$ is given by equation (32) and is equal to 0.73782 for q_a equal to 0.80176). The shape of the channel walls is that required to result in the prescribed velocity distribution used in example III but with linearized compressible flow and for q_a equal to 0.80176. From continuity considerations the upstream channel width is 1.5385 times the downstream width. As in example III, the inner wall of the elbow first

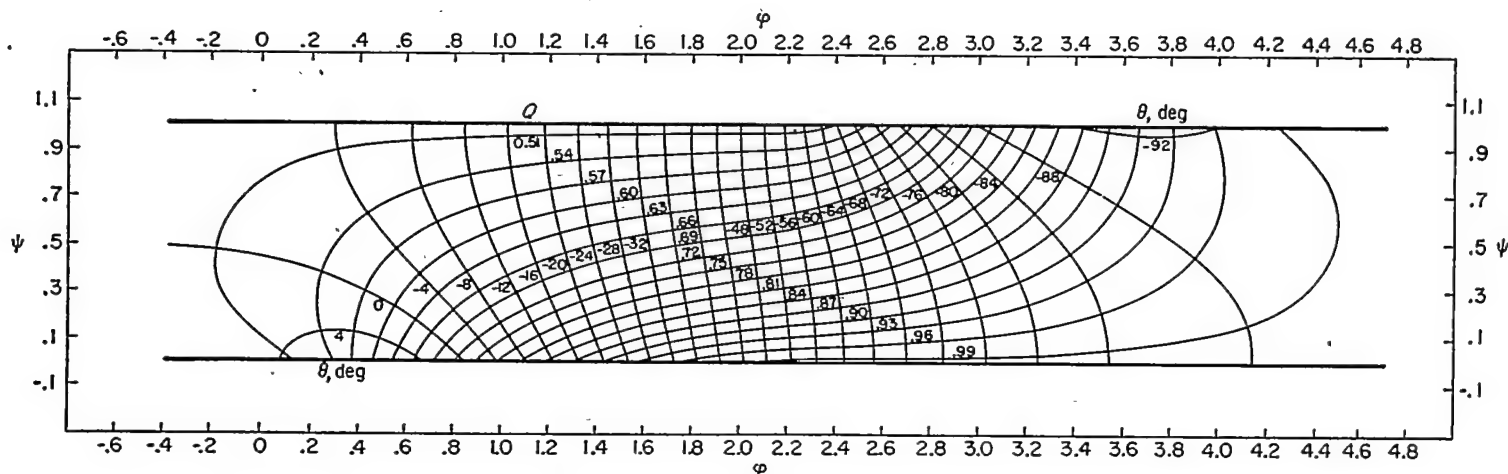


FIGURE 14.—Lines of constant velocity Q and flow direction θ in transformed $\phi\psi$ -plane for example III. Incompressible flow; prescribed velocity given in figures 2 and 13.

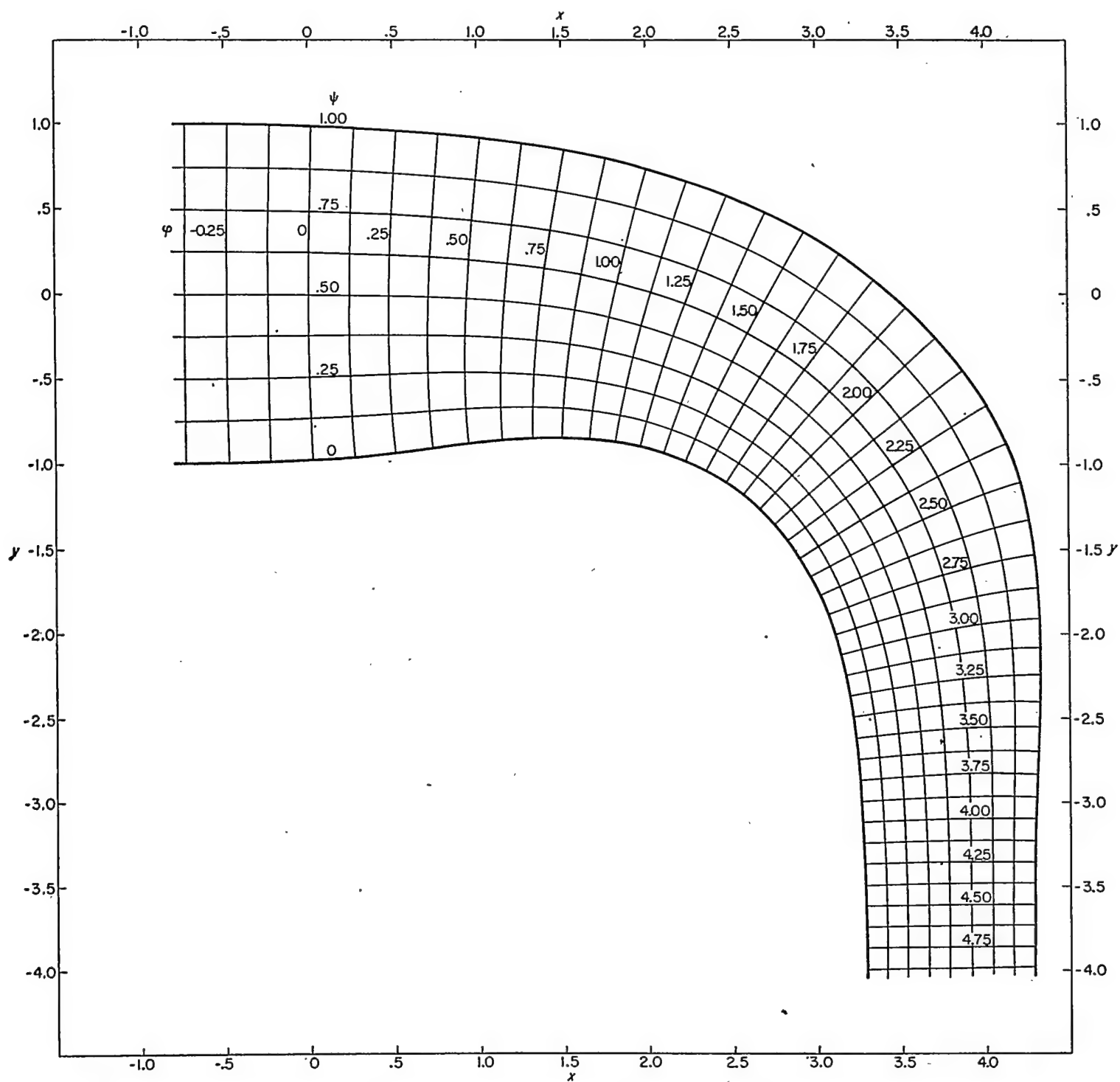


FIGURE 15.—Streamlines and velocity-potential lines in physical xy -plane for example III. Incompressible flow; prescribed velocity given in figures 2 and 13.

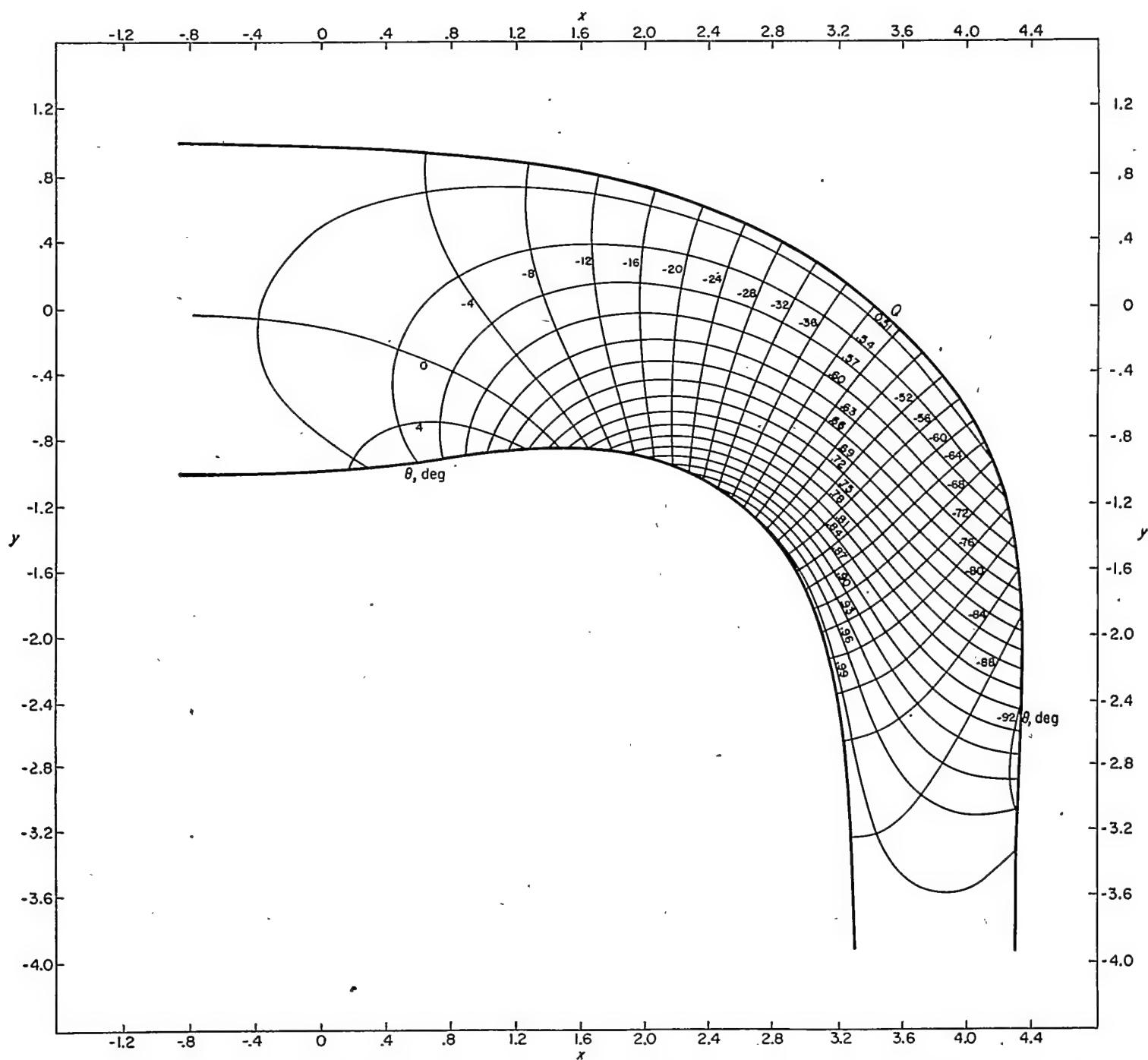


FIGURE 16.—Lines of constant velocity Q and flow direction θ in physical xy -plane for example III. Incompressible flow; prescribed velocity given in figures 2 and 13.

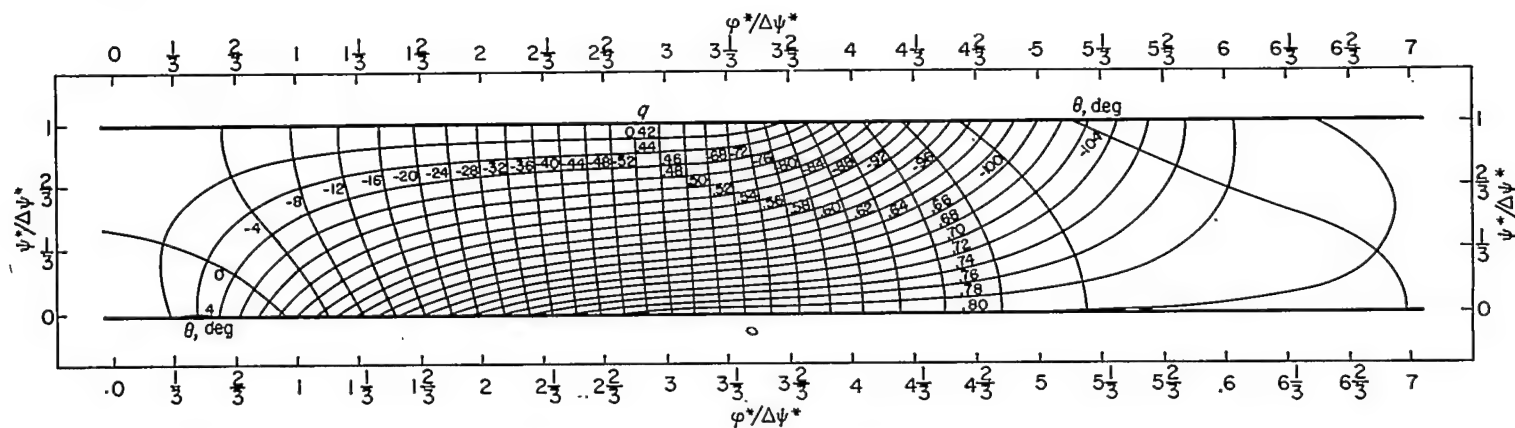


FIGURE 17.—Lines of constant velocity q and flow direction θ in transformed $\phi^*\psi^*$ -plane for example IV. Linearized compressible flow; prescribed velocity as function of arc length along channel walls same as for example III (fig. 2) and with q_a equal to 0.80176.

turns in the opposite direction to the elbow turning angle. As usual, the streamlines and velocity-potential lines are orthogonal.

In figure 19, lines of constant q and θ are plotted in the physical xy -plane. The lines of constant q and θ are not, in general, orthogonal.

EXAMPLE V

The fifth numerical example is the design of an elbow with the same prescribed velocity Q , as a function of arc length, used in examples III and IV but for compressible flow ($\gamma=1.4$).

Prescribed velocity distribution.—The prescribed velocity distribution Q is the same as that for examples III and IV but with q_a equal to 0.79927. The variation in Q with s along one channel wall is plotted in figure 2.

Results.—The results of example V are presented in figures 20 and 21 and in tables V and VI.

In figure 20, lines of constant $\phi/\Delta\psi$ and $\psi/\Delta\psi$ are plotted in the physical xy -plane (where the constant $\Delta\psi$ is given by equation (26) and is equal to 0.71054 for q_a equal to 0.79927). The shape of the channel walls is that required to result in the prescribed velocity distribution used in examples III and IV but with compressible flow ($\gamma=1.4$) and for q_a equal to 0.79927. The upstream channel width is 1.5412 times the downstream width, and the turning angle is 105.31° compared with 104.07° for linearized compressible flow (example IV) and 89.36° for incompressible flow (example III). The streamlines and velocity-potential lines are orthogonal.

The shape of the elbow for compressible flow (example V, fig. 20) is nearly the same as the shape of the elbow for linearized compressible flow (example IV, fig. 18). Therefore, in figure 21 the contours of the walls for both examples are compared. The difference in contours is very small and it is concluded that, if a nonviscous gas with arbitrary γ (1.4, for example) were to flow through a channel designed for linearized compressible flow ($\gamma=-1.0$), the resulting velocity distribution along the channel walls would be nearly the velocity distribution prescribed for the linearized compressible flow, at least if the linearized flow were selected (by the choice of q_a and q_b) so that the densities were equal for both types of flow at the maximum and minimum velocities

and if the ratio of these prescribed velocities is not too large (2:1 in the numerical examples). This conclusion is important because the design method for linearized compressible flow is considerably faster than the design method for compressible flow with γ other than -1.0 .

PART II

SOLUTION BY GREEN'S FUNCTION

In part II a method of solution for the design of two-dimensional channels with prescribed velocity distributions along the walls is developed by means of the appropriate Green's function. The method applies to incompressible and linearized compressible, irrotational flow. One numerical example is presented for an accelerating elbow with linearized compressible flow and with the same prescribed conditions as example IV of part I.

METHOD OF SOLUTION

The method of solution by Green's function is in conjunction with a formula derived from Green's theorem.

PRELIMINARY CONSIDERATIONS

Stream function Ψ .—In part II it is convenient to define the stream function by Ψ , where for incompressible flow

$$d\Psi = \frac{\pi}{2} d\psi \quad (39a)$$

and for linearized compressible flow ($\gamma=-1.0$)

$$d\Psi = \frac{\pi d\psi^*}{2\Delta\psi^*} \quad (39b)$$

For both types of flow Ψ varies from zero along the right side of the channel, when faced in the direction of flow, to $\pi/2$ along the left side.

Velocity potential Φ .—In part II it is convenient to define the velocity potential by Φ , where for incompressible flow

$$d\Phi = \frac{\pi}{2} d\phi \quad (40a)$$

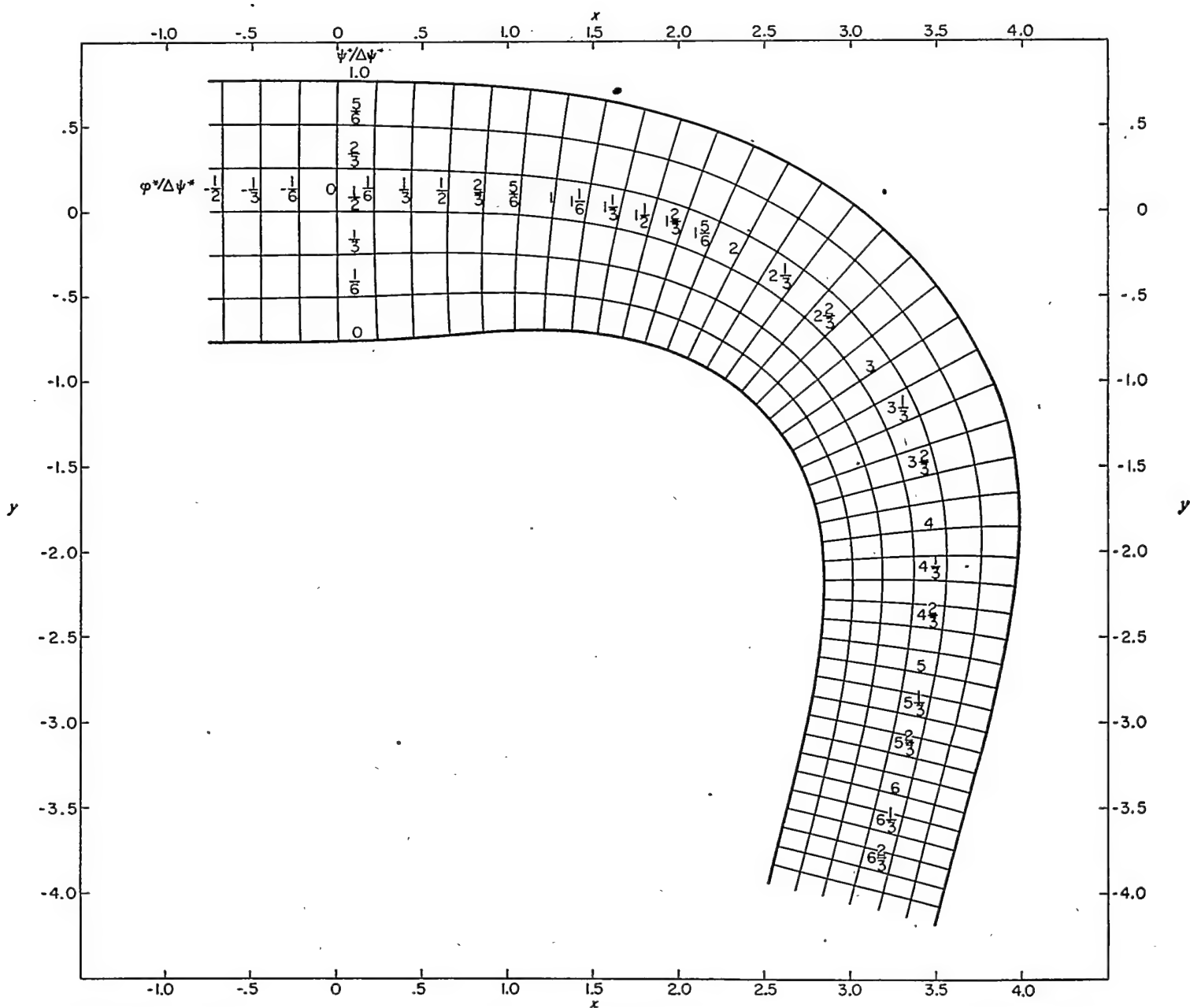


FIGURE 18.—Streamlines and velocity-potential lines in physical xy -plane for example IV. Linearized compressible flow; prescribed velocity as function of arc length along channel walls same as for example III (fig. 2) and with q_∞ equal to 0.80170.

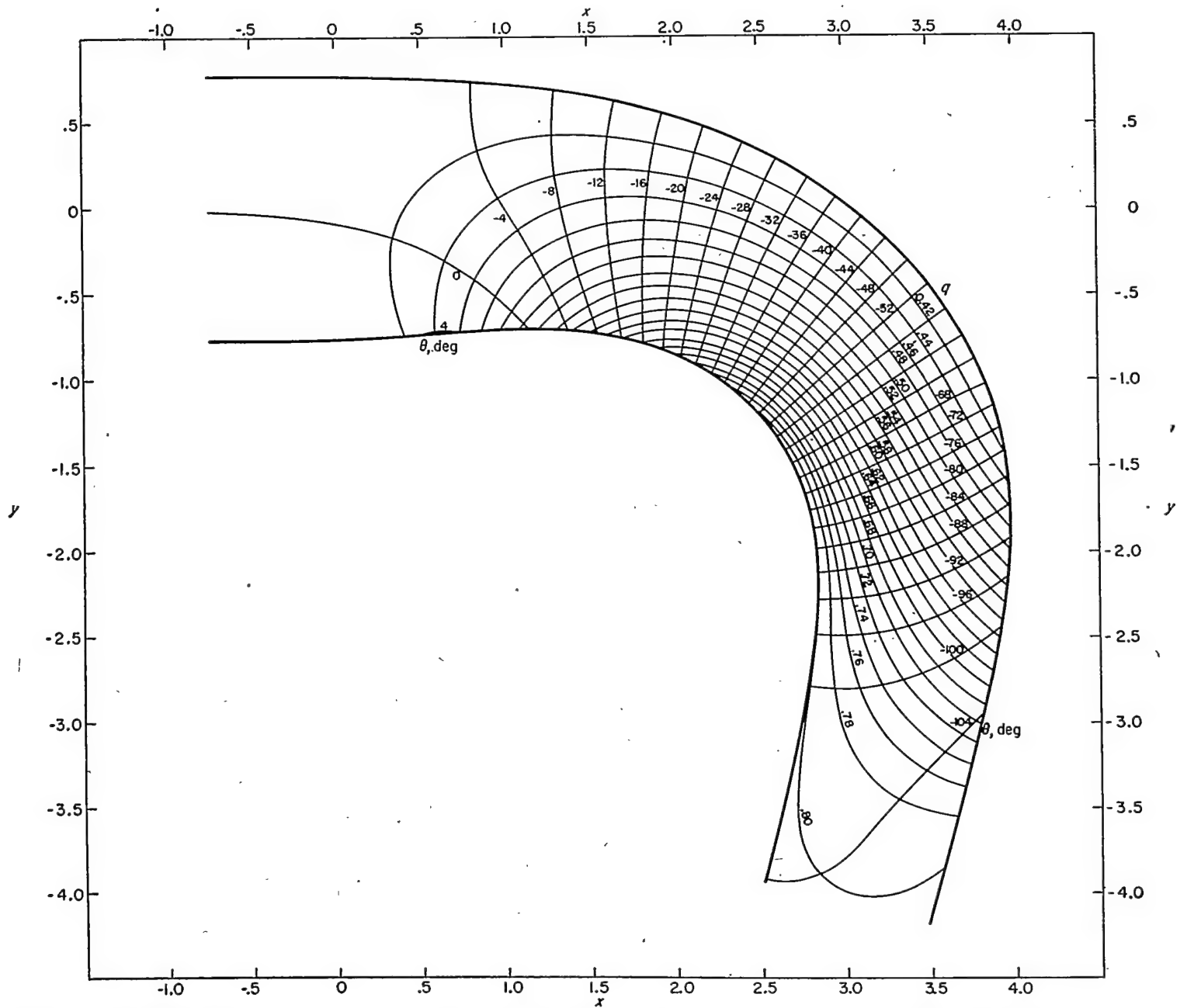


FIGURE 19.—Lines of constant velocity q and flow direction θ in physical xy -plane for example IV. Linearized compressible flow; prescribed velocity as function of arc length along channel walls same as for example III (fig. 2) and with q_0 equal to 0.80176.

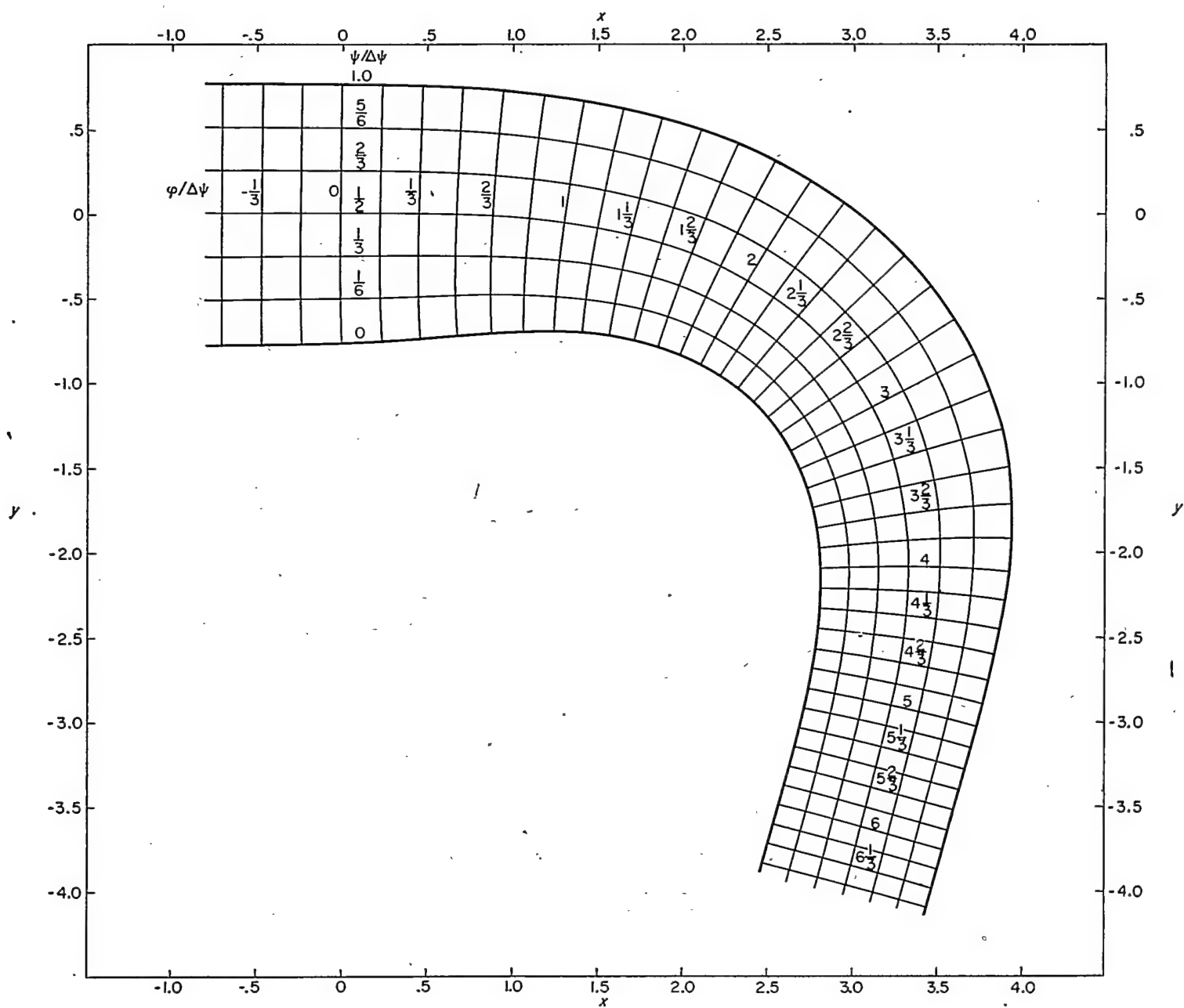


FIGURE 20.—Streamlines and velocity-potential lines in physical xy -plane for example V. Compressible flow ($\gamma=1.4$); prescribed velocity as function of arc length along channel walls same as for examples III and IV (fig. 2) but with g_s equal to 0.79927.

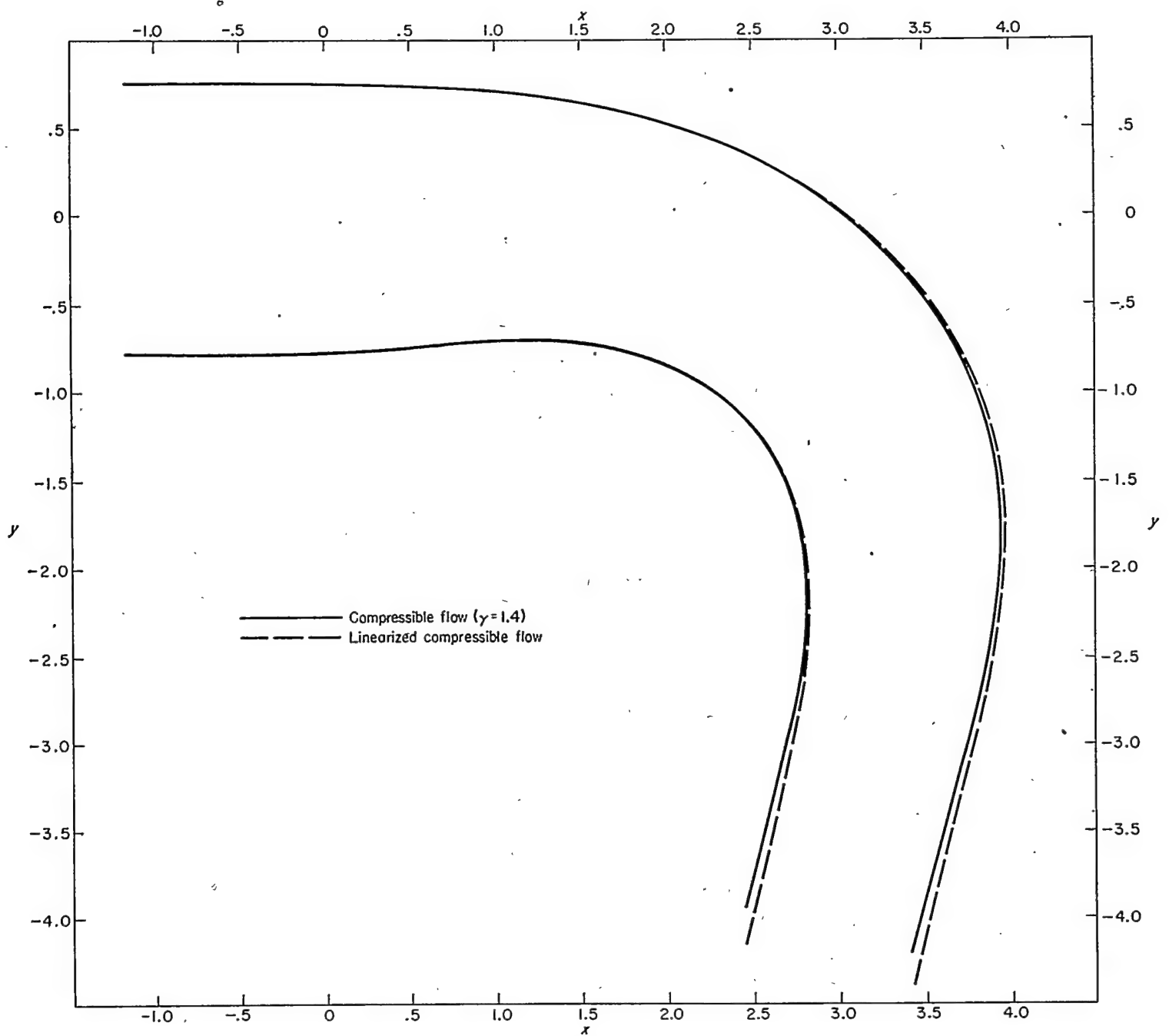


FIGURE 21.—Comparison of channel-wall shapes for compressible flow (example V) with γ equal to 1.4 and for linearized compressible flow (example IV) for same prescribed velocity as function of arc length along channel walls (fig. 2).

and for linearized compressible flow

$$d\Phi = \frac{\pi}{2} \frac{d\psi^*}{\Delta\psi^*} \quad (40b)$$

Channel-wall coordinates.—From part I the distribution of channel-wall coordinates x and y along the boundaries of constant Ψ equal to 0 and $\pi/2$ in the transformed $\Phi\Psi$ -plane is given by

$$x = \frac{2}{\pi} \Delta\psi^* \int_{\Psi}^{\pi/2} \frac{\cos \theta}{q^*} d\Phi \quad (41a)$$

and

$$y = \frac{2}{\pi} \Delta\psi^* \int_{\Psi}^{\pi/2} \frac{\sin \theta}{q^*} d\Phi \quad (41b)$$

for linearized compressible flow, and for incompressible flow is given by

$$x = \frac{2}{\pi} \int_{\Psi}^{\pi/2} \frac{\cos \theta}{Q} d\Phi \quad (42a)$$

and

$$y = \frac{2}{\pi} \int_{\Psi}^{\pi/2} \frac{\sin \theta}{Q} d\Phi \quad (42b)$$

where the constants of integration are selected to give known (specified) values of x or y at one value of Φ along each boundary. Because q^* and Q are known functions of Φ from the prescribed velocity as a function of arc length along the channel walls, the shape of the channel walls in the physical xy -plane is given by equation (41) or (42) if θ is determined as a function of Φ along the channel walls. In part II the solution for θ as a function of Φ along the channel walls in the $\Phi\Psi$ -plane is obtained by Green's function.

SOLUTION BY GREEN'S FUNCTION

Continuity.—From part I the continuity equation becomes in the transformed $\Phi\Psi$ -plane

$$\frac{\partial \log_e V}{\partial \Phi} + \frac{\partial \theta}{\partial \Psi} = 0 \quad (43a)$$

where for incompressible flow

$$V = Q \quad (43b)$$

and for linearized compressible flow

$$V = \frac{q^*}{1 + \sqrt{1 + q^{*2}}} \quad (43c)$$

Irrotational motion.—From part I the equation for irrotational motion becomes in the transformed $\Phi\Psi$ -plane

$$\frac{\partial \log_e V}{\partial \Psi} - \frac{\partial \theta}{\partial \Phi} = 0 \quad (44)$$

Integral equation for $\theta(\Phi_o, \Psi_o)$.—From equations (43a) and (44)

$$\frac{\partial^2 \theta}{\partial \Phi^2} + \frac{\partial^2 \theta}{\partial \Psi^2} = 0 \quad (45)$$

so that from appendix E the value of θ at a point (Φ_o, Ψ_o)

within, or on, the channel walls in the transformed $\Phi\Psi$ -plane is given by the integral equation

$$\theta(\Phi_o, \Psi_o) = \frac{-1}{2\pi} \int_{-\infty}^{\infty} \left[\left(G \frac{\partial \log_e V}{\partial \Phi} \right)_{\frac{\pi}{2}} - \left(G \frac{\partial \log_e V}{\partial \Phi} \right)_0 \right] d\Phi \quad (46)$$

where the subscripts 0 and $\frac{\pi}{2}$ refer to the channel-wall boundaries along which Ψ is 0 and $\frac{\pi}{2}$, respectively, and G is the Green's function of the second kind for the channel, which is an infinite strip of width $\frac{\pi}{2}$ extending in the Φ -direction to $\pm \infty$.

Green's function G .—The Green's function of the second kind G for the infinite channel in the $\Phi\Psi$ -plane is given along the channel-wall boundaries (Ψ equals 0 and $\frac{\pi}{2}$) by (appendix F)

$$G_{0 \text{ or } \frac{\pi}{2}} = -\log_e [\cosh^2(\Phi - \Phi_o) - \cos^2(\Psi - \Psi_o)] \quad (47)$$

where (Φ, Ψ) is any point on the channel-wall boundary and (Φ_o, Ψ_o) is the point in the channel or on the boundary at which θ is to be determined.

Numerical integration for $\theta(\Phi_o, \Psi_o)$.—From equations (46) and (47)

$$\begin{aligned} 2\pi\theta(\Phi_o, \Psi_o) = & \int_{-\infty}^{\infty} \left\{ \frac{\partial \log_e V}{\partial \Phi} \log_e [\cosh^2(\Phi - \Phi_o) - \right. \\ & \left. \sin^2 \Psi_o] \right\}_{\frac{\pi}{2}} d(\Phi - \Phi_o) - \\ & \int_{-\infty}^{\infty} \left\{ \frac{\partial \log_e V}{\partial \Phi} \log_e [\cosh^2(\Phi - \Phi_o) - \right. \\ & \left. \cos^2 \Psi_o] \right\}_0 d(\Phi - \Phi_o) \end{aligned} \quad (48)$$

in which the independent variable of integration has been changed from $d\Phi$ to $d(\Phi - \Phi_o)$ so that the origin, for purposes of integration, lies at Φ_o rather than $\Phi = 0$. If for small changes in $(\Phi - \Phi_o)$, that is, for small $\Delta\Phi$, the term $\frac{\partial \log_e V}{\partial \Phi}$ may be considered constant and equal to its average value over the interval $\Delta\Phi$, then

$$\frac{\partial \log_e V}{\partial \Phi} = \frac{\Delta \log_e V}{\Delta \Phi}$$

and equation (48) becomes

$$\begin{aligned} 2\pi\theta(\Phi_o, \Psi_o) = & \sum_{(\Phi - \Phi_o) = -\infty}^{\infty} \left\{ \frac{\Delta \log_e V}{\Delta \Phi} \int_{(\Phi - \Phi_o)}^{(\Phi - \Phi_o) + \Delta \Phi} \log_e [\cosh^2(\Phi - \Phi_o) - \right. \\ & \left. \sin^2 \Psi_o] d(\Phi - \Phi_o) \right\}_{\frac{\pi}{2}} - \\ & \sum_{(\Phi - \Phi_o) = -\infty}^{\infty} \left\{ \frac{\Delta \log_e V}{\Delta \Phi} \int_{(\Phi - \Phi_o)}^{(\Phi - \Phi_o) + \Delta \Phi} \log_e [\cosh^2(\Phi - \Phi_o) - \right. \\ & \left. \cos^2 \Psi_o] d(\Phi - \Phi_o) \right\}_0 \end{aligned} \quad (49)$$

where the summation sign is understood to mean that the quantity within the braces is summed over the entire range of $(\Phi - \Phi_0)$ between $\pm \infty$.

Equation (49) determines θ at any point in the flow field (channel). For a point (Φ_0, Ψ_0) on the channel walls Ψ_0 is equal to 0 or $\pi/2$ and the integrands in equation (49) become

$$2 \log_e \cosh |(\Phi - \Phi_0)|$$

or

$$2 \log_e \sinh |(\Phi - \Phi_0)|$$

so that equation (49) becomes

$$\pi\theta(\Phi_0, \Psi_0) = \sum_{(\Phi - \Phi_0)=-\infty}^{\infty} \left[\left(\frac{\Delta \log_e V}{\Delta \Phi} \Delta I \right)_{\frac{\pi}{2}} - \left(\frac{\Delta \log_e V}{\Delta \Phi} \Delta I \right)_0 \right] \quad (50a)$$

where

$$\Delta I = I_{(\Phi - \Phi_0) + \Delta \Phi} - I_{(\Phi - \Phi_0)} \quad (50b)$$

$$\left. \begin{aligned} I_{\frac{\pi}{2}} &= \alpha \text{ if } \Psi_0 = 0 \\ I_{\frac{\pi}{2}} &= \beta \text{ if } \Psi_0 = \frac{\pi}{2} \\ I_0 &= \alpha \text{ if } \Psi_0 = \frac{\pi}{2} \\ I_0 &= \beta \text{ if } \Psi_0 = 0 \end{aligned} \right\} \quad (50c)$$

where

$$\alpha = \pm \int_0^{|\Phi - \Phi_0|} \log_e \cosh |(\Phi - \Phi_0)| d|(\Phi - \Phi_0)| \quad (50d)$$

$$\beta = \pm \int_0^{|\Phi - \Phi_0|} \log_e \sinh |(\Phi - \Phi_0)| d|(\Phi - \Phi_0)| \quad (50e)$$

where the + signs apply for positive values of $(\Phi - \Phi_0)$ and the - signs apply for negative values of $(\Phi - \Phi_0)$. Methods of evaluating α and β are given in appendix G, and tabulated values are given for a wide range of $|(\Phi - \Phi_0)|$ in table VII. Equation (50a) determines $\theta(\Phi_0, \Psi_0)$ at any point on the channel-wall boundaries. Thus from equations (41a) and (41b) or (42a) and (42b) the coordinates for the channel-wall shape in the physical xy -plane can be determined.

NUMERICAL PROCEDURE

The numerical procedure for the channel design solution by Green's function is the same, except for minor details, for incompressible and linearized compressible flow. The stepwise procedure is outlined as follows:

(1) For incompressible flow the velocity Q and for linearized compressible flow the velocity q , or which is the same thing the velocity Q and the constant downstream velocity q_∞ , are specified as functions of arc length along the channel walls

$$Q = Q(s) \quad (51a)$$

or

$$q = q(s) \quad (51b)$$

where s is arbitrarily equal to 0 at that point along one channel wall where the velocity first begins to vary.

(2) Compute V as a function of s from equations (43b) and (51a) for incompressible flow or from equations (13b), (14b), (43c), and (51b) for linearized compressible flow

$$V = V(s) \quad (52)$$

(3) Compute Φ as a function of s from equations (4) and (40a) for incompressible flow or from equations (16), (32), (40b), and (51b) for linearized compressible flow. In equation (32) ρ_a^* is obtained from equations (8a), (13a), and (14a). For arbitrary distributions of Q or q equation (40a) or (40b) is integrated numerically by using, for example, Simpson's one-third rule. Thus

$$\Phi = \Phi(s) \quad (53)$$

(4) From equations (52) and (53) V and Φ are known functions of s so that

$$V = V(\Phi) \quad (54)$$

Thus V is a known function of Φ along the channel-wall boundaries in the transformed $\Phi\Psi$ -plane.

(5) If the prescribed velocity distribution along one wall is different from that along the other, the channel will, in general, turn the flow. This turning angle $\Delta\theta$ is given by equation (H5) in appendix H. If the turning angle is unsatisfactory, a new distribution of velocity as a function of s (eqs. (51a) and (51b)) is prescribed and steps (1) to (5) repeated until the desired value of $\Delta\theta$ is obtained. Equation (H5) is integrated numerically by using Simpson's one-third rule, for example, and equation (54).

(6) The channel-wall boundaries are straight parallel lines of constant Ψ equal to 0 and $\pi/2$, and extending to $\pm \infty$ in the Φ -direction. Along these boundaries of constant Ψ , a series of equally spaced points are located at each of which the flow direction θ and the x, y -coordinates of the channel walls will be determined by numerical integration. In order to use the tables of α and β presented in this report, the point spacing $\Delta\Phi$ must be an even multiple of $\pi/24$. Thus the smallest point spacing $\pi/24$ is equal to $1/2$ of the channel width ($\pi/2$). For a particular prescribed velocity distribution along the channel walls the accuracy of the solution increases, and so does the amount of computing, as the point spacing is reduced. The error for a given point spacing depends on the prescribed velocity distribution, and its order of magnitude is given by the leading term of the error series of the formula used for numerical integration (table VIII, ref. 4, for example). For the numerical example presented in part II of this report the point spacing $\Delta\Phi$ was $\pi/12$. From equation (54)

$$\frac{\Delta \log_e V}{\Delta \Phi} = \frac{(\log_e V)_{\Phi + \Delta \Phi} - (\log_e V)_{\Phi}}{\Delta \Phi} \quad (55)$$

where the subscripts Φ and $\Phi + \Delta\Phi$ refer to adjacent points along the channel boundaries.

(7) The value of θ at each point (Φ_0, Ψ_0) on the channel-wall boundaries is obtained from equation (50a) in which $(\Delta \log_e V)/\Delta\Phi$ is given by equation (55) and ΔI is given by equations (50b), (50c), and table VII. Note that in equation

(50a) the origin has been moved to Φ_0 by changing from Φ to $(\Phi - \Phi_0)$. Thus the value of $(\Delta \log_e V)/\Delta \Phi$ for a given value of $(\Phi - \Phi_0)$ varies with Φ_0 .

(8) The physical x, y -coordinates at each point on the channel-wall boundaries are obtained by the numerical integration of equations (42a) and (42b) for incompressible flow, or equations (41a) and (41b) for linearized compressible flow where $\Delta \psi^*$ is given by equation (32). The constants of integration in equations (41) and (42) are selected to give known values of x and y at upstream or downstream positions where flow conditions can be considered uniform.

NUMERICAL EXAMPLE

The channel design method of part II has been applied to the design of an elbow for the same conditions as example IV of part I. The design is for an accelerating elbow with no local decelerations of the prescribed velocities along the channel walls and with linearized compressible flow.

Prescribed velocity distribution.—The prescribed velocity distribution along the channel walls is the same as that for example IV of part I. The prescribed velocity as a function of Φ is plotted in figure 22.

Results.—As indicated in table VIII, the elbow design resulting from the prescribed velocities given in figure 22 is the same as that obtained by relaxation methods (fig. 21) for the same prescribed conditions (example IV, part I).

The solution obtained by Green's function (part II) required one experienced computer 3 days, whereas the solution by relaxation methods (part I) required about 10 days. The relaxation solutions provide additional information, such as the distribution of velocity across the channel; but for the most part this additional information is of secondary importance, and the design of channels by Green's function is more rapid and therefore to be preferred over the design by relaxation methods.

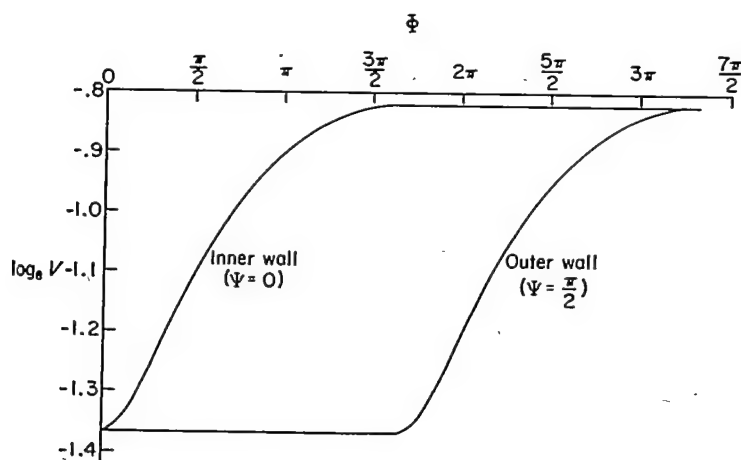


FIGURE 22.—Variation in prescribed values of $\log_e V$ with Φ along channel walls of numerical example in part II.

SUMMARY OF RESULTS AND CONCLUSIONS

A general method of design is developed for two-dimensional unbranched channels with prescribed velocities as a function of arc length along the channel walls. The method is developed for both compressible and incompressible, irrotational, nonviscous flow and applies to the design of elbows, diffusers, nozzles, and so forth. Two types of compressible flow are considered: the general type with arbitrary value for the ratio of specific heats γ (1.4, for example) and the linearized type in which γ is equal to -1.0 . In part I solutions are obtained by relaxation methods on a transformed plane the coordinates of which are the streamlines and velocity-potential lines in the physical plane; in part II solutions are obtained by a Green's function. The method of solution in part I gives complete information concerning the flow throughout the channel, whereas the method of solution in part II gives the channel-wall coordinates only.

Five numerical examples are given in part I and the results are presented by (1) lines of constant velocity and flow direction or lines of constant physical coordinates in the transformed plane and (2) streamlines and velocity-potential lines or lines of constant velocity and flow direction in the physical plane. Among the five examples are three elbow designs for the same prescribed velocity as a function of arc length along the channel walls but with incompressible, linearized compressible, and compressible flow. The numerical results of these three elbow designs are tabulated to enable a detailed comparison of the three designs.

The shapes of the elbows for compressible flow and for linearized compressible flow are very nearly the same; and it is concluded that, if a nonviscous gas with arbitrary γ (1.4, for example) were to flow through a channel designed for linearized compressible flow ($\gamma = -1.0$), the resulting velocity distribution along the channel walls would be nearly the velocity distribution prescribed for the linearized compressible flow. This conclusion is important because the design method for linearized compressible flow is considerably faster than that for compressible flow.

One numerical example is presented in part II for an accelerating elbow with linearized compressible flow. The elbow shape obtained from the solution by Green's function in part II is the same as that obtained from a solution by relaxation methods in part I for the same prescribed conditions. The time required for the calculations was considerably less for the solution by Green's function.

LEWIS FLIGHT PROPULSION LABORATORY

NATIONAL ADVISORY COMMITTEE FOR AERONAUTICS

CLEVELAND, OHIO, July 25, 1951

APPENDIX A

SYMBOLS

The following symbols are used in this report:

A, B, C, D	coefficients, equation (29)	θ	flow direction in physical xy -plane (measured in counterclockwise direction from positive x -axis)
A, B	arbitrary constants, equation (C1a)	$\Delta\theta$	channel turning angle, equation (12)
B_1, B_2, \dots	Bernoulli's numbers	ρ	density (expressed as ratio of stagnation density)
c	constant, equation (E3)	ρ^*	density in linearized compressible flow and related to ρ by equation (13a)
G	Green's function of the second kind, equations (E2) and (47)	Φ	velocity potential used as Cartesian coordinate in transformed $\Phi\Psi$ -plane and related to φ or φ^* by equation (40a) or (40b), respectively
I	integral (α or β)	φ and φ^*	velocity potential for incompressible and linearized compressible flow, respectively, equations (4) and (16)
k_1	coefficient, equation (14a)	Ψ	stream function used as Cartesian coordinate in transformed $\Phi\Psi$ -plane and related to ψ or ψ^* by equation (39a) or (39b), respectively
k_2	coefficient, equation (14b)	ψ and ψ^*	stream function for incompressible and linearized compressible flow, respectively, equations (3) and (15)
l	length of closed boundary	$\Delta\psi^*$	boundary value of ψ^* , for linearized compressible flow, along left channel wall when faced in the direction of flow, equation (32)
n	distance in xy -plane measured normal to direction of flow (expressed as ratio of characteristic length equal to channel width downstream at infinity)	ω	any harmonic function in $\Phi\Psi$ -plane
p	static pressure (expressed as ratio of stagnation density multiplied by stagnation speed of sound squared)	Subscripts:	
Q	velocity (expressed as ratio of characteristic velocity equal to constant channel velocity downstream at infinity)	a, b	quantities related to two velocities (q_a and q_b , respectively) for which density given by equation (8a) is equal to density ρ given by equations (13), (13a), and (13b)
q	velocity (expressed as ratio of stagnation speed of sound)	d	conditions downstream at infinity
q^*	velocity used in linearized compressible flow and related to q by equation (13b)	o	point in $\Phi\Psi$ -plane at which θ is determined
r	distance from any point in $\Phi\Psi$ -plane to point (Φ_o, Ψ_o) at which logarithmic singularity exists	u	conditions upstream at infinity
s	distance in xy -plane measured along direction of flow (expressed as ratio of characteristic length equal to channel width downstream at infinity)	$\Delta\psi^*$	left channel wall, when faced in direction of flow, along which ψ^* is equal to $\Delta\psi^*$
u	velocity parameter related to q^* by equation (18)	$(\Phi - \Phi_o)$	point at $(\Phi - \Phi_o)$ on either channel-wall boundary
V	velocity parameter defined by equations (43b) and (43c) for incompressible and linearized compressible flow, respectively	$(\Phi - \Phi_o) + \Delta\Phi$	point at $[(\Phi - \Phi_o) + \Delta\Phi]$ on either channel-wall boundary
w, w_1, w_2	complex functions defined by equations (F3), (F1a), and (F2a), respectively	$\varphi, \psi, \varphi^*, \psi^*$	along lines of constant φ, ψ, φ^* , and ψ^* , respectively
x, y	Cartesian coordinates in physical plane (expressed as ratios of characteristic length equal to channel width downstream at infinity)	0	right channel wall, when faced in direction of flow, along which Ψ, ψ , or ψ^* is equal to 0
z	complex coordinate, equation (F1b)	1.0	left channel wall, when faced in direction of flow, along which ψ is equal to 1.0
\bar{z}	conjugate of z	$\frac{\pi}{2}$	left channel wall, when faced in direction of flow, along which Ψ is equal to $\frac{\pi}{2}$
α	integral, equation (50d)		
β	integral, equation (50e)		
γ	ratio of specific heats		
Δ	finite increment		
δ	increment of		

APPENDIX B

EQUATIONS OF CONTINUITY AND IRROTATIONAL FLUID MOTION IN TERMS OF TRANSFORMED φ, ψ -COORDINATES

Consider the two-dimensional irrotational motion of a fluid particle in the physical xy -plane. The fluid particle is defined by adjacent streamlines (constant ψ) and velocity-potential lines (constant φ) spaced δn and δs apart as indicated in figure 23. The velocity Q is parallel to the streamlines and normal to the velocity-potential lines.

Continuity.—From continuity considerations of the fluid particle in figure 23

$$\frac{\partial}{\partial s} (\rho Q \delta n) = 0$$

or

$$\frac{\partial \log_e \rho}{\partial s} + \frac{\partial \log_e Q}{\partial s} + \frac{1}{\delta n} \frac{\partial (\delta n)}{\partial s} = 0 \quad (B1)$$

But, from geometrical considerations (ref. 5, p. 167, for example)

$$\frac{1}{\delta n} \frac{\partial (\delta n)}{\partial s} = \frac{\partial \theta}{\partial n} \quad (B2a)$$

and

$$\frac{1}{\delta s} \frac{\partial (\delta s)}{\partial n} = -\frac{\partial \theta}{\partial s} \quad (B2b)$$

so that equation (B1) becomes

$$\frac{\partial \log_e \rho}{\partial s} + \frac{\partial \log_e Q}{\partial s} + \frac{\partial \theta}{\partial n} = 0$$

or

$$\frac{\partial \log_e \rho}{\partial \varphi} \frac{d\varphi}{ds} + \frac{\partial \log_e Q}{\partial \varphi} \frac{d\varphi}{ds} + \frac{\partial \theta}{\partial \psi} \frac{d\psi}{dn} = 0$$

which, combined with equations (3) and (4), becomes

$$\frac{1}{\rho} \left(\frac{\partial \log_e \rho}{\partial \varphi} + \frac{\partial \log_e Q}{\partial \varphi} \right) + \frac{\partial \theta}{\partial \psi} = 0 \quad (5)$$

Equation (5) is the continuity equation expressed in terms of φ, ψ -coordinates.

Irrotational fluid motion.—For irrotational motion of the fluid particle in figure 23

$$\frac{\partial}{\partial n} (Q \delta s) = 0$$

or

$$\frac{\partial \log_e Q}{\partial n} + \frac{1}{\delta s} \frac{\partial (\delta s)}{\partial n} = 0 \quad (B3)$$

But, from equations (B2b) and (B3)

$$\frac{\partial \log_e Q}{\partial n} - \frac{\partial \theta}{\partial s} = 0$$

or

$$\frac{\partial \log_e Q}{\partial \psi} \frac{d\psi}{dn} - \frac{\partial \theta}{\partial \varphi} \frac{d\varphi}{ds} = 0$$

which, combined with equations (3) and (4), becomes

$$\rho \frac{\partial \log_e Q}{\partial \psi} - \frac{\partial \theta}{\partial \varphi} = 0 \quad (6)$$

Equation (6) is the equation for irrotational fluid motion expressed in terms of the φ, ψ -coordinates.

APPENDIX C

RELATION BETWEEN VELOCITY AND DENSITY ASSUMING LINEAR VARIATION IN PRESSURE WITH SPECIFIC VOLUME

The approximate, linear relation between pressure p and specific volume $1/\rho$ first suggested by Chaplygin (ref. 6) is given by

$$p = A - \frac{B}{\rho} \quad (C1a)$$

from which

$$\frac{dp}{d\rho} = \frac{B}{\rho^2} \quad (C1b)$$

where A and B are arbitrary constants.

If p denotes the static pressure expressed as a ratio of the stagnation density multiplied by the stagnation speed of sound squared, Bernoulli's equation is

$$\frac{dp}{\rho} + q dq = 0$$

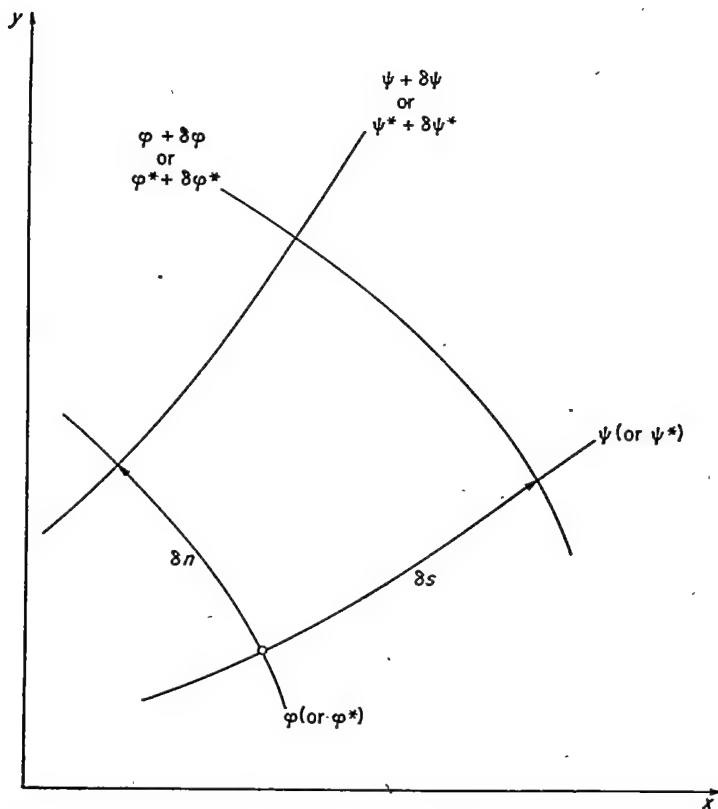


FIGURE 23.—Fluid particle bounded by streamlines and velocity-potential lines in physical xy -plane.

which combined with equation (C1b) integrates to give the approximate relation between velocity and density

$$\frac{B}{2\rho^2} - \frac{q^2}{2} = \text{constant} \quad (\text{C2})$$

For convenience equation (C2) can be written as

$$\frac{1}{\rho^{*2}} - q^{*2} = 1$$

or

$$\rho^* = (1 + q^{*2})^{-1/2} \quad (\text{13})$$

where

$$\rho^* = k_1 \rho \quad (\text{13a})$$

and

$$q^* = k_2 q \quad (\text{13b})$$

The constants k_1 and k_2 replace the two arbitrary constants in equation (C2), and their values are determined so that for any two arbitrary values of q (designated by q_a and q_b) the values of ρ given by equation (13) equal the values of ρ given by equation (8a). Thus the values of ρ given by equation (13) for q equal to q_a or q_b are correct; for all other values of q the values of ρ are approximate. The constants k_1 and k_2 are determined from the conditions

$$\left. \begin{aligned} \rho_a^* &= k_1 \rho_a \\ q_a^* &= k_2 q_a \\ \rho_b^* &= k_1 \rho_b \\ q_b^* &= k_2 q_b \end{aligned} \right\} \quad (\text{C3})$$

From equation (13) and the conditions given by equation (C3)

$$k_1 = \frac{1}{\rho_a} \sqrt{\frac{1 - \left(\frac{\rho_a q_a}{\rho_b q_b}\right)^2}{1 - \left(\frac{q_a}{q_b}\right)^2}} \quad (\text{14a})$$

and

$$k_2 = \frac{1}{q_b} \sqrt{\frac{\left(\frac{\rho_a}{\rho_b}\right)^2 - 1}{1 - \left(\frac{\rho_a q_a}{\rho_b q_b}\right)^2}} \quad (\text{14b})$$

where ρ_a and ρ_b are determined by equation (8a) for the selected values of q_a and q_b , respectively.

The values of q_a and q_b might, for example, be selected to equal the maximum and minimum values of q (which values of q must occur on the channel walls and are therefore known). Also, the values of q_a and q_b might be selected to equal the upstream and downstream velocities q_u and q_d . In this case the upstream and downstream channel widths would then satisfy continuity for a gas with the correct value of γ (1.4, for example). If the upstream and downstream velocities are equal, their value and the value of some other velocity (the maximum or minimum velocity, for example) can be selected for q_a and q_b ; or, if desired, q_a can be equal to q_b , in which case if

$$q_a = q + \epsilon \text{ where } \epsilon \rightarrow 0$$

$$q_b = q$$

it can be shown from equations (14a) and (14b) that

$$k_1 = \frac{1}{\rho} \sqrt{\frac{1 - \frac{\gamma+1}{2} q^2}{1 - \frac{\gamma-1}{2} q^2}} \quad (\text{C4a})$$

and

$$k_2 = \sqrt{\frac{1}{1 - \frac{\gamma+1}{2} q^2}} \quad (\text{C4b})$$

This latter case, in which $q_a = q_b = q$, corresponds to the method used by Chaplygin (ref. 6) and Kármán-Tsien (ref. 8) in which the correct relation between p and $\frac{1}{\rho}$ is replaced by a straight line (eq. (C1a)) that is tangent to the correct relation at one point (where $q_a = q_b$).

APPENDIX D

EQUATIONS OF CONTINUITY AND IRROTATIONAL FLUID MOTION IN TERMS OF TRANSFORMED φ^* , ψ^* -COORDINATES

Consider the two-dimensional irrotational motion of a fluid particle in the physical xy -plane. The fluid particle is defined by adjacent streamlines (constant ψ^*) and velocity-potential lines (constant φ^*) spaced δn and δs apart as indicated in figure 23. The velocity q^* is parallel to the streamlines and normal to the velocity-potential lines.

Continuity.—From continuity considerations of the fluid particle in figure 23

$$\frac{\partial}{\partial s} (\rho^* q^* \delta n) = 0$$

or

$$\frac{\partial \log_e \rho^*}{\partial s} + \frac{\partial \log_e q^*}{\partial s} + \frac{1}{\delta n} \frac{\partial (\delta n)}{\partial s} = 0$$

which combined with equation (B2a) becomes

$$\frac{\partial \log_e \rho^*}{\partial \varphi^*} \frac{d\varphi^*}{ds} + \frac{\partial \log_e q^*}{\partial \varphi^*} \frac{d\varphi^*}{ds} + \frac{\partial \theta}{\partial \psi^*} \frac{d\psi^*}{dn} = 0$$

or, from equations (15) and (16)

$$\frac{1}{\rho^*} \left(\frac{\partial \log_e \rho^*}{\partial \varphi^*} + \frac{\partial \log_e q^*}{\partial \varphi^*} \right) + \frac{\partial \theta}{\partial \psi^*} = 0 \quad (\text{D1})$$

But, from equation (13)

$$\frac{1}{\rho^*} \frac{\partial \log_e \rho^*}{\partial \varphi^*} = \frac{-q^{*2}}{\sqrt{1+q^{*2}}} \frac{\partial \log_e q^*}{\partial \varphi^*}$$

so that equation (D1) becomes

$$\frac{1}{\sqrt{1+q^{*2}}} \frac{\partial \log_e q^*}{\partial \varphi^*} + \frac{\partial \theta}{\partial \psi^*} = 0 \quad (\text{D2})$$

Finally, if

$$u = \frac{q^*}{1 + \sqrt{1 + q^{*2}}} \quad (18)$$

then

$$\frac{\partial \log_e q^*}{\sqrt{1 + q^{*2}}} = \partial \log_e u \quad (D3)$$

so that equation (D2) becomes

$$\frac{\partial \log_e u}{\partial \varphi^*} + \frac{\partial \theta}{\partial \psi^*} = 0 \quad (17)$$

Equation (17) is the continuity equation expressed in terms of φ^*, ψ^* -coordinates and $\log_e u$.

Irrotational fluid motion.—For irrotational motion of the fluid particle in figure 23

$$\frac{\partial}{\partial n} (q^* \delta s) = 0$$

or

$$\frac{\partial \log_e q^*}{\partial n} + \frac{1}{\delta s} \frac{\partial (\delta s)}{\partial n} = 0$$

which combined with equation (B2b) becomes

$$\frac{\partial \log_e q^*}{\partial \psi^*} \frac{d\psi^*}{dn} - \frac{\partial \theta}{\partial \varphi^*} \frac{d\varphi^*}{ds} = 0$$

or, from equations (13), (15), and (16)

$$\frac{1}{\sqrt{1 + q^{*2}}} \frac{\partial \log_e q^*}{\partial \psi^*} - \frac{\partial \theta}{\partial \varphi^*} = 0 \quad (D4)$$

Finally, from equations (D3) and (D4)

$$\frac{\partial \log_e u}{\partial \psi^*} - \frac{\partial \theta}{\partial \varphi^*} = 0 \quad (20)$$

Equation (20) is the equation for irrotational fluid motion expressed in terms of φ^*, ψ^* -coordinates and $\log_e u$.

APPENDIX E

INTEGRAL EQUATION FOR $\theta(\Phi, \Psi)$

If the distribution of the angle $\theta(\Phi, \Psi)$ in the transformed $\Phi\Psi$ -plane is harmonic, that is, satisfies equation (45) within and on the channel walls (Ψ equals 0 and $\frac{\pi}{2}$), then from Green's theorem and the theorem of mean value it can be shown that the value of θ at a point (Φ_o, Ψ_o) within (or on) the channel walls is given by (ref. 9, p. 204, for example)

$$\theta(\Phi_o, \Psi_o) = \frac{1}{2\pi} \left[\int_{-\infty}^{\infty} \left(\theta \frac{\partial G}{\partial \Psi} - G \frac{\partial \theta}{\partial \Psi} \right)_0 d\Phi - \int_{\infty}^{-\infty} \left(-\theta \frac{\partial G}{\partial \Psi} + G \frac{\partial \theta}{\partial \Psi} \right)_{\frac{\pi}{2}} d\Phi \right] \quad (E1)$$

where the two integrals on the right side of equation (E1) represent the line integral around the channel walls in the counterclockwise direction with the signs adjusted so that $\frac{\partial}{\partial \Psi}$ represents the inner normal to the path of integration.

The function $G(\Phi, \Psi)$ in equation (E1) is of the form (ref. 9, p. 204)

$$G(\Phi, \Psi) = \log_e \frac{1}{r} + \omega(\Phi, \Psi) \quad (E2)$$

where r is the distance from any point (Φ, Ψ) to the point (Φ_o, Ψ_o) and where $\omega(\Phi, \Psi)$ is an arbitrary function that is harmonic within and on the channel walls. (Thus from equation (E2), $G(\Phi, \Psi)$ is harmonic within and on the channel walls except at the point (Φ_o, Ψ_o) where a logarithmic singularity exists.) Because the harmonic function $\omega(\Phi, \Psi)$ is arbitrary, the function $G(\Phi, \Psi)$ can be selected so that along

the channel-wall boundaries (Ψ equals 0 and $\frac{\pi}{2}$) $\frac{\partial G}{\partial \Psi}$ is a constant c given by the following equation (obtained from notes presented by Tamarkin and Feller in the 1941 Summer Session for Advanced Instruction and Research in Mechanics at Brown Univ.):

$$c = \frac{2\pi}{l} \quad (E3)$$

where l is the length of the path along which the line integral is taken. For the path under consideration l is infinite and therefore $G(\Phi, \Psi)$ can be selected so that $\frac{\partial G}{\partial \Psi}$ is zero along the channel walls. A function with this property is a Green's function of the second kind. Equation (E1) becomes

$$\theta(\Phi_o, \Psi_o) = \frac{1}{2\pi} \int_{-\infty}^{\infty} \left[\left(G \frac{\partial \theta}{\partial \Psi} \right)_{\frac{\pi}{2}} - \left(G \frac{\partial \theta}{\partial \Psi} \right)_0 \right] d\Phi$$

or, combined with equation (43a)

$$\theta(\Phi_o, \Psi_o) = \frac{-1}{2\pi} \int_{-\infty}^{\infty} \left[\left(G \frac{\partial \log_e V}{\partial \Phi} \right)_{\frac{\pi}{2}} - \left(G \frac{\partial \log_e V}{\partial \Phi} \right)_0 \right] d\Phi \quad (46)$$

Along the channel walls $\frac{\partial \log_e V}{\partial \Phi}$ is known from the prescribed velocity distribution so that, after the proper Green's function G has been determined (appendix F), equation (46) determines the value of θ at any point (Φ_o, Ψ_o) . The value of $\theta(\Phi_o, \Psi_o)$ given by equation (46) can be adjusted by an arbitrary constant of integration to give a specified value of θ at one point in the flow field.

APPENDIX F

GREEN'S FUNCTION OF SECOND KIND

From appendix E Green's function of the second kind G satisfies the condition

$$\frac{\partial G}{\partial \Psi} = 0$$

along the channel walls, which are straight and parallel boundaries (Ψ equals 0 and $\frac{\pi}{2}$) extending to $\pm \infty$ in the Φ -direction, and satisfies the equation

$$\frac{\partial^2 G}{\partial \Phi^2} + \frac{\partial^2 G}{\partial \Psi^2} = 0$$

everywhere in the channel except at the point (Φ_0, Ψ_0) where G has a logarithmic pole. For these conditions the Green's function G can be obtained by analogy from the velocity potential for incompressible flow into a point sink at (Φ_0, Ψ_0) between straight parallel boundaries at Ψ equal to 0 and $\frac{\pi}{2}$. The logarithmic pole for G at (Φ_0, Ψ_0) corresponds to the point sink, and the condition $\frac{\partial G}{\partial \Psi} = 0$ at the boundaries corresponds to zero velocity, that is, no flow normal to the boundaries.

The velocity potential for fluid flow with the boundary conditions just described is obtained from two infinite series of point sinks with the sinks of each series spaced π distance apart in the Ψ -direction, and the two series arranged by the method of images in such a manner that no flow crosses the boundaries, that is, $\frac{\partial G}{\partial \Psi} = 0$. This arrangement of point sinks is shown in figure 24.

The complex function w_1 for the first infinite series of point sinks is given by (ref. 10, p. 112, for example)

$$w_1 = -\log_e \sinh(z - z_0) \quad (F1a)$$

where

$$z = \Phi + i\Psi \quad (F1b)$$

The complex function w_2 for the second infinite series of point sinks (mirror image of the first series in order to prevent flow across the boundaries Ψ equals 0 and $\frac{\pi}{2}$) is given by

$$w_2 = -\log_e \sinh(z - \bar{z}_0) \quad (F2a)$$

where

$$\bar{z} = \Phi - i\Psi \quad (F2b)$$

The complex function w for the combined flow becomes from equations (F1a) to (F2b)

$$w = w_1 + w_2 = -\log_e \sinh[(\Phi - \Phi_0) + i(\Psi - \Psi_0)] - \log_e \sinh[(\Phi - \Phi_0) + i(\Psi + \Psi_0)] \quad (F3)$$

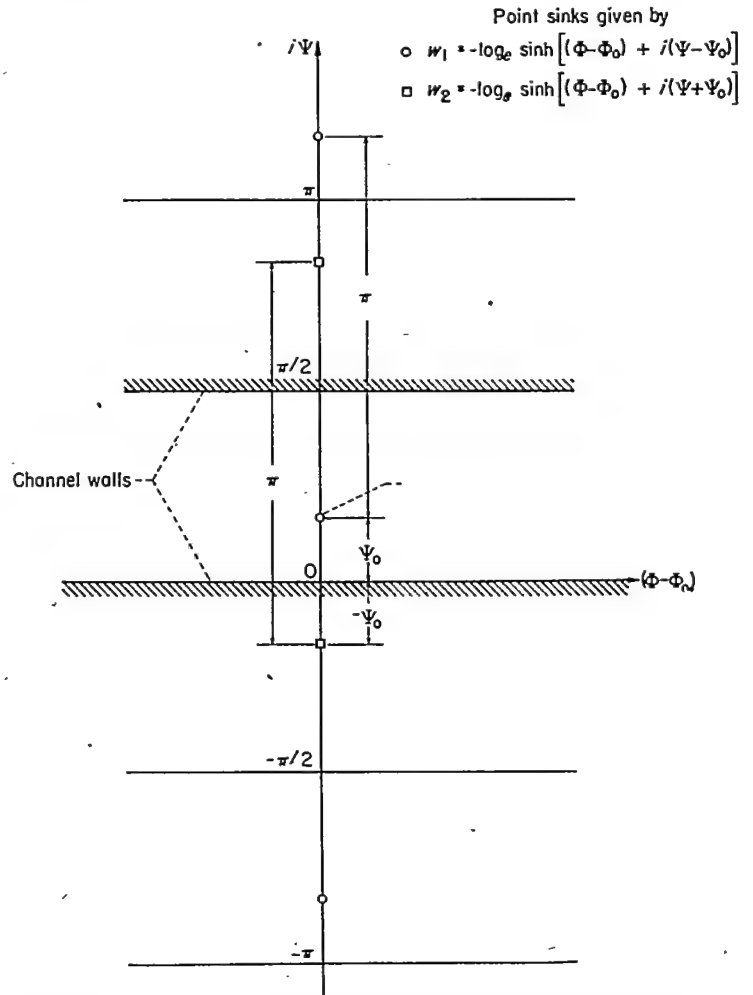


FIGURE 24.—Two infinite series of point sinks required in the development of Green's function of the second kind G .

The Green's function of the second kind G corresponds to the velocity potential for the incompressible flow and is therefore given by the real part of equation (F3)

$$G = -\frac{1}{2} \log_e [\cosh^2(\Phi - \Phi_0) - \cos^2(\Psi - \Psi_0)][\cosh^2(\Phi - \Phi_0) - \cos^2(\Psi + \Psi_0)] \quad (F4)$$

But along the channel walls Ψ is equal to 0 or $\frac{\pi}{2}$ so that

$$\cos^2(\Psi + \Psi_0) = \cos^2(\Psi - \Psi_0)$$

and equation (F4) becomes

$$G_{0 \text{ or } \frac{\pi}{2}} = -\log_e [\cosh^2(\Phi - \Phi_0) - \cos^2(\Psi - \Psi_0)] \quad (47)$$

Equation (47) gives the Green's function of the second kind along the channel walls (straight parallel lines of constant Ψ equal to 0 and $\frac{\pi}{2}$ and extending to $\pm \infty$ in the Φ -direction).

APPENDIX G

EVALUATION OF α AND β

Several techniques, depending on the magnitude of the upper limit $|(\Phi - \Phi_0)|$, were used to evaluate the integrals α and β given by equations (50d) and (50e). Each integral is treated separately in this appendix, and the values of $(\Phi - \Phi_0)$ for the upper limit $|(\Phi - \Phi_0)|$ are considered positive. For negative values of $(\Phi - \Phi_0)$ the magnitudes of I (that is, of α or β) are equal for corresponding values of $|(\Phi - \Phi_0)|$ but opposite in sign. As a result the values of ΔI have the same sign.

INTEGRAL α

Small and medium values of $(\Phi - \Phi_0)$.—For small and medium values of the upper limit of integration $(\Phi - \Phi_0)$ in equation (50d), that is, for $0 \leq (\Phi - \Phi_0) \leq 60\pi/24$, the integral α is evaluated by Simpson's one-third rule using increments of $(\Phi - \Phi_0)$ equal to $\pi/48$.

Large values of $(\Phi - \Phi_0)$.—For large values of $(\Phi - \Phi_0)$, that is, for $(\Phi - \Phi_0) > 60\pi/24$, the integrand in equation (50d) becomes

$$\log_e \cosh (\Phi - \Phi_0) \approx (\Phi - \Phi_0) - \log_e 2 \quad (G1)$$

so that equation (50d) becomes

$$\begin{aligned} \alpha &\approx \int_0^{60\pi/24} \log_e \cosh (\Phi - \Phi_0) d(\Phi - \Phi_0) + \\ &\quad \int_{60\pi/24}^{(\Phi - \Phi_0)} [(\Phi - \Phi_0) - \log_e 2] d(\Phi - \Phi_0) \\ &\approx 25.809782 + \left[\frac{(\Phi - \Phi_0)^2}{2} - 0.693147(\Phi - \Phi_0) - 25.398552 \right] \\ &\approx 0.411230 - 0.693147(\Phi - \Phi_0) + \frac{1}{2}(\Phi - \Phi_0)^2 \end{aligned} \quad (G2)$$

Equation (G2) gives values of α for values of $(\Phi - \Phi_0)$ equal to or greater than $60\pi/24$. Values of the integral α are tabulated in table VII for a range of $|(\Phi - \Phi_0)|$ between 0 and $100\pi/24$ in increments of $\pi/24$. For negative values of $(\Phi - \Phi_0)$ the sign of α is negative.

INTEGRAL β

Small values of $(\Phi - \Phi_0)$.—For $(\Phi - \Phi_0)$ equal to zero the integrand of equation (50e) becomes infinite so that Simpson's one-third rule cannot be used to evaluate β in this region of $(\Phi - \Phi_0)$, as was done for α . However, equation (50e) integrates by parts to give

$$\begin{aligned} \int_0^{(\Phi - \Phi_0)} \log_e \sinh (\Phi - \Phi_0) d(\Phi - \Phi_0) &= (\Phi - \Phi_0) \log_e \sinh (\Phi - \Phi_0) - \\ &\quad \int_0^{(\Phi - \Phi_0)} (\Phi - \Phi_0) \operatorname{ctnh} (\Phi - \Phi_0) d(\Phi - \Phi_0) \end{aligned} \quad (G3)$$

where the integrand $(\Phi - \Phi_0) \operatorname{ctnh} (\Phi - \Phi_0)$ on the right side of equation (G3) can be expanded in the following series form:

$$\begin{aligned} (\Phi - \Phi_0) \operatorname{ctnh} (\Phi - \Phi_0) &= 1 + \frac{2^2 B_1 (\Phi - \Phi_0)^2}{2!} - \frac{2^4 B_3 (\Phi - \Phi_0)^4}{4!} + \\ &\quad \frac{2^6 B_5 (\Phi - \Phi_0)^6}{6!} - \frac{2^8 B_7 (\Phi - \Phi_0)^8}{8!} + \frac{2^{10} B_9 (\Phi - \Phi_0)^{10}}{10!} - \\ &\quad \frac{2^{12} B_{11} (\Phi - \Phi_0)^{12}}{12!} + \dots \end{aligned} \quad (G4)$$

where B_1, B_3 , and so forth, are Bernoulli's numbers (ref. 11, p. 90, for example). From equations (G3) and (G4)

$$\begin{aligned} \beta &= (\Phi - \Phi_0) \log_e \sinh (\Phi - \Phi_0) - (\Phi - \Phi_0) - \frac{(\Phi - \Phi_0)^3}{9} + \frac{(\Phi - \Phi_0)^5}{225} - \\ &\quad \frac{2(\Phi - \Phi_0)^7}{6615} + \frac{(\Phi - \Phi_0)^9}{42,525} - \frac{2(\Phi - \Phi_0)^{11}}{1,029,105} + \frac{1382(\Phi - \Phi_0)^{13}}{8,300,667,375} - \dots \end{aligned} \quad (G5)$$

Equation (G5) was used to obtain β as a function of $(\Phi - \Phi_0)$ for $0 \leq (\Phi - \Phi_0) \leq 8\pi/24$.

Medium values of $(\Phi - \Phi_0)$.—For medium values of the upper limit of integration $(\Phi - \Phi_0)$ in equation (50e), that is, for $8\pi/24 < (\Phi - \Phi_0) \leq 60\pi/24$, the integral β is evaluated by Simpson's one-third rule as was done for α .

Large values of $(\Phi - \Phi_0)$.—For large values of $(\Phi - \Phi_0)$, that is, for $(\Phi - \Phi_0) > 60\pi/24$, the integrand in equation (50e) becomes

$$\log_e \sinh (\Phi - \Phi_0) \approx (\Phi - \Phi_0) - \log_e 2 \quad (G6)$$

so that equation (50e) becomes

$$\begin{aligned} \beta &\approx \int_0^{60\pi/24} \log_e \sinh (\Phi - \Phi_0) d(\Phi - \Phi_0) + \\ &\quad \int_{60\pi/24}^{(\Phi - \Phi_0)} [(\Phi - \Phi_0) - \log_e 2] d(\Phi - \Phi_0) \\ &\approx 24.576082 + \left[\frac{(\Phi - \Phi_0)^2}{2} - 0.693147(\Phi - \Phi_0) - 25.398552 \right] \\ &\approx -0.822470 - 0.693147(\Phi - \Phi_0) + \frac{1}{2}(\Phi - \Phi_0)^2 \end{aligned} \quad (G7)$$

Equation (G7) gives values of β for values of $(\Phi - \Phi_0)$ equal to or greater than $60\pi/24$. Values of the integral β are tabulated in table VII for a range of $|(\Phi - \Phi_0)|$ between 0 and $100\pi/24$ in increments of $\pi/24$. For negative values of $(\Phi - \Phi_0)$, the sign of β changes.

APPENDIX H

CHANNEL TURNING ANGLE

If the prescribed velocity distribution along one channel wall differs from the distribution along the other wall, then in general the channel deflects an amount $\Delta\theta$, which is the difference in flow direction far downstream and far upstream

of the region in which the prescribed velocity distribution varies. Thus,

$$\Delta\theta = \theta_d - \theta_u \quad (H1)$$

For large values of $|\Phi - \Phi_0|$ such as occur far upstream and far downstream of the region in which the prescribed velocity varies along the channel walls

$$\cosh^2 (\Phi - \Phi_0) \gg \cos^2 (\Psi - \Psi_0)$$

so that from equation (47)

$$G_0 = G_{\frac{\pi}{2}} = -2[|(\Phi - \Phi_0)| - \log_e 2] \quad (\text{H2})$$

Far upstream $\Phi_0 < \Phi$ so that

$$|(\Phi - \Phi_0)| = (\Phi - \Phi_0)$$

and because V is harmonic

$$\int_{-\infty}^{\infty} \left[\left(\frac{\partial \log_e V}{\partial \Phi} \right)_{\frac{\pi}{2}} - \left(\frac{\partial \log_e V}{\partial \Phi} \right)_0 \right] d\Phi = 0$$

so that equation (H2) substituted into equation (46) gives

$$\theta_u = \frac{1}{\pi} \int_{-\infty}^{\infty} \Phi \left[\left(\frac{\partial \log_e V}{\partial \Phi} \right)_{\frac{\pi}{2}} - \left(\frac{\partial \log_e V}{\partial \Phi} \right)_0 \right] d\Phi \quad (\text{H3})$$

Likewise, far downstream $\Phi_0 > \Phi$ so that

$$|(\Phi - \Phi_0)| = -(\Phi - \Phi_0)$$

and equation (H2) substituted into equation (46) gives

$$\theta_d = \frac{-1}{\pi} \int_{-\infty}^{\infty} \Phi \left[\left(\frac{\partial \log_e V}{\partial \Phi} \right)_{\frac{\pi}{2}} - \left(\frac{\partial \log_e V}{\partial \Phi} \right)_0 \right] d\Phi \quad (\text{H4})$$

From equations (H1), (H3), and (H4)

$$\Delta\theta = \frac{-2}{\pi} \int_{-\infty}^{\infty} \Phi \left[\left(\frac{\partial \log_e V}{\partial \Phi} \right)_{\frac{\pi}{2}} - \left(\frac{\partial \log_e V}{\partial \Phi} \right)_0 \right] d\Phi \quad (\text{H5})$$

Equation (H5) determines the channel turning angle $\Delta\theta$.

REFERENCES

1. Carrier, G. F.: Elbows for Accelerated Flow. Jour. Appl. Mech., vol. 14, no. 2, June 1947, pp. A-108-A-112.
2. Lighthill, M. J.: A New Method of Two-Dimensional Aerodynamic Design. R. & M. No. 2112, British A. R. C., 1945.
3. Clauser, Francis H.: Two-Dimensional Compressible Flows Having Arbitrarily Specified Pressure Distributions for Gases with Gamma Equal to Minus One. Rep. NOLR 1132, Symposium on Theoretical Compressible Flow, U. S. Naval Ordnance Lab., June 28, 1949, pp. 1-33.
4. Southwell, R. V.: Relaxation Methods in Theoretical Physics. Clarendon Press (Oxford), 1946.
5. Liepmann, Hans Wolfgang, and Puckett, Allen E.: Introduction to Aerodynamics of a Compressible Fluid. John Wiley & Sons, Inc., 1947.
6. Chaplygin, S.: Gas Jets. NACA TM 1063, 1944.
7. Emmons, Howard W.: The Numerical Solution of Partial Differential Equations. Quart. Appl. Math., vol. II, no. 3, Oct. 1944, pp. 173-195.
8. Tsien, Hsue-Shen: Two-Dimensional Subsonic Flow of Compressible Fluids. Jour. Aero. Sci., vol. 6, no. 10, Aug. 1939, pp. 399-407.
9. Osgood, William Fogg: Functions of a Complex Variable. G. E. Stechert & Co. (New York), 1942.
10. Streeter, Victor L.: Fluid Dynamics. McGraw-Hill Book Co., Inc. (New York), 1948.
11. Peirce, B. O.: A Short Table of Integrals. Third ed., Ginn and Company (Boston), 1929.

TABLE I—DISTRIBUTION OF VELOCITY Q AND FLOW DIRECTION θ IN TRANSFORMED ψ -PLANE FOR EXAMPLE III (ELBOW WITH INCOMPRESSIBLE FLOW)[Prescribed variation in Q with arc length s along channel walls plotted in fig. 2; $Q_0=0.5$, $Q_1=1.0$, $\Delta\theta=89.36^\circ$]

ψ	0		0.125		0.250		0.375		0.500		0.625		0.750		0.875		1.000	
	Q	θ	Q	θ	Q	θ	Q	θ	Q	θ	Q	θ	Q	θ	Q	θ	Q	θ
-2.000	0.5000	0	0.5000	0	0.5000	0	0.5000	0	0.5000	0	0.5000	0	0.5000	0	0.5000	0	0.5000	0
-1.875	.5000	.01	.5000	.01	.5000	.00	.5000	.00	.5000	.00	.5000	.00	.5000	.00	.5000	-.01	.5000	-.01
-1.750	.5000	.01	.5000	.01	.5000	.01	.5000	.01	.5000	.00	.5000	.00	.5000	-.01	.5000	-.01	.5000	-.01
-1.625	.5000	.01	.5000	.01	.5000	.01	.5000	.01	.5000	.01	.5000	.01	.5000	-.01	.5000	-.01	.5000	-.01
-1.500	.5000	.02	.5000	.02	.5000	.01	.5000	.01	.5000	.01	.5000	.01	.5000	-.01	.5000	-.02	.5000	-.02
-1.375	.5000	.03	.5000	.03	.5000	.02	.5000	.02	.5000	.02	.5000	.02	.5000	-.02	.5000	-.03	.5000	-.03
-1.250	.5000	.04	.5000	.04	.5000	.03	.5000	.03	.5000	.03	.5000	.03	.5000	-.03	.5000	-.04	.5000	-.04
-1.125	.5000	.06	.5000	.06	.5000	.04	.5000	.04	.5000	.04	.5000	.04	.5000	-.04	.5000	-.06	.5000	-.06
-1.000	.5000	.09	.5000	.09	.5000	.06	.5000	.06	.5000	.06	.5000	.06	.5000	-.06	.5000	-.09	.5000	-.09
-.875	.5000	.14	.5000	.14	.5000	.10	.5000	.10	.5000	.08	.5000	.08	.5000	-.08	.5000	-.14	.5000	-.14
-.750	.5000	.20	.5000	.20	.5000	.18	.5000	.18	.5000	.17	.5000	.17	.5000	-.17	.5000	-.20	.5000	-.20
-.625	.5000	.30	.5000	.30	.5000	.27	.5000	.27	.5000	.25	.5000	.25	.5000	-.25	.5000	-.30	.5000	-.30
-.500	.5000	.45	.5000	.45	.5000	.40	.5000	.40	.5000	.38	.5000	.38	.5000	-.38	.5000	-.45	.5000	-.45
-.375	.5000	.69	.5000	.69	.5000	.60	.5000	.60	.5000	.56	.5000	.56	.5000	-.56	.5000	-.69	.5000	-.69
-.250	.5000	1.04	.5000	1.04	.5000	.89	.5000	.89	.5000	.82	.5000	.82	.5000	-.82	.5000	1.04	.5000	1.04
-.125	.5000	1.63	.5000	1.63	.5000	1.34	.5000	1.34	.5000	1.24	.5000	1.24	.5000	-.88	.5000	1.63	.5000	1.63
0	.5000	2.73	.5000	2.73	.5000	2.04	.5000	2.04	.5000	1.86	.5000	1.86	.5000	-.99	.5000	2.73	.5000	2.73
.125	.5097	5.06	.5097	5.06	.5097	3.21	.5097	3.21	.5097	2.78	.5097	2.78	.5097	-1.50	.5097	5.06	.5097	5.06
.250	.5154	6.83	.5154	6.83	.5154	4.02	.5154	4.02	.5154	3.44	.5154	3.44	.5154	-2.24	.5154	6.83	.5154	6.83
.375	.5215	7.36	.5215	7.36	.5215	4.02	.5215	4.02	.5215	3.44	.5215	3.44	.5215	-2.24	.5215	7.36	.5215	7.36
.500	.5283	6.69	.5283	6.69	.5283	3.19	.5283	3.19	.5283	2.78	.5283	2.78	.5283	-2.24	.5283	6.69	.5283	6.69
.625	.5356	4.95	.5356	4.95	.5356	1.62	.5356	1.62	.5356	1.34	.5356	1.34	.5356	-1.89	.5356	4.95	.5356	4.95
.750	.5434	2.40	.5434	2.40	.5434	-.82	.5434	-.82	.5434	-.82	.5434	-.82	.5434	-1.89	.5434	2.40	.5434	2.40
.875	.5517	-.81	.5517	-.81	.5517	-3.76	.5517	-3.76	.5517	-3.76	.5517	-3.76	.5517	-11.09	.5517	-.81	.5517	-.81
1.000	.5605	-4.52	.5605	-4.52	.5605	-7.18	.5605	-7.18	.5605	-11.34	.5605	-11.34	.5605	-17.90	.5605	-4.52	.5605	-4.52
1.125	.5697	-8.64	.5697	-8.64	.5697	-11.01	.5697	-11.01	.5697	-16.14	.5697	-16.14	.5697	-25.19	.5697	-8.64	.5697	-8.64
1.250	.5793	-13.03	.5793	-13.03	.5793	-15.16	.5793	-15.16	.5793	-21.77	.5793	-21.77	.5793	-33.77	.5793	-13.03	.5793	-13.03
1.375	.5893	-17.77	.5893	-17.77	.5893	-19.59	.5893	-19.59	.5893	-28.66	.5893	-28.66	.5893	-42.63	.5893	-17.77	.5893	-17.77
1.500	.5997	-22.67	.5997	-22.67	.5997	-24.22	.5997	-24.22	.5997	-35.84	.5997	-35.84	.5997	-56.69	.5997	-22.67	.5997	-22.67
1.625	.6105	-27.72	.6105	-27.72	.6105	-29.03	.6105	-29.03	.6105	-43.25	.6105	-43.25	.6105	-72.39	.6105	-27.72	.6105	-27.72
1.750	.6217	-32.88	.6217	-32.88	.6217	-33.95	.6217	-33.95	.6217	-50.64	.6217	-50.64	.6217	-92.39	.6217	-32.88	.6217	-32.88
1.875	.6334	-38.10	.6334	-38.10	.6334	-38.94	.6334	-38.94	.6334	-58.64	.6334	-58.64	.6334	-118.88	.6334	-38.10	.6334	-38.10
2.000	.6456	-43.30	.6456	-43.30	.6456	-43.91	.6456	-43.91	.6456	-68.69	.6456	-68.69	.6456	-148.88	.6456	-43.30	.6456	-43.30
2.125	.6583	-48.43	.6583	-48.43	.6583	-48.83	.6583	-48.83	.6583	-77.77	.6583	-77.77	.6583	-182.39	.6583	-48.43	.6583	-48.43
2.250	.6715	-53.54	.6715	-53.54	.6715	-53.57	.6715	-53.57	.6715	-88.64	.6715	-88.64	.6715	-220.88	.6715	-53.54	.6715	-53.54
2.375	.6851	-58.64	.6851	-58.64	.6851	-58.01	.6851	-58.01	.6851	-101.14	.6851	-101.14	.6851	-263.88	.6851	-58.64	.6851	-58.64
2.500	.6991	-63.73	.6991	-63.73	.6991	-62.61	.6991	-62.61	.6991	-115.14	.6991	-115.14	.6991	-311.88	.6991	-63.73	.6991	-63.73
2.625	.7134	-68.81	.7134	-68.81	.7134	-60.01	.7134	-60.01	.7134	-130.14	.7134	-130.14	.7134	-364.88	.7134	-68.81	.7134	-68.81
2.750	.7281	-73.88	.7281	-73.88	.7281	-65.14	.7281	-65.14	.7281	-146.14	.7281	-146.14	.7281	-422.88	.7281	-73.88	.7281	-73.88
2.875	.7432	-78.93	.7432	-78.93	.7432	-70.07	.7432	-70.07	.7432	-163.14	.7432	-163.14	.7432	-485.88	.7432	-78.93	.7432	-78.93
3.000	.7587	-83.96	.7587	-83.96	.7587	-75.12	.7587	-75.12	.7587	-181.14	.7587	-181.14	.7587	-553.88	.7587	-83.96	.7587	-83.96
3.125	.7746	-88.96	.7746	-88.96	.7746	-80.17	.7746	-80.17	.7746	-200.14	.7746	-200.14	.7746	-626.88	.7746	-88.96	.7746	-88.96
3.250	.7909	-93.93	.7909	-93.93	.7909	-85.22	.7909	-85.22	.7909	-220.14	.7909	-220.14	.7909	-704.88	.7909	-93.93	.7909	-93.93
3.375	.8076	-98.88	.8076	-98.88	.8076	-90.27	.8076	-90.27	.8076	-241.14	.8076	-241.14	.8076	-787.88	.8076	-98.88	.8076	-98.88
3.500	.8247	-103.81	.8247	-103.81	.8247	-95.32	.8247	-95.32	.8247	-263.14	.8247	-263.14	.8247	-875.88	.8247	-103.81	.8247	-103.81
3.625	.8422	-108.72	.8422	-108.72	.8422	-100.37	.8422	-100.37	.8422	-286.14	.8422	-286.14	.8422	-968.88	.8422	-108.72	.8422	-108.72
3.750	.8601	-113.61	.8601	-113.61	.8601	-105.42	.8601	-105.42	.8601	-310.14	.8601	-310.14	.8601	-1066.88	.8601	-113.61	.8601	-113.61
3.875	.8784	-118.48	.8784	-118.48	.8784	-110.47	.8784	-110.47	.8784	-335.14	.8784	-335.14	.8784	-1169.88	.8784	-118.48	.8784	-118.48
4.000	.8971	-123.33	.8971	-123.33	.8971	-115.52	.8971	-115.52	.8971	-361.14	.8971	-361.14	.8971	-1277.88	.8971	-123.33	.8971	-123.33
4.125	.9162	-128.16	.9162	-128.16	.9162	-120.57	.9162	-120.57	.9162	-388.14	.9162	-388.14	.9162	-1390.88	.9162	-128.16	.9162	-128.16
4.250	.9357	-132.96	.9357	-132.96	.9357	-125.62	.9357	-125.62	.9357	-416.14	.9357	-416.14	.9357	-1508.88	.9357	-132.96	.9357	-132.96
4.375	.9556	-137.73	.9556	-137.73	.9556	-130.67	.9556	-130.67	.9556	-445.14	.9556	-445.14	.9556	-1631.88	.9556	-137.73	.9556	-137.73
4.500	.9759	-142.48	.9759	-142.48	.9759	-135.72	.9759	-135.72	.9759	-475.14	.9759	-475.14	.9759	-1759.88	.9759	-142.48	.9759	-142.48
4.625	.9966	-147.21	.9966	-147.21	.9966	-140.77	.9966	-140.77	.9966	-506.14	.9966	-506.14	.9966	-1892.88	.9966	-147.21	.9966	-147.21
4.750	1.0177	-151.92	1.0177	-151.92	1.0177	-145.82	1.0177	-145.82	1.0177	-538.14	1.0177	-538.14	1.0177	-2030.88	1.0177	-151.92	1.0177	-151.92
4.875	1.0392	-156.61	1.0392	-156.61	1.0392	-150.87	1.0392	-150.87	1.0392	-571.14	1.0392	-571.14	1.0392	-2173.88	1.0392	-156.61	1.0392	-156.61
5.000	1.0611	-161.28	1.0611	-161.28	1.0611	-155.92	1.0611	-155.92	1.0611	-605.14	1.0611	-605.14	1.0611	-2321.88	1.0611	-161.28	1.0611	-161.28
5.125	1.0834	-165.93	1.0834	-165.93	1.0834	-160.97	1.0834	-160.97	1.0834	-640.14	1.0834	-640.14	1.0834	-2474.88	1.0834	-165.93	1.0834	-165.93
5.250	1.1061	-170.56	1.1061	-170.56	1.1061	-166.02	1.1061	-166.02	1.1061	-676.14	1.1061	-676.14	1.1061	-2632.88	1.1061	-170.56	1.1061	-170.56
5.375	1.1292	-175.17	1.1292	-175.17	1.1292	-171.07	1.1292	-171.07	1.1292	-713.14	1.1292	-713.14	1.1292	-2795.88	1.1292	-175.17	1.1292	-175.17
5.500	1.1527	-179.76	1.1527	-179.76	1.1527	-176.12	1.1527	-176.12	1.1527	-751.14	1.1527	-751.14	1.1527	-2963.88	1.1527	-179.76	1.1527	-179.76
5.625	1.1766	-184.33	1.1766	-184.33	1.1766	-181.17	1.1766	-181.17	1.1766	-790.14	1.1766	-790.14	1.1766	-3136.88	1.1766	-184.33	1.1766	-184.33
5.750	1.2009	-188.88	1.2009	-188.88	1.2009	-186.22	1.2009	-186.22	1.2009	-830.14	1.2009	-830.14	1.2009	-3314.88	1.2009	-188.88	1.2009	-188.88

TABLE II—DISTRIBUTION OF PHYSICAL COORDINATES x AND y IN TRANSFORMED ψ -PLANE FOR EXAMPLE III (ELBOW WITH INCOMPRESSIBLE FLOW)[Prescribed variation in Q with arc length s along channel walls plotted in fig. 2; $Q_0=0.5$, $Q_d=1.0$, $\Delta\theta=89.36^\circ$]

φ	0		0.125		0.250		0.375		0.500		0.625		0.750		0.875		1.000	
	x	y	x	y	x	y	x	y	x	y	x	y	x	y	x	y	x	y
-2.000	-3.978	-0.998	-3.978	-0.748	-3.978	-0.498	-3.978	-0.248	-3.978	0.002	-3.978	0.252	-3.978	0.502	-3.978	0.752	-3.978	1.002
-1.875	-3.727	-0.998	-3.728	-0.748	-3.728	-0.498	-3.728	-0.248	-3.728	0.002	-3.728	0.252	-3.728	0.502	-3.728	0.752	-3.727	1.002
-1.750	-3.477	-0.998	-3.478	-0.748	-3.478	-0.498	-3.478	-0.248	-3.478	0.002	-3.478	0.252	-3.478	0.502	-3.478	0.752	-3.477	1.002
-1.625	-3.227	-0.998	-3.228	-0.748	-3.228	-0.498	-3.228	-0.248	-3.228	0.002	-3.228	0.252	-3.228	0.502	-3.228	0.752	-3.227	1.002
-1.500	-2.977	-0.998	-2.977	-0.748	-2.978	-0.498	-2.978	-0.248	-2.978	0.002	-2.978	0.252	-2.978	0.502	-2.978	0.752	-2.977	1.002
-1.375	-2.727	-0.998	-2.728	-0.748	-2.728	-0.498	-2.728	-0.248	-2.728	0.002	-2.728	0.252	-2.728	0.502	-2.728	0.752	-2.727	1.002
-1.250	-2.477	-0.997	-2.478	-0.747	-2.478	-0.498	-2.478	-0.248	-2.478	0.002	-2.478	0.252	-2.478	0.502	-2.478	0.752	-2.477	1.002
-1.125	-2.227	-0.997	-2.228	-0.747	-2.228	-0.497	-2.228	-0.248	-2.228	0.002	-2.228	0.252	-2.228	0.502	-2.228	0.752	-2.227	1.002
-1.000	-1.977	-0.997	-1.978	-0.747	-1.978	-0.497	-1.978	-0.247	-1.978	0.002	-1.978	0.252	-1.978	0.501	-1.978	0.751	-1.977	1.001
-0.875	-1.727	-0.996	-1.728	-0.747	-1.728	-0.497	-1.728	-0.247	-1.729	0.002	-1.729	0.252	-1.729	0.501	-1.729	0.751	-1.727	1.001
-0.750	-1.477	-0.996	-1.478	-0.746	-1.479	-0.496	-1.479	-0.247	-1.480	0.002	-1.479	0.251	-1.479	0.501	-1.478	0.750	-1.477	1.000
-0.625	-1.227	-0.995	-1.228	-0.746	-1.230	-0.496	-1.230	-0.247	-1.231	0.002	-1.230	0.251	-1.230	0.500	-1.229	0.749	-1.227	0.999
-0.500	-0.977	-0.993	-0.979	-0.743	-0.981	-0.495	-0.982	-0.246	-0.982	0.002	-0.982	0.250	-0.981	0.499	-0.979	0.748	-0.977	0.997
-0.375	-0.727	-0.990	-0.730	-0.741	-0.733	-0.493	-0.734	-0.245	-0.735	0.002	-0.734	0.249	-0.732	0.497	-0.730	0.746	-0.727	0.995
-0.250	-0.478	-0.987	-0.482	-0.738	-0.485	-0.491	-0.487	-0.244	-0.488	0.002	-0.487	0.248	-0.484	0.495	-0.481	0.743	-0.477	0.992
-0.125	-0.228	-0.981	-0.235	-0.733	-0.239	-0.487	-0.242	-0.242	-0.243	0.001	-0.241	0.245	-0.238	0.491	-0.233	0.739	-0.227	0.987
0	0.022	-0.972	0.011	-0.726	0.004	-0.482	0.000	-0.240	0.000	0.000	0.003	0.242	0.008	0.488	0.015	0.732	0.023	0.981
0.125	0.270	-0.965	0.254	-0.715	0.243	-0.476	0.239	-0.239	0.240	-0.002	0.245	0.237	0.252	0.479	0.261	0.724	0.273	0.971
0.250	0.510	-0.930	0.489	-0.700	0.477	-0.469	0.472	-0.238	0.476	-0.006	0.484	0.229	0.494	0.468	0.507	0.711	0.522	0.958
0.375	0.754	-0.901	0.713	-0.684	0.702	-0.463	0.700	-0.239	0.707	-0.013	0.719	0.218	0.734	0.454	0.751	0.695	0.772	0.941
0.500	0.942	-0.875	0.925	-0.670	0.918	-0.460	0.921	-0.244	0.933	-0.024	0.950	0.202	0.970	0.434	0.994	0.672	1.021	0.917
0.625	1.139	-0.855	1.129	-0.662	1.128	-0.461	1.136	-0.254	1.153	-0.041	1.177	0.180	1.204	0.408	1.234	0.643	1.269	0.896
0.750	1.322	-0.843	1.321	-0.660	1.327	-0.470	1.343	-0.271	1.387	-0.064	1.398	0.151	1.433	0.375	1.472	0.607	1.516	0.848
0.875	1.495	-0.840	1.502	-0.668	1.518	-0.486	1.542	-0.295	1.575	-0.095	1.614	0.113	1.658	0.332	1.707	0.560	1.761	0.798
1.000	1.658	-0.848	1.675	-0.684	1.701	-0.511	1.734	-0.328	1.776	-0.135	1.824	0.067	1.879	0.279	1.938	0.503	2.003	0.738
1.125	1.812	-0.868	1.840	-0.710	1.875	-0.545	1.915	-0.370	1.969	-0.185	2.028	0.010	2.094	0.216	2.165	0.435	2.242	0.665
1.250	1.958	-0.893	1.995	-0.747	2.041	-0.590	2.094	-0.423	2.156	-0.245	2.225	-0.068	2.302	0.142	2.386	0.354	2.477	0.578
1.375	2.096	-0.931	2.143	-0.793	2.198	-0.644	2.262	-0.485	2.334	-0.316	2.415	-0.137	2.501	0.055	2.601	0.260	2.705	0.477
1.500	2.226	-0.979	2.282	-0.849	2.348	-0.709	2.422	-0.558	2.504	-0.398	2.596	-0.228	2.697	-0.044	2.807	0.162	2.927	0.361
1.625	2.347	-1.038	2.413	-0.914	2.488	-0.783	2.572	-0.642	2.665	-0.491	2.768	-0.330	2.882	-0.156	3.005	0.030	3.139	0.229
1.750	2.461	-1.102	2.535	-0.989	2.621	-0.867	2.713	-0.735	2.816	-0.594	2.930	-0.444	3.055	-0.281	3.192	-0.106	3.341	0.082
1.875	2.566	-1.177	2.649	-1.073	2.741	-0.960	2.844	-0.838	2.957	-0.708	3.081	-0.569	3.218	-0.418	3.363	-0.255	3.531	-0.081
2.000	2.662	-1.260	2.753	-1.164	2.853	-1.061	2.964	-0.950	3.086	-0.831	3.219	-0.705	3.367	-0.567	3.529	-0.418	3.706	-0.259
2.125	2.749	-1.350	2.847	-1.264	2.956	-1.170	3.074	-1.070	3.202	-0.953	3.344	-0.850	3.501	-0.727	3.675	-0.594	3.865	-0.451
2.250	2.828	-1.447	2.932	-1.369	3.047	-1.286	3.172	-1.197	3.307	-1.062	3.455	-0.960	3.620	-0.895	3.803	-0.780	4.004	-0.653
2.375	2.899	-1.550	3.008	-1.481	3.128	-1.407	3.258	-1.329	3.398	-1.247	3.550	-1.160	3.721	-1.070	3.910	-0.977	4.119	-0.880
2.500	2.961	-1.650	3.075	-1.598	3.199	-1.533	3.332	-1.466	3.476	-1.395	3.631	-1.322	3.803	-1.249	3.991	-1.177	4.203	-1.105
2.625	3.016	-1.771	3.134	-1.718	3.260	-1.663	3.396	-1.605	3.611	-1.516	3.697	-1.485	3.869	-1.428	4.058	-1.374	4.259	-1.324
2.750	3.064	-1.886	3.184	-1.841	3.313	-1.794	3.450	-1.746	3.695	-1.697	3.751	-1.648	3.919	-1.601	4.100	-1.565	4.294	-1.532
2.875	3.105	-2.005	3.227	-1.966	3.357	-1.927	3.494	-1.887	3.638	-1.847	3.792	-1.803	3.958	-1.775	4.130	-1.748	4.314	-1.727
3.000	3.139	-2.125	3.263	-2.092	3.393	-2.050	3.530	-2.028	3.673	-1.996	3.824	-1.985	3.983	-1.941	4.160	-1.923	4.334	-1.911
3.125	3.168	-2.246	3.292	-2.219	3.423	-2.193	3.550	-2.167	3.700	-2.142	3.848	-2.119	4.002	-2.101	4.162	-2.089	4.328	-2.084
3.250	3.191	-2.369	3.317	-2.347	3.447	-2.328	3.582	-2.305	3.721	-2.285	3.886	-2.267	4.015	-2.258	4.168	-2.249	4.326	-2.247
3.375	3.211	-2.493	3.337	-2.475	3.466	-2.457	3.600	-2.411	3.737	-2.426	3.879	-2.413	4.024	-2.405	4.171	-2.401	4.323	-2.402
3.500	3.227	-2.617	3.352	-2.602	3.481	-2.688	3.614	-2.576	3.749	-2.561	3.888	-2.555	4.029	-2.549	4.173	-2.548	4.317	-2.551
3.625	3.239	-2.741	3.365	-2.729	3.493	-2.719	3.624	-2.709	3.768	-2.700	3.894	-2.693	4.032	-2.690	4.171	-2.690	4.311	-2.693
3.750	3.249	-2.865	3.375	-2.856	3.503	-2.848	3.633	-2.840	3.764	-2.834	3.898	-2.829	4.033	-2.827	4.169	-2.828	4.305	-2.832
3.875	3.257	-2.990	3.383	-2.983	3.510	-2.976	3.639	-2.971	3.769	-2.966	3.901	-2.962	4.033	-2.961	4.166	-2.962	4.299	-2.966
4.000	3.264	-3.115	3.389	-3.109	3.516	-3.104	3.644	-3.100	3.773	-3.096	3.905	-3.093	4.033	-3.093	4.164	-3.094	4.294	-3.097
4.125	3.269	-3.240	3.394	-3.235	3.520	-3.231	3.648	-3.228	3.776	-3.225	3.905	-3.223	4.033	-3.223	4.162	-3.223	4.290	-3.226
4.250	3.273	-3.365	3.398	-3.361	3.524	-3.358	3.651	-3.355	3.778	-3.352	3.906	-3.351	4.033	-3.350	4.160	-3.351	4.287	-3.353
4.375	3.276	-3.490	3.401	-3.487	3.527	-3.484	3.653	-3.482	3.780	-3.480	3.907	-3.478	4.033	-3.478	4.160	-3.478	4.286	-3.478
4.500	3.279	-3.615	3.404	-3.612	3.529	-3.610	3.655	-3.608	3.781	-3.606	3.908	-3.605	4.034	-3.604	4.159	-3.603	4.285	-3.603
4.625	3.281	-3.740	3.406	-3.738	3.531	-3.736	3.657	-3.734	3.783	-3.732	3.909	-3.731	4.034	-3.730	4.160	-3.729	4.285	-3.729
4.750	3.283	-3.865	3.408	-3.863	3.533	-3.861	3.659	-3.859	3.784	-3.858								

TABLE III—DISTRIBUTION OF VELOCITY q AND FLOW DIRECTION θ IN TRANSFORMED $\varphi^*\psi^*$ -PLANE
FOR EXAMPLE IV (ELBOW WITH LINEARIZED COMPRESSIBLE FLOW)[Prescribed variation in Q with arc length s along channel walls plotted in fig. 2; $Q_0=0.5$, $Q_1=1.0$, $q_1=0.80176$, $\Delta\psi^*=0.73782$, $\Delta\theta=104.07^\circ$]

$\frac{\psi^*}{\Delta\psi^*}$	0		$\frac{1}{4}$		$\frac{1}{2}$		$\frac{3}{4}$		$\frac{5}{8}$		$\frac{6}{8}$		1.0	
	q	θ	q	θ	q	θ	q	θ	q	θ	q	θ	q	θ
-11/8	0.4009	0	0.4009	0	0.4009	0	0.4009	0	0.4009	0	0.4009	0	0.4009	0
-10/8	.4009	.01	.4009	.01	.4009	.00	.4009	.00	.4009	.00	.4009	.01	.4009	-.01
-9/8	.4009	.01	.4009	.01	.4010	.01	.4010	.00	.4010	-.01	.4009	-.01	.4009	-.01
-8/8	.4009	.02	.4010	.02	.4010	.01	.4010	.00	.4010	-.01	.4010	-.02	.4009	-.02
-7/8	.4009	.03	.4010	.03	.4011	.01	.4011	.00	.4011	-.01	.4010	-.02	.4009	-.03
-6/8	.4009	.05	.4011	.04	.4012	.02	.4013	.00	.4013	-.02	.4011	-.04	.4009	-.05
-5/8	.4009	.08	.4012	.07	.4015	.04	.4015	.00	.4014	-.04	.4012	-.07	.4009	-.08
-4/8	.4009	.14	.4015	.12	.4019	.07	.4020	.00	.4018	-.07	.4014	-.11	.4009	-.13
-3/8	.4009	.24	.4019	.20	.4025	.11	.4027	-.01	.4024	-.11	.4017	-.18	.4009	-.21
-2/8	.4009	.40	.4026	.33	.4037	.17	.4039	-.03	.4035	-.20	.4022	-.31	.4009	-.35
-1/8	.4009	.70	.4041	.57	.4057	.27	.4059	-.05	.4048	-.33	.4030	-.50	.4009	-.60
0	.4009	1.31	.4070	.96	.4093	.36	.4090	-.17	.4071	-.58	.4042	-.84	.4009	-.92
1/8	.4072	2.82	.4141	1.49	.4155	.43	.4139	-.40	.4104	-.99	.4053	-1.34	.4009	-1.45
2/8	.4243	3.88	.4268	1.77	.4251	.24	.4207	-.87	.4148	-1.63	.4080	-2.07	.4009	-2.22
3/8	.4489	4.00	.4444	1.46	.4377	-.38	.4295	-1.70	.4202	-2.50	.4106	-3.11	.4009	-3.28
4/8	.4780	3.17	.4654	.50	.4526	-1.49	.4396	-2.92	.4285	-3.90	.4135	-4.46	.4009	-4.05
5/8	.5094	1.44	.4882	-1.17	.4639	-3.16	.4506	-4.62	.4333	-5.63	.4167	-6.21	.4009	-6.41
6/8	.5415	-.88	.5118	-3.43	.4857	-6.34	.4621	-6.76	.4403	-7.75	.4200	-8.33	.4009	-8.52
7/8	.5732	-4.00	.5353	-6.23	.5024	-8.01	.4734	-9.35	.4472	-10.29	.4232	-10.85	.4009	-11.04
8/8	.6038	-7.48	.5578	-9.48	.5186	-11.10	.4844	-12.34	.4539	-13.22	.4262	-13.74	.4009	-13.91
9/8	.6329	-11.35	.5793	-13.12	.5340	-14.67	.4947	-16.70	.4601	-16.49	.4291	-16.97	.4009	-17.13
10/8	.6602	-15.62	.5994	-17.09	.5482	-18.37	.5043	-19.38	.4659	-20.09	.4317	-20.62	.4009	-20.07
11/8	.6855	-19.96	.6178	-21.33	.5613	-22.46	.5181	-23.34	.4712	-23.93	.4341	-24.37	.4009	-24.49
12/8	.7086	-24.62	.6346	-25.80	.5732	-26.79	.5210	-27.66	.4759	-28.12	.4362	-28.46	.4009	-28.58
13/8	.7293	-29.46	.6496	-30.47	.5837	-31.32	.5281	-32.00	.4801	-32.49	.4381	-32.70	.4009	-32.89
14/8	.7477	-34.45	.6629	-35.31	.5931	-36.03	.5343	-36.62	.4838	-37.05	.4398	-37.81	.4009	-37.40
15/8	.7636	-39.56	.6744	-40.27	.6013	-36.89	.5393	-41.39	.4872	-41.77	.4413	-42.00	.4009	-42.08
16/8	.7769	-44.76	.6842	-45.34	.6084	-45.86	.5447	-46.30	.4902	-46.64	.4437	-46.85	.4009	-46.83
17/8	.7876	-50.02	.6924	-50.47	.6146	-50.90	.5492	-51.30	.4931	-51.63	.4440	-51.85	.4009	-51.83
18/8	.7953	-55.27	.6991	-55.61	.6202	-55.98	.5537	-56.36	.4961	-56.72	.4456	-56.98	.4009	-57.08
19/8	.8001	-60.49	.7045	-60.72	.6257	-61.06	.5586	-61.47	.4999	-61.91	.4477	-62.28	.4009	-62.44
20/8	.8018	-65.55	.7091	-65.68	.6315	-66.03	.5647	-66.53	.5035	-67.13	.4515	-67.79	.4009	-68.16
21/8	.8018	-70.32	.7135	-70.45	.6385	-70.85	.5700	-71.49	.5142	-72.37	.4568	-73.46	.4009	-74.80
22/8	.8018	-74.81	.7186	-74.96	.6471	-75.43	.5783	-76.22	.5222	-77.36	.4745	-78.91	.4009	-81.03
23/8	.8018	-78.97	.7245	-79.15	.6573	-76.38	.5878	-80.59	.5441	-81.93	.4948	-83.79	.4009	-86.33
24/8	.8018	-82.82	.7311	-83.01	.6690	-83.59	.6138	-84.87	.5641	-86.02	.5190	-88.01	.4009	-90.09
25/8	.8018	-86.28	.7381	-86.48	.6816	-87.07	.6313	-88.08	.5860	-89.55	.5455	-91.55	.4009	-94.10
26/8	.8018	-89.37	.7462	-89.56	.6947	-90.15	.6404	-91.14	.6089	-92.57	.5729	-94.48	.4009	-96.03
27/8	.8018	-92.07	.7523	-92.25	.7077	-92.81	.6678	-93.75	.6318	-95.10	.6002	-96.88	.4009	-99.11
28/8	.8018	-94.40	.7591	-94.57	.7203	-95.09	.6852	-95.97	.6540	-97.21	.6268	-98.83	.4009	-100.83
29/8	.8018	-96.39	.7654	-96.54	.7321	-97.02	.7020	-97.82	.6763	-98.94	.6522	-100.39	.4009	-102.17
30/8	.8018	-98.05	.7713	-98.20	.7432	-98.62	.7177	-99.34	.6952	-100.34	.6769	-101.63	.4009	-103.19
31/8	.8018	-99.44	.7766	-99.56	.7532	-99.94	.7321	-100.68	.7135	-101.46	.6978	-102.69	.4009	-103.05
32/8	.8018	-100.56	.7813	-100.67	.7623	-101.01	.7451	-101.66	.7301	-102.33	.7178	-103.31	.4009	-104.49
33/8	.8018	-101.47	.7855	-101.57	.7702	-101.85	.7566	-102.33	.7449	-102.99	.7357	-103.83	.4009	-104.84
34/8	.8018	-102.18	.7890	-102.28	.7772	-102.51	.7667	-102.91	.7580	-103.47	.7515	-104.18	.4009	-105.03
35/8	.8018	-102.73	.7921	-102.80	.7831	-103.00	.7753	-103.34	.7691	-103.80	.7651	-104.39	.4009	-105.10
36/8	.8018	-103.14	.7946	-103.20	.7880	-103.37	.7825	-103.64	.7785	-104.01	.7764	-104.48	.4009	-105.05
37/8	.8018	-103.45	.7966	-103.49	.7920	-103.62	.7883	-103.83	.7860	-104.12	.7855	-104.49	.4009	-104.91
38/8	.8018	-103.66	.7982	-103.69	.7950	-103.79	.7927	-103.95	.7917	-104.16	.7923	-104.42	.4009	-104.71
39/8	.8018	-103.81	.7994	-103.83	.7973	-103.90	.7960	-104.02	.7957	-104.16	.7968	-104.33	.4009	-104.49
40/8	.8018	-103.90	.8002	-103.92	.7989	-103.97	.7982	-104.05	.7982	-104.14	.7993	-104.23	.4009	-104.28
41/8	.8018	-103.97	.8008	-103.98	.8000	-104.01	.7996	-104.06	.7997	-104.11	.8004	-104.16	.4009	-104.18
42/8	.8018	-104.00	.8011	-104.01	.8006	-104.03	.8004	-104.06	.8005	-104.09	.8010	-104.12	.4009	-104.13
43/8	.8018	-104.03	.8014	-104.03	.8011	-104.05	.8009	-104.06	.8010	-104.08	.8013	-104.10	.4009	-104.10
44/8	.8018	-104.04	.8015	-104.05	.8013	-104.05	.8013	-104.06	.8015	-104.08	.8016	-104.08	.4009	-104.09
45/8	.8018	-104.05	.8016	-104.05	.8015	-104.06	.8015	-104.07	.8016	-104.07	.8016	-104.08	.4009	-104.08
46/8	.8018	-104.06	.8017	-104.06	.8016	-104.06	.8016	-104.07	.8016	-104.07	.8017	-104.07	.4009	-104.07
47/8	.8018	-104.06	.8017	-104.06	.8017	-104.06	.8017	-104.07	.8017	-104.07	.8017	-104.07	.4009	-104.07
48/8	.8018	-104.06	.8017	-104.06	.8017	-104.06	.8017	-104.07	.8017	-104.07	.8017	-104.07	.4009	-104.07
49/8	.8018	-104.06	.8017	-104.06	.8017	-104.06	.8017	-104.07	.8017	-104.07	.8017	-104.07	.4009	-104.07
50/8	.8018	-104.06	.8018	-104.06	.8018	-104.06	.8018	-104.07	.8018	-104.07	.8018	-104.07	.4009	-104.07

TABLE IV—DISTRIBUTION OF PHYSICAL COORDINATES x AND y IN TRANSFORMED $\varphi^*\psi^*$ -PLANE FOR EXAMPLE IV (ELBOW WITH LINERARIZED COMPRESSIBLE FLOW)[Prescribed variation in Q with arc length s along channel walls plotted in fig. 2; $Q_0=0.5$, $Q_1=1.0$, $q_1=0.80176$, $\Delta\psi^*=0.73782$, $\Delta\theta=104.07^\circ$]

$\frac{\psi^*}{\Delta\psi^*}$	0		$\frac{1}{6}$		$\frac{1}{3}$		$\frac{1}{2}$		$\frac{2}{3}$		$\frac{5}{6}$		1.0	
	x	y	x	y	x	y	x	y	x	y	x	y	x	y
-11/8	-2.466	-0.789	-2.466	-0.512	-2.466	-0.256	-2.466	0.001	-2.466	0.257	-2.466	0.513	-2.466	0.770
-10/8	-2.241	-0.789	-2.241	-0.512	-2.241	-0.256	-2.241	0.001	-2.241	0.257	-2.241	0.513	-2.241	0.770
-9/8	-2.016	-0.789	-2.016	-0.512	-2.016	-0.256	-2.016	0.001	-2.016	0.257	-2.016	0.513	-2.016	0.770
-8/8	-1.791	-0.789	-1.791	-0.512	-1.791	-0.256	-1.791	0.001	-1.791	0.257	-1.791	0.513	-1.791	0.770
-7/8	-1.566	-0.789	-1.566	-0.512	-1.566	-0.256	-1.566	0.001	-1.566	0.257	-1.566	0.513	-1.566	0.770
-6/8	-1.341	-0.789	-1.341	-0.512	-1.341	-0.256	-1.341	0.001	-1.341	0.257	-1.341	0.513	-1.341	0.770
-5/8	-1.116	-0.789	-1.116	-0.512	-1.116	-0.256	-1.116	0.001	-1.116	0.257	-1.116	0.513	-1.116	0.770
-4/8	-0.891	-0.789	-0.891	-0.512	-0.891	-0.256	-0.891	0.001	-0.891	0.257	-0.891	0.513	-0.891	0.770
-3/8	-0.666	-0.789	-0.666	-0.512	-0.666	-0.256	-0.666	0.001	-0.666	0.257	-0.666	0.513	-0.666	0.770
-2/8	-0.441	-0.789	-0.441	-0.512	-0.441	-0.256	-0.441	0.001	-0.441	0.257	-0.441	0.513	-0.441	0.770
-1/8	-0.216	-0.789	-0.216	-0.512	-0.216	-0.256	-0.216	0.000	-0.216	0.257	-0.216	0.513	-0.216	0.770
0	0.008	-0.760	0.003	-0.505	0.000	-0.252	0.000	0.000	0.002	0.253	0.005	0.507	0.009	0.763
1/8	0.233	-0.752	0.223	-0.500	0.219	-0.251	0.219	-0.001	0.222	0.250	0.228	0.503	0.234	0.758
2/8	0.450	-0.739	0.438	-0.494	0.434	-0.249	0.438	-0.003	0.441	0.245	0.449	0.496	0.459	0.751
3/8	0.666	-0.724	0.645	-0.488	0.643	-0.250	0.648	-0.008	0.657	0.237	0.670	0.486	0.684	0.740
4/8	0.851	-0.712	0.844	-0.485	0.846	-0.253	0.855	-0.016	0.870	0.225	0.888	0.472	0.908	0.725
5/8	1.033	-0.704	1.033	-0.485	1.042	-0.261	1.057	-0.029	1.079	0.208	1.104	0.452	1.132	0.703
6/8	1.205	-0.703	1.213	-0.492	1.230	-0.274	1.254	-0.049	1.284	0.184	1.318	0.425	1.355	0.674
7/8	1.366	-0.710	1.386	-0.507	1.411	-0.285	1.445	-0.076	1.485	0.153	1.529	0.389	1.577	0.636
8/8	1.519	-0.725	1.548	-0.529	1.586	-0.325	1.630	-0.111	1.681	0.112	1.737	0.344	1.797	0.587
9/8	1.663	-0.749	1.704	-0.560	1.753	-0.363	1.809	-0.166	1.871	0.061	1.940	0.288	2.013	0.527
10/8	1.798	-0.781	1.852	-0.600	1.913	-0.410	1.981	-0.210	2.056	0.000	2.138	0.221	2.226	0.455
11/8	1.926	-0.822	1.992	-0.649	2.065	-0.466	2.146	-0.274	2.235	-0.072	2.331	0.142	2.434	0.368
12/8	2.046	-0.871	2.124	-0.706	2.209	-0.532	2.304	-0.349	2.406	-0.156	2.517	0.050	2.635	0.268
13/8	2.157	-0.928	2.247	-0.772	2.346	-0.608	2.453	-0.435	2.569	-0.251	2.694	-0.055	2.829	0.153
14/8	2.261	-0.993	2.363	-0.847	2.473	-0.693	2.593	-0.530	2.723	-0.357	2.862	-0.173	3.013	0.024
15/8	2.356	-1.064	2.469	-0.930	2.591	-0.787	2.723	-0.636	2.866	-0.476	3.020	-0.304	3.186	-0.120
16/8	2.443	-1.143	2.567	-1.020	2.700	-0.889	2.843	-0.751	2.999	-0.604	3.166	-0.447	3.346	-0.278
17/8	2.521	-1.228	2.655	-1.117	2.798	-1.000	2.952	-0.875	3.118	-0.743	3.298	-0.601	3.492	-0.449
18/8	2.590	-1.318	2.732	-1.220	2.885	-1.117	3.049	-1.007	3.225	-0.890	3.416	-0.766	3.623	-0.632
19/8	2.650	-1.414	2.800	-1.330	2.960	-1.240	3.132	-1.146	3.317	-1.046	3.518	-0.940	3.736	-0.826
20/8	2.701	-1.514	2.858	-1.443	3.024	-1.369	3.203	-1.290	3.395	-1.208	3.603	-1.122	3.830	-1.030
21/8	2.743	-1.619	2.905	-1.561	3.076	-1.501	3.259	-1.438	3.456	-1.374	3.669	-1.309	3.901	-1.242
22/8	2.777	-1.726	2.942	-1.681	3.117	-1.635	3.303	-1.588	3.501	-1.541	3.715	-1.496	3.947	-1.455
23/8	2.803	-1.836	2.970	-1.803	3.147	-1.770	3.333	-1.737	3.531	-1.707	3.743	-1.680	3.969	-1.661
24/8	2.820	-1.947	2.990	-1.926	3.167	-1.905	3.353	-1.885	3.548	-1.869	3.755	-1.858	3.974	-1.856
25/8	2.831	-2.059	3.001	-2.048	3.177	-2.038	3.362	-2.030	3.554	-2.026	3.756	-2.027	3.966	-2.038
26/8	2.835	-2.171	3.005	-2.169	3.181	-2.169	3.363	-2.171	3.552	-2.177	3.747	-2.189	3.950	-2.209
27/8	2.834	-2.283	3.003	-2.290	3.177	-2.297	3.357	-2.308	3.542	-2.322	3.732	-2.342	3.927	-2.369
28/8	2.827	-2.396	2.996	-2.409	3.168	-2.423	3.345	-2.440	3.527	-2.461	3.712	-2.487	3.900	-2.520
29/8	2.817	-2.508	2.984	-2.527	3.155	-2.547	3.330	-2.570	3.508	-2.596	3.688	-2.626	3.871	-2.663
30/8	2.803	-2.619	2.969	-2.643	3.139	-2.668	3.311	-2.695	3.485	-2.725	3.662	-2.760	3.841	-2.799
31/8	2.786	-2.731	2.951	-2.758	3.119	-2.787	3.289	-2.818	3.461	-2.851	3.635	-2.888	3.809	-2.929
32/8	2.766	-2.841	2.931	-2.872	3.097	-2.904	3.266	-2.938	3.435	-2.973	3.606	-3.012	3.777	-3.055
33/8	2.744	-2.952	2.908	-2.985	3.074	-3.019	3.241	-3.055	3.409	-3.093	3.577	-3.133	3.746	-3.176
34/8	2.721	-3.062	2.885	-3.097	3.049	-3.133	3.215	-3.171	3.381	-3.209	3.548	-3.250	3.714	-3.294
35/8	2.697	-3.172	2.860	-3.209	3.024	-3.246	3.188	-3.284	3.353	-3.324	3.518	-3.366	3.683	-3.409
36/8	2.672	-3.281	2.834	-3.319	2.998	-3.358	3.161	-3.397	3.325	-3.437	3.489	-3.479	3.653	-3.522
37/8	2.646	-3.391	2.808	-3.430	2.971	-3.469	3.134	-3.509	3.297	-3.549	3.460	-3.591	3.623	-3.633
38/8	2.620	-3.500	2.782	-3.540	2.944	-3.579	3.107	-3.619	3.269	-3.660	3.432	-3.701	3.594	-3.744
39/8	2.593	-3.609	2.755	-3.649	2.917	-3.689	3.079	-3.730	3.241	-3.770	3.403	-3.811	3.565	-3.853
40/8	2.566	-3.719	2.728	-3.759	2.890	-3.799	3.052	-3.839	3.214	-3.880	3.376	-3.921	3.537	-3.962
41/8	2.539	-3.828	2.701	-3.868	2.862	-3.908	3.024	-3.949	3.186	-3.990	3.348	-4.030	3.510	-4.071
42/8	2.512	-3.937	2.673	-3.977	2.835	-4.018	2.997	-4.058	3.159	-4.099	3.320	-4.139	3.482	-4.180
43/8	2.484	-4.046	2.646	-4.087	2.808	-4.127	2.970	-4.168	3.131	-4.208	3.293	-4.249	3.455	-4.289
44/8	2.457	-4.155	2.619	-4.196	2.780	-4.236	2.942	-4.277	3.104	-4.317	3.266	-4.358	3.427	-4.398
45/8	2.430	-4.264	2.591	-4.305	2.753	-4.345	2.915	-4.386	3.077	-4.426	3.238	-4.467	3.400	-4.507
46/8	2.402	-4.374	2.564	-4.414	2.726	-4.455	2.887	-4.495	3.049	-4.536	3.211	-4.576	3.372	-4.617
47/8	2.376	-4.483	2.537	-4.523	2.698	-4.564	2.860	-4.604	3.022	-4.645	3.183	-4.685	3.345	-4.726
48/8	2.348	-4.592	2.509	-4.632	2.671	-4.673	2.833	-4.713	2.994	-4.754	3.156	-4.794	3.318	-4.835
49/8	2.320	-4.701	2.482	-4.741	2.644	-4.782	2.806	-4.822	2.967	-4.863	3.129	-4.903	3.290	-4.944
50/8	2.293	-4.810	2.455	-4.851	2.616	-4.891	2.778	-4.932	2.940	-4.972	3.101	-5.013	3.263	-5.053

TABLE VI—DISTRIBUTION OF PHYSICAL COORDINATES x AND y IN TRANSFORMED $\varphi\psi$ -PLANE FOR EXAMPLE V (ELBOW WITH COMPRESSIBLE FLOW ($\gamma=1.4$))[Prescribed variation in Q with arc length s along channel walls plotted in fig. 2; $Q_u=0.5$, $Q_d=1.0$, $g_d=0.79927$, $\Delta\psi=0.71054$, $\Delta\theta=105.31^\circ$]

$\frac{\varphi}{\Delta\psi}$	0		$\frac{1}{16}$		$\frac{1}{8}$		$\frac{3}{16}$		$\frac{1}{2}$		$\frac{5}{8}$		1.0	
	x	y	x	y	x	y	x	y	x	y	x	y	x	y
-12/6	-2.832	-0.770	-2.832	-0.513	-2.832	-0.256	-2.832	0.001	-2.832	0.258	-2.832	0.514	-2.832	0.771
-11/6	-2.695	-0.770	-2.695	-0.513	-2.695	-0.256	-2.695	0.001	-2.695	0.258	-2.695	0.514	-2.695	0.771
-10/6	-2.358	-0.770	-2.358	-0.513	-2.358	-0.256	-2.358	0.001	-2.358	0.258	-2.358	0.514	-2.358	0.771
-9/6	-2.122	-0.770	-2.122	-0.513	-2.122	-0.256	-2.122	0.001	-2.122	0.258	-2.122	0.514	-2.122	0.771
-8/6	-1.885	-0.770	-1.885	-0.513	-1.885	-0.256	-1.885	0.001	-1.885	0.258	-1.885	0.514	-1.885	0.771
-7/6	-1.648	-0.770	-1.648	-0.513	-1.648	-0.256	-1.648	0.001	-1.648	0.257	-1.648	0.514	-1.648	0.771
-6/6	-1.411	-0.769	-1.411	-0.513	-1.411	-0.256	-1.411	0.001	-1.411	0.257	-1.411	0.514	-1.411	0.771
-5/6	-1.174	-0.769	-1.175	-0.512	-1.175	-0.256	-1.175	0.001	-1.175	0.257	-1.175	0.514	-1.175	0.771
-4/6	-0.937	-0.769	-0.938	-0.512	-0.939	-0.256	-0.939	0.001	-0.938	0.257	-0.938	0.513	-0.937	0.770
-3/6	-0.701	-0.768	-0.702	-0.511	-0.702	-0.255	-0.703	0.001	-0.702	0.257	-0.702	0.513	-0.701	0.769
-2/6	-0.464	-0.767	-0.466	-0.510	-0.467	-0.255	-0.467	0.001	-0.467	0.256	-0.465	0.512	-0.464	0.768
-1/6	-0.227	-0.764	-0.230	-0.508	-0.232	-0.254	-0.233	0.001	-0.232	0.255	-0.230	0.510	-0.227	0.766
0	0.009	-0.760	0.004	-0.505	0.000	-0.252	0.000	0.000	0.002	0.253	0.005	0.507	0.010	0.763
1/6	0.245	-0.750	0.235	-0.499	0.230	-0.250	0.230	0.001	0.234	0.250	0.240	0.502	0.247	0.758
2/6	0.473	-0.735	0.460	-0.492	0.456	-0.249	0.458	0.004	0.463	0.244	0.473	0.495	0.484	0.749
3/6	0.688	-0.719	0.677	-0.485	0.675	-0.249	0.680	0.009	0.690	0.235	0.704	0.483	0.720	0.737
4/6	0.891	-0.705	0.884	-0.482	0.887	-0.253	0.897	0.019	0.913	0.220	0.934	0.466	0.956	0.719
5/6	1.080	-0.697	1.081	-0.483	1.091	-0.263	1.109	0.035	1.132	0.200	1.161	0.443	1.192	0.693
6/6	1.257	-0.698	1.268	-0.492	1.287	-0.279	1.314	0.058	1.347	0.173	1.385	0.411	1.426	0.669
7/6	1.424	-0.707	1.446	-0.510	1.475	-0.304	1.513	0.089	1.556	0.135	1.605	0.369	1.659	0.615
8/6	1.581	-0.726	1.615	-0.537	1.656	-0.338	1.705	0.130	1.760	0.088	1.822	0.317	1.888	0.558
9/6	1.729	-0.755	1.775	-0.574	1.828	-0.383	1.890	0.182	1.958	0.029	2.033	0.252	2.115	0.488
10/6	1.867	-0.794	1.926	-0.620	1.992	-0.438	2.067	0.245	2.149	-0.042	2.239	0.174	2.336	0.403
11/6	1.997	-0.842	2.069	-0.677	2.148	-0.503	2.236	0.320	2.332	-0.125	2.437	0.082	2.550	0.303
12/6	2.117	-0.899	2.202	-0.743	2.295	-0.579	2.396	0.406	2.507	-0.221	2.627	-0.024	2.757	0.187
13/6	2.229	-0.966	2.326	-0.820	2.432	-0.666	2.546	0.503	2.671	-0.330	2.806	-0.145	2.953	0.055
14/6	2.331	-1.040	2.441	-0.905	2.558	-0.763	2.686	0.612	2.824	-0.452	2.974	-0.279	3.137	-0.094
15/6	2.424	-1.122	2.545	-0.999	2.674	-0.869	2.814	0.732	2.965	-0.585	3.129	-0.428	3.308	-0.258
16/6	2.506	-1.211	2.638	-1.100	2.778	-0.984	2.929	0.862	3.092	-0.730	3.270	-0.589	3.463	-0.438
17/6	2.579	-1.306	2.720	-1.209	2.870	-1.108	3.031	1.000	3.205	-0.886	3.394	-0.762	3.601	-0.629
18/6	2.642	-1.407	2.791	-1.325	2.949	-1.238	3.118	1.147	3.301	-1.050	3.501	-0.946	3.719	-0.834
19/6	2.694	-1.513	2.850	-1.445	3.015	-1.374	3.191	1.299	3.381	-1.221	3.588	-1.138	3.816	-1.050
20/6	2.737	-1.624	2.898	-1.570	3.068	-1.514	3.248	1.456	3.443	-1.396	3.654	-1.335	3.887	-1.274
21/6	2.770	-1.738	2.935	-1.697	3.107	-1.656	3.290	1.614	3.486	-1.572	3.698	-1.533	3.928	-1.499
22/6	2.794	-1.854	2.961	-1.826	3.135	-1.799	3.319	1.772	3.513	-1.747	3.722	-1.727	3.945	-1.714
23/6	2.809	-1.971	2.977	-1.956	3.152	-1.940	3.334	1.927	3.527	-1.917	3.729	-1.912	3.944	-1.916
24/6	2.816	-2.089	2.985	-2.085	3.159	-2.081	3.339	2.079	3.528	-2.081	3.724	-2.089	3.929	-2.106
25/6	2.816	-2.208	2.985	-2.212	3.157	-2.218	3.336	2.226	3.520	-2.238	3.710	-2.256	3.906	-2.281
26/6	2.810	-2.326	2.978	-2.339	3.149	-2.353	3.325	2.369	3.505	-2.369	3.689	-2.414	3.878	-2.448
27/6	2.799	-2.444	2.965	-2.463	3.135	-2.484	3.308	2.507	3.484	-2.533	3.664	-2.564	3.846	-2.601
28/6	2.783	-2.561	2.948	-2.586	3.116	-2.613	3.287	2.641	3.460	-2.672	3.635	-2.708	3.812	-2.748
29/6	2.763	-2.678	2.928	-2.708	3.094	-2.739	3.263	2.771	3.433	-2.807	3.604	-2.845	3.777	-2.887
30/6	2.740	-2.794	2.904	-2.828	3.069	-2.862	3.236	2.898	3.404	-2.936	3.573	-2.977	3.742	-3.021
31/6	2.715	-2.910	2.879	-2.947	3.043	-2.984	3.208	3.022	3.374	-3.063	3.540	-3.105	3.707	-3.150
32/6	2.689	-3.025	2.851	-3.064	3.014	-3.104	3.178	3.144	3.342	-3.186	3.507	-3.229	3.672	-3.274
33/6	2.660	-3.140	2.822	-3.181	2.985	-3.222	3.148	3.264	3.311	-3.307	3.474	-3.351	3.637	-3.396
34/6	2.631	-3.255	2.793	-3.297	2.954	-3.339	3.117	3.382	3.279	-3.425	3.441	-3.470	3.603	-3.515
35/6	2.601	-3.369	2.762	-3.412	2.924	-3.455	3.085	3.498	3.247	-3.542	3.409	-3.587	3.570	-3.632
36/6	2.570	-3.484	2.731	-3.527	2.893	-3.571	3.054	3.614	3.215	-3.658	3.376	-3.703	3.537	-3.748
37/6	2.540	-3.598	2.701	-3.642	2.862	-3.685	3.023	3.729	3.184	-3.773	3.344	-3.818	3.505	-3.882
38/6	2.509	-3.712	2.669	-3.756	2.830	-3.800	2.991	3.844	3.152	-3.888	3.313	-3.932	3.474	-3.977
39/6	2.477	-3.827	2.638	-3.871	2.799	-3.915	2.960	3.959	3.121	-4.003	3.281	-4.047	3.442	-4.091
40/6	2.446	-3.941	2.607	-3.985	2.768	-4.029	2.929	4.073	3.089	-4.117	3.250	-4.161	3.411	-4.205
41/6	2.415	-4.055	2.576	-4.099	2.736	-4.143	2.897	4.187	3.058	-4.232	3.219	-4.275	3.380	-4.319
42/6	2.384	-4.169	2.544	-4.213	2.705	-4.257	2.866	4.301	3.027	-4.345	3.187	-4.389	3.348	-4.433
43/6	2.352	-4.284	2.513	-4.328	2.674	-4.372	2.835	4.416	2.995	-4.460	3.156	-4.504	3.317	-4.548
44/6	2.321	-4.398	2.482	-4.442	2.643	-4.486	2.803	4.530	2.964	-4.574	3.125	-4.618	3.286	-4.662

TABLE VII—TABULATED VALUES OF THE INTEGRALS α AND β FOR A RANGE OF $|(\Phi-\Phi_0)|$

[Computational methods given in appendix G]

$ (\Phi-\Phi_0) $	$\alpha^{(1)}$	$\Delta I = \Delta \alpha$		$\beta^{(1)}$	$\Delta I = \Delta \beta$	
		$\Delta \alpha$ ($\Delta \Phi = \pi/24$)	$\Delta \alpha$ ($\Delta \Phi = 2\pi/24$)		$\Delta \beta$ ($\Delta \Phi = \pi/24$)	$\Delta \beta$ ($\Delta \Phi = 2\pi/24$)
0	0	0.000373	0.002970	0	-0.396937	-0.611680
1($\pi/24$)	.000373	.002597		-.396937	-.214723	
2($\pi/24$)	.002970	.006972	.020331	-.611680	-.144746	-.242791
3($\pi/24$)	.009942	.013359		-.756406	-.098045	
4($\pi/24$)	.023301	.021574	.052976	-.854451	-.062035	-.094079
5($\pi/24$)	.044875	.031402		-.916486	-.032044	
6($\pi/24$)	.076277	.042620	.097632	-.948530	-.005816	.012092
7($\pi/24$)	.118897	.055012		-.954346	.017908	
8($\pi/24$)	.173909	.068374	.150903	-.936438	.038996	.100542
9($\pi/24$)	.242283	.082529		-.896542	.060646	
10($\pi/24$)	.324812	.097324	.209951	-.835896	.080497	.180181
11($\pi/24$)	.422136	.112627		-.755399	.099684	
12($\pi/24$)	.534763	.128335	.272697	-.656715	.118377	.255075
13($\pi/24$)	.663098	.144362		-.537338	.136698	
14($\pi/24$)	.807460	.160636	.337741	-.400640	.154739	.327305
15($\pi/24$)	.968096	.177105		-.245901	.172566	
16($\pi/24$)	1.145201	.193725	.404188	-.073335	.190232	.398006
17($\pi/24$)	1.338926	.210463		.116897	.207774	
18($\pi/24$)	1.549389	.227290	.471478	.324671	.225221	.467817
19($\pi/24$)	1.776679	.244188		.548892	.242596	
20($\pi/24$)	2.020867	.261141	.539276	.792488	.259915	.537106
21($\pi/24$)	2.282008	.278135		1.052403	.277191	
22($\pi/24$)	2.560143	.295161	.607373	1.329594	.294435	.606089
23($\pi/24$)	2.855304	.312212		1.624029	.311654	
24($\pi/24$)	3.167516	.329283	.675652	1.935683	.328853	.674890
25($\pi/24$)	3.496799	.346369		2.264536	.346037	
26($\pi/24$)	3.843168	.363465	.744035	2.610573	.363210	.743585
27($\pi/24$)	4.206633	.380570		2.973783	.380375	
28($\pi/24$)	4.587203	.397682	.812482	3.354158	.397531	.812215
29($\pi/24$)	4.984885	.414800		3.751689	.414684	
30($\pi/24$)	5.399685	.431922	.880967	4.166373	.431832	.880808
31($\pi/24$)	5.831607	.449045		4.598205	.448976	
32($\pi/24$)	6.280652	.466173	.949474	5.047181	.466120	.949380
33($\pi/24$)	6.746825	.483301		5.513301	.483260	
34($\pi/24$)	7.230126	.500431	1.017993	5.996561	.500400	1.017938
35($\pi/24$)	7.730557	.517562		6.496961	.517538	
36($\pi/24$)	8.248119	.534694	1.086521	7.014499	.534676	1.086488
37($\pi/24$)	8.782813	.551827		7.549175	.551812	
38($\pi/24$)	9.334640	.568960	1.156053	8.100987	.568949	1.156034
39($\pi/24$)	9.903600	.586093		8.669936	.586085	
40($\pi/24$)	10.489693	.603227	1.223588	9.256021	.603220	1.223576
41($\pi/24$)	11.092920	.620361		9.859241	.620356	
42($\pi/24$)	11.713281	.637496	1.292125	10.470597	.637492	1.292118
43($\pi/24$)	12.350777	.654629		11.117089	.654626	
44($\pi/24$)	13.005406	.671764	1.360662	11.771715	.671762	1.360658
45($\pi/24$)	13.677170	.688898		12.443477	.688896	
46($\pi/24$)	14.366068	.706033	1.429200	13.132373	.706032	1.429196
47($\pi/24$)	15.072101	.723167		13.838405	.723166	
48($\pi/24$)	15.795268	.740303	1.497739	14.561571	.740302	1.497738
49($\pi/24$)	16.535571	.757436		15.301873	.757436	

(1) For negative values of $(\Phi-\Phi_0)$ the signs of α and β change, but the signs of $\Delta\alpha$ and $\Delta\beta$ remain unchanged.

TABLE VII—TABULATED VALUES OF THE INTEGRALS α AND β FOR A RANGE OF $|\Phi - \Phi_0|$ —Concluded.

[Computation methods given in appendix G.]

$ \Phi - \Phi_0 $	$\alpha^{(1)}$	$\Delta I = \Delta \alpha$		$\beta^{(2)}$	$\Delta I = \Delta \beta$	
		$\Delta_1 \alpha$ ($\Delta \Phi = \pi/24$)	$\Delta_2 \alpha$ ($\Delta \Phi = 2\pi/24$)		$\Delta_1 \beta$ ($\Delta \Phi = \pi/24$)	$\Delta_2 \beta$ ($\Delta \Phi = 2\pi/24$)
50($\pi/24$)	17.293007	0.774572	1.566278	16.059309	0.774571	1.566276
51($\pi/24$)	18.067879	.791706		16.833880	.791705	
52($\pi/24$)	18.859285	.808840	1.634816	17.625585	.808841	1.634816
53($\pi/24$)	19.668125	.825976		18.434426	.825975	
54($\pi/24$)	20.494101	.843110	1.703355	19.260401	.843110	1.703354
55($\pi/24$)	21.337211	.860245		20.103511	.860244	
56($\pi/24$)	22.197458	.877379	1.771893	20.963755	.877380	1.771894
57($\pi/24$)	23.074835	.894514		21.841135	.894514	
58($\pi/24$)	23.969349	.911649	1.840433	22.735649	.911649	1.840433
59($\pi/24$)	24.880998	.928784		23.647298	.928784	
60($\pi/24$)	25.809782	.945912	1.908968	24.576082	.945912	1.908968
61($\pi/24$)	26.755694	.963056		25.521994	.963056	
62($\pi/24$)	27.718750	.980190	1.977507	26.485050	.980190	1.977507
63($\pi/24$)	28.698940	.997317		27.465240	.997317	
64($\pi/24$)	29.696257	1.014460	2.046044	28.462557	1.014460	2.046044
65($\pi/24$)	30.710717	1.031594		29.477017	1.031594	
66($\pi/24$)	31.742311	1.048722	2.114585	30.508611	1.048722	2.114585
67($\pi/24$)	32.791033	1.065863		31.557333	1.065863	
68($\pi/24$)	33.856896	1.082999	2.183123	32.623196	1.082999	2.183123
69($\pi/24$)	34.939895	1.100134		33.706195	1.100134	
70($\pi/24$)	36.040029	1.117260	2.251663	34.806329	1.117260	2.251663
71($\pi/24$)	37.157289	1.134403		35.923589	1.134403	
72($\pi/24$)	38.291692	1.151538	2.320201	37.057992	1.151538	2.320201
73($\pi/24$)	39.443230	1.168663		38.209530	1.168663	
74($\pi/24$)	40.611893	1.185808	2.388740	39.378193	1.185808	2.388740
75($\pi/24$)	41.797701	1.202942		40.564001	1.202942	
76($\pi/24$)	43.000643	1.220067	2.457279	41.766943	1.220067	2.457279
77($\pi/24$)	44.220710	1.237212		42.987010	1.237212	
78($\pi/24$)	45.457922	1.254347	2.525818	44.224222	1.254347	2.525818
79($\pi/24$)	46.712269	1.271481		45.478569	1.271481	
80($\pi/24$)	47.983750	1.288606	2.594357	46.750050	1.288606	2.594357
81($\pi/24$)	49.272356	1.305751		48.038656	1.305751	
82($\pi/24$)	50.578107	1.322885	2.662895	49.344407	1.322885	2.662895
83($\pi/24$)	51.900992	1.340010		50.667292	1.340010	
84($\pi/24$)	53.241002	1.357156	2.731435	52.007302	1.357156	2.731435
85($\pi/24$)	54.598168	1.374289		53.364458	1.374289	
86($\pi/24$)	55.972447	1.391414	2.799974	54.738747	1.391414	2.799973
87($\pi/24$)	57.363861	1.408560		56.130161	1.408560	
88($\pi/24$)	58.772421	1.425694	2.868512	57.538720	1.425694	2.868513
89($\pi/24$)	60.198115	1.442818		58.964415	1.442818	
90($\pi/24$)	61.640933	1.459964	2.937052	60.407233	1.459964	2.937052
91($\pi/24$)	63.100897	1.477098		61.867197	1.477098	
92($\pi/24$)	64.577995	1.494233	3.005590	63.344295	1.494233	3.005590
93($\pi/24$)	66.072228	1.511357		64.838528	1.511357	
94($\pi/24$)	67.583535	1.528503	3.074130	66.349835	1.528503	3.074130
95($\pi/24$)	69.112088	1.545637		67.878388	1.545637	
96($\pi/24$)	70.657725	1.562761	3.142668	69.424025	1.562761	3.142668
97($\pi/24$)	72.220486	1.579907		70.986786	1.579907	
98($\pi/24$)	73.800393	1.597042	3.211206	72.566693	1.597042	3.211206
99($\pi/24$)	75.397435	1.614164		74.163785	1.614164	
100($\pi/24$) ⁽³⁾	77.011699			75.777899		

⁽¹⁾ For negative values of $(\Phi - \Phi_0)$ the signs of α and β change, but the signs of $\Delta \alpha$ and $\Delta \beta$ remain unchanged.⁽²⁾ For values of $|\Phi - \Phi_0| > 100(\pi/24)$ use equation (G2) for α and equation (G7) for β .

TABLE VIII—COMPARISON OF ELBOW DESIGNS OBTAINED FROM SOLUTIONS BY RELAXATION METHODS AND BY GREEN'S FUNCTION

[Linearized compressible flow; prescribed velocity distribution given in figs. 2 and 22.]

ϕ	$\Psi=0$ (Inner wall)									$\Psi=\pi/2$ (Outer wall)								
	Q	q	Solution by relaxation methods (Part I)			Solution by Green's function (Part II)			Q	q	Solution by relaxation methods (Part I)			Solution by Green's function (Part II)			δ (deg)	δ (deg)
			x	y	δ (deg)	x	y	δ (deg)			x	y	δ (deg)	x	y	δ (deg)		
-22($\pi/24$)	0.5000	0.4009	-2.466	-0.769	0	-2.466	-0.769	0	0.5000	0.4009	-2.466	0.770	0	-2.466	0.770	0		
-20($\pi/24$)	.5000	.4009	-2.241	-.769	.01	-2.241	-.769	.01	.5000	.4009	-2.241	.770	-.01	-2.241	.770	-.01		
-18($\pi/24$)	.5000	.4009	-2.016	-.769	.01	-2.016	-.769	.01	.5000	.4009	-2.016	.770	-.01	-2.016	.770	-.01		
-16($\pi/24$)	.5000	.4009	-1.791	-.769	.02	-1.791	-.769	.02	.5000	.4009	-1.791	.779	-.02	-1.791	.779	-.02		
-14($\pi/24$)	.5000	.4009	-1.566	-.768	.03	-1.566	-.768	.03	.5000	.4009	-1.566	.770	-.03	-1.566	.770	-.03		
-12($\pi/24$)	.5000	.4009	-1.341	-.768	.05	-1.341	-.768	.05	.5000	.4009	-1.341	.769	-.05	-1.341	.770	-.05		
-10($\pi/24$)	.5000	.4009	-1.116	-.768	.08	-1.116	-.768	.08	.5000	.4009	-1.116	.769	-.08	-1.116	.769	-.08		
-8($\pi/24$)	.5000	.4009	-.891	-.768	.14	-.891	-.768	.14	.5000	.4009	-.891	.769	-.13	-.891	.769	-.13		
-6($\pi/24$)	.5000	.4009	-.666	-.767	.24	-.666	-.767	.24	.5000	.4009	-.666	.768	-.21	-.666	.768	-.22		
-4($\pi/24$)	.5000	.4009	-.441	-.766	.40	-.441	-.766	.41	.5000	.4009	-.441	.767	-.35	-.441	.767	-.30		
-2($\pi/24$)	.5000	.4009	-.216	-.763	.70	-.216	-.763	.74	.5000	.4009	-.216	.765	-.66	-.216	.765	-.59		
0	.5000	.4009	.008	-.760	1.31	.010	-.759	1.52	.5000	.4009	.009	.763	-.92	.009	.762	-.91		
2($\pi/24$)	.5079	.4072	.233	-.762	2.82	.233	-.761	2.76	.5000	.4009	.224	.768	-1.45	.234	.768	-1.45		
4($\pi/24$)	.5293	.4243	.450	-.739	3.88	.449	-.738	3.76	.5000	.4009	.459	.761	-2.22	.459	.760	-2.21		
6($\pi/24$)	.5599	.4489	.656	-.724	4.00	.656	-.724	3.89	.5000	.4009	.684	.740	-3.28	.684	.740	-3.29		
8($\pi/24$)	.5962	.4780	.851	-.712	3.17	.850	-.713	3.07	.5000	.4009	.908	.725	-4.65	.908	.721	-4.68		
10($\pi/24$)	.6354	.5094	1.033	-.704	1.44	1.033	-.705	1.38	.5000	.4009	1.132	.703	-6.41	1.132	.702	-6.43		
12($\pi/24$)	.6754	.5415	1.205	-.703	-.98	1.205	-.704	-1.04	.5000	.4009	1.355	.674	-8.52	1.355	.673	-8.56		
14($\pi/24$)	.7149	.5732	1.368	-.710	-4.00	1.367	-.711	-4.04	.5000	.4009	1.577	.636	-11.04	1.577	.635	-11.06		
16($\pi/24$)	.7531	.6038	1.519	-.725	-7.48	1.519	-.727	-7.51	.5000	.4009	1.797	.587	-13.91	1.797	.586	-13.91		
18($\pi/24$)	.7894	.6329	1.663	-.749	-11.35	1.663	-.750	-11.37	.5000	.4009	2.013	.527	-17.13	2.013	.526	-17.16		
20($\pi/24$)	.8235	.6602	1.798	-.781	-15.82	1.799	-.783	-15.84	.5000	.4009	2.226	.455	-20.67	2.226	.453	-20.69		
22($\pi/24$)	.8550	.6855	1.926	-.822	-19.96	1.926	-.823	-19.98	.5000	.4009	2.434	.368	-24.49	2.434	.367	-24.52		
24($\pi/24$)	.8838	.7086	2.046	-.871	-24.62	2.046	-.871	-24.63	.5000	.4009	2.635	.268	-28.68	2.635	.266	-28.69		
26($\pi/24$)	.9097	.7293	2.157	-.928	-29.46	2.158	-.929	-29.47	.5000	.4009	2.829	.163	-32.89	2.828	.162	-32.90		
28($\pi/24$)	.9326	.7477	2.261	-.993	-34.45	2.261	-.994	-34.46	.5000	.4009	3.013	.024	-37.40	3.012	.022	-37.41		
30($\pi/24$)	.9534	.7636	2.356	-1.064	-39.56	2.356	-1.066	-39.57	.5000	.4009	3.186	-.120	-42.08	3.185	-.122	-42.09		
32($\pi/24$)	.9690	.7769	2.443	-1.143	-44.76	2.443	-1.144	-44.77	.5000	.4009	3.346	-.278	-46.93	3.346	-.279	-46.94		
34($\pi/24$)	.9822	.7875	2.521	-1.228	-50.02	2.521	-1.229	-50.01	.5000	.4009	3.492	-.449	-51.93	3.492	-.450	-51.91		
36($\pi/24$)	.9919	.7953	2.590	-1.318	-55.27	2.590	-1.320	-55.27	.5000	.4009	3.623	-.632	-57.08	3.623	-.633	-57.10		
38($\pi/24$)	.9979	.8001	2.650	-1.414	-60.49	2.650	-1.415	-60.47	.5000	.4009	3.736	-.826	-62.44	3.736	-.828	-62.49		
40($\pi/24$)	1.0000	.8018	2.701	-1.514	-65.55	2.701	-1.516	-65.51	.5000	.4009	3.830	-1.030	-68.16	3.829	-1.034	-68.37		
42($\pi/24$)	1.0000	.8018	2.743	-1.619	-70.32	2.744	-1.620	-70.29	.5079	.4072	3.901	-1.242	-74.80	3.901	-1.244	-74.75		
44($\pi/24$)	1.0000	.8018	2.777	-1.726	-74.81	2.777	-1.727	-74.78	.5293	.4243	3.947	-1.455	-81.03	3.945	-1.456	-81.01		
46($\pi/24$)	1.0000	.8018	2.803	-1.836	-78.97	2.803	-1.837	-78.96	.5599	.4489	3.969	-1.661	-86.33	3.969	-1.662	-86.23		
48($\pi/24$)	1.0000	.8018	2.820	-1.947	-82.82	2.821	-1.948	-82.80	.5962	.4780	3.974	-1.856	-90.69	3.975	-1.858	-90.59		
50($\pi/24$)	1.0000	.8018	2.831	-2.059	-86.28	2.831	-2.059	-86.26	.6354	.5094	3.966	-2.038	-94.16	3.967	-2.040	-94.09		
52($\pi/24$)	1.0000	.8018	2.835	-2.171	-89.37	2.836	-2.172	-89.34	.6754	.5415	3.950	-2.209	-96.93	3.951	-2.210	-96.88		
54($\pi/24$)	1.0000	.8018	2.834	-2.283	-92.07	2.834	-2.285	-92.04	.7149	.5732	3.927	-2.369	-99.11	3.928	-2.371	-99.07		
56($\pi/24$)	1.0000	.8018	2.827	-2.396	-94.40	2.828	-2.397	-94.37	.7531	.6038	3.900	-2.520	-100.83	3.901	-2.522	-100.80		
58($\pi/24$)	1.0000	.8018	2.817	-2.508	-96.39	2.817	-2.509	-96.36	.7894	.6329	3.871	-2.663	-102.17	3.872	-2.665	-102.14		
60($\pi/24$)	1.0000	.8018	2.803	-2.619	-98.05	2.803	-2.620	-98.03	.8235	.6602	3.841	-2.799	-103.19	3.842	-2.801	-103.17		
62($\pi/24$)	1.0000	.8018	2.788	-2.731	-99.44	2.786	-2.732	-99.42	.8550	.6855	3.809	-2.929	-103.95	3.810	-2.931	-103.91		
64($\pi/24$)	1.0000	.8018	2.766	-2.841	-100.56	2.767	-2.842	-100.55	.8838	.7086	3.777	-3.055	-104.49	3.778	-3.056	-104.48		
66($\pi/24$)	1.0000	.8018	2.744	-2.952	-101.47	2.745	-2.953	-101.45	.9097	.7293	3.746	-3.176	-104.84	3.746	-3.178	-104.83		
68($\pi/24$)	1.0000	.8018	2.721	-3.062	-102.18	2.722	-3.063	-102.17	.9326	.7477	3.714	-3.294	-105.03	3.715	-3.296	-105.03		
70($\pi/24$)	1.0000	.8018	2.697	-3.173	-102.73	2.698	-3.173	-102.72	.9524	.7636	3.683	-3.409	-105.10	3.684	-3.411	-105.09		
72($\pi/24$)	1.0000	.8018	2.672	-3.281	-103.14	2.672	-3.283	-103.14	.9690	.7769	3.653	-3.522	-105.05	3.654	-3.524	-105.01		
74($\pi/24$)	1.0000	.8018	2.646	-3.391	-103.45	2.647	-3.392	-103.44	.9822	.7875	3.623	-3.633	-104.91	3.624	-3.635	-104.91		
76($\pi/24$)	1.0000	.8018	2.620	-3.500	-103.66	2.620	-3.501	-103.66	.9919	.7953	3.594	-3.744	-104.71	3.595	-3.746	-104.72		
78($\pi/24$)	1.0000	.8018	2.593	-3.609	-103.81	2.594	-3.611	-103.79	.9979	.8001	3.565	-3.853	-104.49	3.566	-3.855	-104.40		
80($\pi/24$)	1.0000	.8018	2.566	-3.719	-103.90	2.567	-3.720	-103.90	1.0000	.8018	3.537	-3.962	-104.28	3.538	-3.964	-104.19		
82($\pi/24$)	1.0000	.8018	2.539	-3.828	-103.97	2.540	-3.829	-103.97	1.0000	.8018	3.510	-4.071	-104.18	3.510	-4.073	-104.30		